Master's thesis

NTNU
Norwegian University of Science and Technology
Faculty of Natural Sciences
Department of Physics

Magnus S. Skjærpe

Superconducting Proximity Effects in Diffusive, Curved Antiferromagnets

Master's thesis in Physics
Supervisor: Sol H. Jacobsen
May 2023

NTNU
Norwegian University of
Science and Technology

Magnus S. Skjærpe

Superconducting Proximity Effects in Diffusive, Curved Antiferromagnets

Master's thesis in Physics
Supervisor: Sol H. Jacobsen
May 2023

Norwegian University of Science and Technology
Faculty of Natural Sciences
Department of Physics

NTNU
Norwegian University of
Science and Technology

Abstract

We apply the framework of curvature to the recently derived quasiclassical Usadel equation for an antiferromagnet-superconductor system. The addition of curvature makes it so we can tune the triplet generation by adjusting the physical parameters of the system. We transform the antiferromagnetic Usadel equation into describing a curvilinear system, which we then use to look at the case of a 1D wire with and without torsion. The main result is a Riccati parametrization of the Usadel equation for antiferromagnets along a curved 1D wire. We also look at the weak proximity equations for the system, and use numerical methods to solve for the density of states and magnetization in the antiferromagnet. The weak proximity equations showed that we needed torsion, in the form of a nanowire helix, in order to get mixing between the singlet and triplet states. In addition, no spin-orbit coupling was needed for mixing to occur when looking at the nanowire helix. Finally, looking at the density of states and magnetization of the electrons in the antiferromagnet indicated that there exist an optimal relationship between the antiferromagnetic exchange energy and the physical parameters of the system for generating triplet components and increased magnetization.

Sammendrag

Vi legger til krumming i den nylig utledede kvasiklassiske Usadel-ligningen for et antiferromagnet-superleder-system. Tillegget av krumning gjør det mulig å justere triplett generasjon ved å endre de fysiske parameterne i systemet. Vi transformerer den antiferromagnetiske Usadel-ligningen til å kunne beskrive et krummet system, som vi deretter bruker til å se på en 1D-ledning med og uten torsjon. Hovedresultatet er en Riccati-parametrisering av Usadel-ligningen for antiferromagneter langs en krummet 1D-ledning. Vi ser også på de svake proksimitetsligningene for systemet, og bruker numeriske metoder for å undersøketilstandstettheten og magnetiseringen i antiferromagneten. De svake proximitetsligningene viste at vi trengte torsjon i nanotråden i form av en helix for å oppnå en miksing mellom singlett- og triplett-tilstandene. I tillegg var det ikke nødvendig med spinn-bane-kobling for at miksingen skulle skje når vi så på helixen. Til slutt viste tilstandstettheten og magnetiseringen til elektronene i antiferromagneten at det eksisterer et optimalt forhold mellom den antiferromagnetiske utvekslingsfeltstyrken og de fysiske parameterne i systemet med tanke på å generere triplett komponenter og sterk magnetisering.

Preface

This document was submitted as a master thesis in physics at the Norwegian University of Science and Technology, under supervision of Sol H. Jacobsen. The duration of the masters program was two years, and consists of 60 ECTS-credits.

First of all, I would like to thank my supervisor Sol H. Jacobsen. I appreciate the time you have spend helping me with the ins and outs of curved superconductors. I would also like to thank Tancredi Salamone for all your guidance, and that you have always been available to ask for help. I am also grateful to Henning Hugdal, Alv Skarpeid and Morten Amundsen for being able to take part in the weekly curvature meetings, where I have learned a lot.

Lastly, I would like to thank my partner Johanne. Without your help I would not be where I am today.

Contents

1 Notation and Units

Vectors will be denoted with a bold font, e.g. $\mathbf{r}$. Covariant, contravariant and physical vector components will be denoted by x^i, x_i, $x_{(i)}$, respectively, where a physical vector means a vector defined in a specific basis, like $v_{(i)}$ for the component of a Cartesian vector in the $\hat{\mathbf{e}}_i$-direction. If it is stated which basis the vector is defined in, physical vector components are implied so we will drop the parenthesis notation.

Matrices will in general be denoted by capital letters, e.g $A, B, ...$ If it is not clear if the capital letters are matrices or not, we will denote them with a bold font similar to vectors. We will use the notation $\underline{\cdot}$ if we want to specify that we have a 2×2 matrix in spin-space. $\hat{\cdot}$ will be used for matrices in 4×4 Nambu particle-hole space and $\check{\cdot}$ will be used for 8×8 matrices in Keldysh space. If a matrix sum or product is taken with non-matching dimensions, is should be interpreted as taking the Kronecker product between the matrix with the smallest dimension and the appropriate identity matrix before multiplication. For example, we have $\check{A}\underline{B} + \hat{C} = \check{A}(\hat{I} \otimes \underline{B}) + (\underline{I} \otimes \hat{C})$. i denotes the complex number, $i = \sqrt{-1}$, and we write complex conjugation as $(a + ib)^* = (a - ib)$. Matrix transposition will be written as M^{T} and Hermitian conjugation as $\psi^\dagger$.

x_i will be used to specify both the position and time coordinate, e.g. $f(x_i) \equiv f(t_i, \mathbf{r}_i)$. The *Pauli matrices*, σ_i, in spin space are defined by:

$$\sigma^0 = \begin{pmatrix} 1 & 0 \\ 0 & 1 \end{pmatrix}, \ \sigma^1 = \begin{pmatrix} 0 & 1 \\ 1 & 0 \end{pmatrix}, \ \sigma^2 = \begin{pmatrix} 0 & -i \\ i & 0 \end{pmatrix}, \ \sigma^3 = \begin{pmatrix} 1 & 0 \\ 0 & -1 \end{pmatrix}. \tag{1.1}$$

We can combine the last three Pauli matrices into a vector called the *Pauli vector*, defined as $\boldsymbol{\sigma} \equiv \sigma^1\hat{\mathbf{e}}_x + \sigma^2\hat{\mathbf{e}}_y + \sigma^3\hat{\mathbf{e}}_y$. Note that one should not confuse the notation used for unit vectors, $\hat{\mathbf{e}}_i$, with the notation for 4×4 matrices. The Pauli matrices in Nambu space are defined in exactly the same way, and will be denoted by τ_i. $\hat{\tau_z} = \mathrm{diag}(1, 1, -1, -1)$ is the 4×4 extension of τ_z, with similar definitions for the rest of the Pauli matrices. We will also use σ to denote spin of a particle with spin σ, ψ_σ. It should be clear from the context if we are talking about spin or the Pauli matrices.

The *commutator* of two operators or matrices are defined as $[\mathbf{A}, \mathbf{B}] = \mathbf{AB} - \mathbf{BA}$, while the *anticommutator* is defined as $\{\mathbf{A}, \mathbf{B}\} = \mathbf{AB} + \mathbf{BA}$.

Partial differentiation will be written with the shorthand $\partial_i f \equiv \frac{\partial f}{\partial i}$, and the gradient is $\nabla \equiv \partial_x\hat{\mathbf{e}}_x + \partial_y\hat{\mathbf{e}}_y + \partial_z\hat{\mathbf{e}}_z$.

The function $\Theta(t_1 - t_2)$ is the Heaviside step function, $\delta(t_1 - t_2)$ is the Dirac delta function, and δ_{ij} is the Kronecker delta. We will also write $\delta(x - x') \equiv \delta(\mathbf{r} - \mathbf{r}')\delta(t - t')$.

In this thesis, we will use natural units where

$$\hbar = c = \epsilon_0 = \mu_0 = k_B = 1, \tag{1.2}$$

where $\hbar$ is the reduced Planck constant, c is the speed of light, ϵ_0 is the vacuum permittivity, μ_0 is the permeability and k_B is the Boltzmann constant. Using these

units where physical constants are chosen as the fundamental scales of the corresponding physical quantities has the advantage of making the notation easier, while still conserving the physics in the equations [1].

2 Introduction

As the technology in the world continues to evolve, so does the energy requirements. Increased interest in e.g. cryptocurrencies have raised the energy consumption in the world dramatically. For instance, the energy consumption of mining Bitcoins alone is estimated in 2023 to be 134.15 TWH/y, about 0.6% of the worlds total energy consumption [2]. This is comparable to the yearly consumption of countries such as Norway and Pakistan [3]. Finding a way to make computer components more energetically efficient could therefore help reduce the worlds emissions, as many processes producing power emits pollution. This is where the use of superconductors comes in. One of the fundamental properties of superconductors is that currents may flow without resistance. This means that, unlike traditional conductors like copper or other metals, superconducting materials can carry electrical current with almost no energy lost to heat due to the resistance in the material. This could result in significantly reduced energy consumption.

Superconductivity emerges due to the formation of bound states of electrons, known as *Cooper pairs* [4]. These electrons usually have opposite momentum and spin. In addition to reducing the energy needed to run different components, the spin of the quasiparticles in the superconductor can be used as information carriers. Not all combinations of spins for the quasiparticles are ideal to use as information carriers. Looking at a superconductor-ferromagnet (SF) system, one problem arises when we consider how the spin of the Cooper pairs interact with the magnetic field. When we put a superconductor in contact with another material, we get a phenomenon known as *the proximity effect* [5–8]. Here, the superconducting Cooper pairs may leak into the material, and thus influence its properties. This effect in a SF system is complicated with the fact that magnetic fields will tend to align spins, and thus break up the Cooper pairs. Spin singlets $|\uparrow\downarrow\rangle - |\downarrow\uparrow\rangle$, and the triplet component $|\uparrow\downarrow\rangle + |\downarrow\uparrow\rangle$ will therefore decay over a short distance. However, if we where to generate triplet components with finite total spins ($|\uparrow\uparrow\rangle$, $|\downarrow\downarrow\rangle$), these can penetrate the ferromagnet over a much longer distance [9–11]. These triplets are known as long range triplets (LRTs), while the triplet decaying over a short distance are known as short range triplet (SRT). Since the LRTs also have a finite spin direction, they can be used to represent 0- or 1-bit in a computer.

It is known that generation of LRTs happens in the presence of magnetic inhomogeneities [12–14]. Another possible source of LRT generation can happen in the presence of spin-orbit coupling (SOC) [9, 15]. Recent studies have also shown how a SF structure with a curved ferromagnet gives rise to SOC, which can be used to tune the triplet generation inside the ferromagnet [16, 17].

The deformation of the material due to bending leads to an additional potential in the material, which for small strains is assumed to be linear in strain [18, 19]. The potential leads to an electric field, which in turn couples to an electron's spin via the Zeeman coupling, leading to an effective spin-orbit coupling. By tuning the curvature of the ferromagnet, one can then adjust the amount of LRTs generated in the system. A possible application of this system could be to use it as a spin logical gate. Using a SFS Josephson junction, one could have a system where singlets and SRTs would not pass through the junction, while the LRTs would. This could then be encoded as 1 when a current passes through, and 0 when no current passes. This would allow for superconductors to be used for transferring information with zero resistance inside a computer.

Recently, Fyhn et.al. developed a method for using the quasiclassical framework to derive an equation of motion for an antiferromagnet-superconductor (AF-S) bilayer. [20] Antiferromagnets have many important advantages over ferromagnets in the context of spintronics, like being more stable and impervious to external magnetic fields while creating negligible magnetic stray fields of their own [21]. This makes them less intrusive to neighboring components, which is important if we want to use antiferromagnets in spintronics systems. Another advantage of antiferromagnets is the fact that their resonance frequency is of the order of terahertz, which allows for fast information processing [22, 23]. This is in comparison to ferromagnets, which have resonance frequencies of the order of gigahertz [24]. The fact that the derivation for the equation of motion for the AF-S system performed by Fyhn et.al. uses the same theoretical framework as for curved SF systems, allows for the possibility of looking at the effects of a curved antiferromagnet using the same framework. Spin transport have been shown to be long range in antiferromagnets [25], and it will therefore be interesting to see how the effect of curvature will affect these processes.

2.1 Superconductivity

Superconductivity is a quantum phenomenon observed in some materials at sufficiently low temperatures, and is characterized by having the ability to conduct electric currents without any resistance and excluding external magnetic fields. Superconductivity was discovered in 1911 by Heike Kamerlingh Onnes [26], but it took many years for the phenomena to be explained. The most used and successful theory to describe superconductors in the BCS theory, named after the creators Bardeen, Cooper and Schrieffer [27]. BSC theory is founded on the idea of Cooper pairs, which is a quasiparticle consisting of pairs of electrons. These pairs form due to an attractive interactions between the electrons, which for most superconductors is mediated by phonons. Superconductivity appears when an attractive interaction works on an ensemble of electron, making it a many-body quantum effect. The overall angular momenta of the Cooper pairs have to bee antisymmetric. This means

we can have Cooper pairs with an odd spin state (singlet) and even spatial part, known as a s-wave superconductor, or an even spin state (triplet) and odd spatial part, known as a p-wave superconductor [28, 29].

One important parameter when discussing superconductivity is the mean field, or *order parameter*. Consider $\hat{\psi}_\sigma(\mathbf{r}, t)$ as the operator annihilating an electron with spin σ at position $\mathbf{r}$ and time t. The order parameter is then defined as

$$\Delta(\mathbf{r}, t) = \lambda \langle \hat{\psi}_\uparrow(\mathbf{r}, t) \hat{\psi}_\downarrow(\mathbf{r}, t) \rangle, \tag{2.1}$$

where $\langle ... \rangle$ denotes a statistical average, and $\lambda > 0$ is the effective coupling constant of the electron-phonon-electron attractive interaction. In general, the order parameter is a complex function, $\Delta = |\Delta| e^{i\varphi}$, where the norm $|\Delta|$ describes the size of the superconducting gap, and φ describes the superconducting phase. When only considering a single superconductor, which will be the case in this thesis, the superconducting phase is not of importance. One can then perform a $U(1)$ gauge transformation in order to cancel the superconducting phase from the equations. We will therefore assume a gauge where Δ is real. Note that for systems with multiple superconductors, such as for the Josephson junction, the superconducting phase is of great importance, and will dictate the transport properties.

2.2 Quantum Mechanics

The building block of elementary quantum mechanics is the wave function, φ. The wave function is most often represented as a *ket vector* $|\varphi\rangle$ in Hilbert space, along with its Hermitian conjugate, the *bra vector* $\langle\varphi|$. The wave function is a representation of the state of a physical system, and can be used to find different observables. All physical observables of the system can be represented in terms of some Hermitian operator A, which acts on the wave function. These operators, along with the wave function, can be used to find the expectation value of physical observables. If a system is prepared in a state $|\varphi\rangle$ at time zero, the observable corresponding to the operator A will, at time t, have the expectation value given by:

$$\langle A \rangle = \langle \varphi | e^{iHt} A e^{-iHt} | \varphi \rangle \,, \tag{2.2}$$

where H is the Hamiltonian operator of the system. The *time evolution operator* $e^{\pm iHt}$ connects the states and measurements defined at different times. Usually, we absorb the time evolution operator into either the states, observables, or both:

- **Schrödinger picture**. Here we absorb the time evolution operator into the states, $e^{-iHt} |\varphi\rangle \equiv |\varphi(t)\rangle$. The expectation value then becomes $\langle A \rangle = \langle \varphi(t) | A | \varphi(t) \rangle$. The time evolution of these states must satisfy the *Schrödinger equation*:

$$i \frac{\mathrm{d}}{\mathrm{d}t} |\varphi(t)\rangle = H |\varphi(t)\rangle \,. \tag{2.3}$$

- **Heisenberg Picture**. In this case, we absorb the time evolution operator into the operators, $e^{iHt}Ae^{-iHt} \equiv A(t)$. The time evolution of these operators satisfy the *Heisenberg equation*:

$$i\frac{\mathrm{d}}{\mathrm{d}t}A(t) = [A(t), H]. \tag{2.4}$$

  Note that if the operator A has an explicit time-dependence, we need to add a term $i\partial_t A$ to the right hand side of the equation.

- **Interaction Picture**. Here we have some of the time evolution in the operators, and some in the states. If we split the Hamiltonian into two parts, H_0 and H_i, we can define the time dependent states as $e^{iH_0t}e^{-iHt}\left|\varphi\right\rangle \equiv \left|\varphi(t)\right\rangle$ and operators as $e^{iH_0t}Ae^{-iH_0t} \equiv A(t)$. The states then follow a Schrödinger equation, while the operators follow a Heisenberg equation:

$$i\frac{\mathrm{d}}{\mathrm{d}t}\left|\varphi(t)\right\rangle = H_i\left|\varphi(t)\right\rangle, \qquad i\frac{\mathrm{d}}{\mathrm{d}t}A(t) = [A(t), H_0]. \tag{2.5}$$

2.2.1 Second Quantization

The systems we will look at will contain a large number of particles. A more convenient way to describe many-particle systems than what was discussed above, is to use the second quantization formalism. Here, fields are thought of as field operators just like e.g. position and momentum are thought of as operators in the first quantization formalism. We introduce a *creation field operator* $\psi^\dagger_\sigma(\mathbf{r}, t)$ that creates an electron with spin σ at position $\mathbf{r}$ and time t, and an *annihilation field operator* $\psi_\sigma(\mathbf{r}, t)$ that destroys the same electron. These field operators act on a state in Fock-space, which is a combination of many single particle states given by $\left|\mathbf{r}_1\sigma_1, \mathbf{r}_2\sigma_2, ..., \mathbf{r}_n\sigma_n\right\rangle = \left|\mathbf{r}_1\sigma_1\right\rangle \otimes ... \otimes \left|\mathbf{r}_n\sigma_n\right\rangle$. Many-particle states can be created by operating with the field operators onto a special *vacuum state*, $\left|0, 0, ..., 0\right\rangle \equiv \left|0\right\rangle$, which contains *zero* electrons:

$$\begin{aligned}\left|\mathbf{r}_1\sigma_1, \mathbf{r}_2\sigma_2, \ldots, \mathbf{r}_n\sigma_n\right\rangle &= \psi^\dagger_{\sigma_1}(\mathbf{r}_1, t)\left|0, \mathbf{r}_2\sigma_2, \ldots, \mathbf{r}_n\sigma_n\right\rangle \\ &= \ldots = \psi^\dagger_{\sigma_1}(\mathbf{r}_1, t)\ldots\psi^\dagger_{\sigma_n}(\mathbf{r}_n, t)\left|0\right\rangle.\end{aligned} \tag{2.6}$$

The electron field operators satisfies the following fermionic anticommutation relations:

$$\{\psi^\dagger_\sigma(\mathbf{r}, t), \psi^\dagger_{\sigma'}(\mathbf{r}', t)\} = 0, \tag{2.7a}$$

$$\{\psi_\sigma(\mathbf{r}, t), \psi^\dagger_{\sigma'}(\mathbf{r}', t)\} = \delta_{\sigma\sigma'}\delta(\mathbf{r} - \mathbf{r}')\delta(t - t'), \tag{2.7b}$$

$$\{\psi_\sigma(\mathbf{r}, t), \psi_{\sigma'}(\mathbf{r}', t)\} = 0. \tag{2.7c}$$

We would like a way to relate the non-interacting Hamiltonian of a single particle in the first quantization formalism to the equivalent non-interaction Hamiltonian for a many-particle system in the second quantization formalism. This relation is given by:

$$\mathcal{H}_0 = \int \mathrm{d}^3\mathbf{r} \sum_\sigma \psi^\dagger_\sigma(\mathbf{r}, t) H_0 \psi_\sigma(\mathbf{r}, t), \tag{2.8}$$

where H_0 is the non-interacting Hamiltonian for a single particle in the first quantization formalism, and $\mathcal{H}_0$ is the corresponding many-particle Hamiltonian in the second quantization formalism.

2.3 Tensors

In this thesis, we will work with curved geometries. It will therefore be convenient to introduce tensors in order to rewrite relevant equations from Cartesian to curved coordinates. In this section we will summarize the most important points for understanding the notation used in this thesis. For a more detailed review, see e.g. [30, 31].

In physics, we use coordinates to describe where physical objects are and how they change. We do this by assigning them a value based on where they are relative to a given coordinate system. For instance, we could use a Cartesian coordinate system to describe the motion of a particle in three dimensions, or a spherical coordinate system to describe a particle moving in some circular motion. While the unit vectors used to describe the different coordinate systems are different, the objects they describe move along the same line regardless of the choice of coordinate system. This is where the use of *tensors* comes inn. Using tensors, we can express equations using notation that is invariant with respect to a change of coordinates. This will become useful later when we want to rewrite equations like the Usadel equation from Cartesian to curved coordinates.

To describe what a tensor is, we have to describe how they change. First, consider a scalar such as the distance between two points in Euclidean space. For a number λ to be a scalar, it has to remain unaffected if we transform from, say, coordinates (x, y, z) to (x', y', z'):

$$\lambda = \lambda', \tag{2.9}$$

where we use the notation $\lambda \equiv \lambda(x, y, z)$ and $\lambda' \equiv \lambda(x', y', z')$. This statement uses how they transform under a change of coordinate systems to formally define what it means for a quantity to be a scalar. In contrast to scalars, vectors are often described as "arrows" that carry information about a magnitude and a direction. The length and magnitude of the vector is independent of any coordinate system, but we can use coordinates to describe the orientation and scaling of the vector along the coordinate axes. Since coordinate systems can change, equations that contains vectors must in some way contain information about how they would behave if we where to change coordinate systems. The next step up from a vector is a tensor, which is described as a mathematical object that is independent of a specific basis, and is defined by how it changes under a transformation of coordinates. Tensors are usually classified by its rank, and can be described by N^{rank} numbers. A rank 0 tensor can be described with $N^0 = 1$ number, and can therefore be represented by a scalar. A rank 1 tensor can be described by N numbers, and can be represented by a vector. Furthermore, a rank 2 tensor can be represented by N^2 numbers, which is

equivalent to a matrix. Note that even though a vector and a matrix can be used to represent a rank 1 and 2 tensor, not all vectors or matrices are tensors. For instance, since we need N^2 numbers to describe a rank 2 tensor, only square matrices can be used as a representation.

The rank of a tensor appears in the number of indices needed to describe the object. For instance, a rank 1 tensor is written as A_i or B^i. The placement of the index is important as it determines how the tensors transform. A_i with a lowered index is called a *covariant* vector, and is said to transform *covariantly*. B^i with a raised index is called a *contravariant* vector, and transforms *contravariantly*. Under a change of coordinate $x \to x'$ they transform as:

$$A'_i = \frac{\partial x^j}{\partial x'^i} A_j, \tag{2.10}$$

$$B'^i = \frac{\partial x'^i}{\partial x^j} B^j, \tag{2.11}$$

where we use Einstein summation convention for summation over each index repeated twice in a product. A general tensor of rank $k+l$ with k raised and l lowered indices $T_{i_1 \dots i_l}{}^{j_1 \dots j_k}$ transforms as a product of l covariant and k contravariant vectors:

$$T'_{i_1 \dots i_l}{}^{j_1 \dots j_k} = \frac{\partial x^{m_1}}{\partial x'^{i_1}} \dots \frac{\partial x^{m_l}}{\partial x'^{i_l}} \frac{\partial x'^{j_1}}{\partial x^{n_1}} \dots \frac{\partial x'^{j_k}}{\partial x^{n_l}} T_{m_1 \dots m_l}{}^{n_1 \dots n_k}. \tag{2.12}$$

The reason we need two different types of vectors is because different physical quantities changes in different ways when we transform coordinate systems. For instance, if we where to change the units of a coordinate system from meters to centimeters, we would *divide* the scale of the coordinate axes by 100, so 1m would now correspond to 1cm. The components of e.g. a velocity vector would however change by being *multiplied* by 100. This change is the inverse of the change for the coordinate axes, and is what happens to a contravariant vector. A gradient with respect to position, for example, has units of distance^{-1}, and changes in the same way as the coordinate axes. This is what happens to a covariant vector.

2.3.1 The Metric Tensor

We will now look at an important tensor called the *metric tensor*. Let us consider the displacement vector $\mathrm{d}\mathbf{r}$, measured in units of length. In Cartesian coordinates, it is given as

$$\mathrm{d}\mathbf{r} = \mathrm{d}x\, \hat{\mathbf{e}}_x + \mathrm{d}y\, \hat{\mathbf{e}}_y + \mathrm{d}z\, \hat{\mathbf{e}}_z, \tag{2.13}$$

while in spherical coordinates it is given as

$$\mathrm{d}\mathbf{r} = \mathrm{d}\rho\, \hat{\mathbf{e}}_\rho + \rho\, \mathrm{d}\theta\, \hat{\mathbf{e}}_\theta + \rho \sin(\theta)\, \mathrm{d}\phi\, \hat{\mathbf{e}}_\phi. \tag{2.14}$$

We can now generalize the differential coordinate displacement for an arbitrary coordinate system by introducing scale factors h_i

$$\mathrm{d}\mathbf{r} = \sum_i h_i\, \mathrm{d}x^i\, \hat{\mathbf{e}}_i. \tag{2.15}$$

Since d$\mathbf{r}$ is given in units of length, the scaling factors h_i makes sure that each coordinate displacement $\mathrm{d}x^i$ has the correct unit of length. The differential coordinate displacement squared is found by taking the scalar product with itself:

$$(\mathrm{d}r)^2 = \sum_{i,j} h_i h_j \hat{\mathbf{e}}_i \cdot \hat{\mathbf{e}}_j \, \mathrm{d}x^i \, \mathrm{d}x^j = \eta_{ij} \, \mathrm{d}x^i \, \mathrm{d}x^j \,, \tag{2.16}$$

where

$$\eta_{ij} = h_i h_j \hat{\mathbf{e}}_i \cdot \hat{\mathbf{e}}_j \tag{2.17}$$

is defined as the covariant form of the metric tensor (remember the summation convention). If we now consider the examples given in equations (2.13) and (2.14), we may write the metric tensor as a square matrix:

$$\eta_{ij}^{\text{Cartesian}} = \begin{pmatrix} 1 & 0 & 0 \\ 0 & 1 & 0 \\ 0 & 0 & 1 \end{pmatrix}, \qquad \eta_{ij}^{\text{Spherical}} = \begin{pmatrix} 1 & 0 & 0 \\ 0 & \rho^2 & 0 \\ 0 & 0 & \rho^2 \sin^2(\theta) \end{pmatrix}. \tag{2.18}$$

Note that if the coordinate systems are orthogonal, then $\hat{\mathbf{e}}_i \cdot \hat{\mathbf{e}}_j = \delta_{ij}$ and the metric tensor is thus diagonal. One important fact is that the covariant and contravariant metric tensor is the inverse of each other, $\eta_{ij}^{-1} = \eta^{ij}$. A fundamental property of the metric tensor is that we can use it to convert between covariant and contravariant vectors:

$$A_i = \eta_{ij} A^j, \qquad A^i = \eta^{ij} A_j. \tag{2.19}$$

This is also the case for a general tensor:

$$\begin{aligned} T_{i_1 \ldots i_{n-1}}{}^{k}{}_{i_{n+1} \ldots i_m}{}^{j_1 \ldots j_l} &= \eta^{k i_n} T_{i_1 \ldots t_m}{}^{j_1 \ldots j_l}, \\ T_{i_1 \ldots i_m}{}^{j_1 \ldots j_{n-1}}{}_{k}{}^{j_{n+1} \ldots j_l} &= \eta_{k j_n} T_{i_1 \ldots t_m}{}^{j_1 \ldots j_l}. \end{aligned} \tag{2.20}$$

Finally, when we refer to a *physical* vector, we mean a vector defined in a given basis, e.g. Cartesian or spherical, and is denoted $A_{(i)}$. This is in contrast to the more general covariant/contravariant vectors which are independent of a basis.

2.3.2 Christoffel Symbols

In the later chapters, we will see that we will end up working with derivatives. We therefore have to look at the transformation properties of the derivative of covariant/contravariant tensors. Consider a contravariant vector x^i in a coordinate system $\mathcal{S}$ that we want to transform to a primed coordinate system $\mathcal{S}'$. We would then use equation (2.11) and write:

$$x'^i = \frac{\partial x'^i}{\partial x^j} x^j \tag{2.21}$$

We can then find the transformation rule for the derivative of a covariant vector by differentiating this equation by some scalar t:

$$\frac{\mathrm{d}x'^i}{\mathrm{d}t} = \frac{\partial x'^i}{\partial x^j} \frac{\mathrm{d}x^j}{\mathrm{d}t} + x^j \frac{\mathrm{d}}{\mathrm{d}t}\left(\frac{\partial x'^i}{\partial x^j}\right) = \frac{\partial x'^i}{\partial x^j} \frac{\mathrm{d}x^j}{\mathrm{d}t} + x^j \frac{\partial^2 x'^i}{\partial x^j \partial x^k} \frac{\mathrm{d}x^k}{\mathrm{d}t} \tag{2.22}$$

The first term is what we would expect if we where to just replace B in equation (2.11) with the derivative of a contravariant vector $\mathrm{d}x^j \,/\, \mathrm{d}t$. If we only had this term, the derivative of the contravariant vector would follow the transformation rule for it to also be a tensor. However, as we can see, we also have a second term involving second derivatives. Ordinary derivatives of tensors are therefore not necessarily tensors, since they do not generally follow definition (2.11). In order to make the derivative have a proper contravariant transformation, we redefine the derivative operator in such a way that this additional second derivative term cancels, which will then preserve the tensorial nature of the transformation. This redefined derivative is called the *coordinate covariant derivative*, denoted by $\mathcal{D}$, first introduced by Ricci and Levi-Civita in 1900 [32]. The coordinate covariant derivative of a contravariant vector A^j with respect to a coordinate x^i is defined as

$$\mathcal{D}_i A^j = \partial_i A^j + \Gamma^j_{ik} A^k, \tag{2.23}$$

where Γ^j_{ik} is known as the *Christoffel symbol* or the *affine connection* and is related to the metric tensor in the way that

$$\Gamma^k_{ij} = \frac{1}{2}\eta^{kl}(\partial_j \eta_{li} + \partial_i \eta_{lj} - \partial_l \eta_{ij}). \tag{2.24}$$

The Christoffel symbol ensures that the coordinate covariant derivative of a tensor remains a tensor, but it is not itself a tensor. Terms including derivatives, such as for the Usadel equation in section 8, will include this coordinate covariant derivative. The coordinate covariant derivative of a covariant vectors is defined similarly, but with a minus sign instead of a plus sign

$$\mathcal{D}_i A_j = \partial_i A_j - \Gamma^j_{ik} A_k. \tag{2.25}$$

2.4 Curvilinear Coordinates

In later chapters, we will look at how a curved material changes the singlet and triplet generation of Cooper pairs inside a S-AF system. For this, it will be convenient to use curvilinear coordinates, which is beneficial when looking at systems with curved symmetries. Curvilinear coordinate systems are characterized by the fact that the coordinate lines may be curved, and the direction of the basis vectors can change depending on the point you look at. Examples of such coordinate systems are spherical and cylindrical coordinates. This section is based on section 3.1 in the thesis by M. Svendsen [30].

Our system will be defined by a set of orthogonal basis vectors $\hat{\boldsymbol{\mathcal{N}}}(s)$, $\hat{\boldsymbol{\mathcal{T}}}(s)$ and $\hat{\boldsymbol{\mathcal{B}}}(s)$ in the normal, tangential and binormal direction respectively. This is a general orthogonal curvilinear coordinate system, defined on the curved structure as shown in figure 1. Here, s is the distance along the arclength from a reference point to the point we are interested in. Since the direction of the basis vectors are functions of the arclength parameter, they will point in different directions depending on which point on the surface we look at.

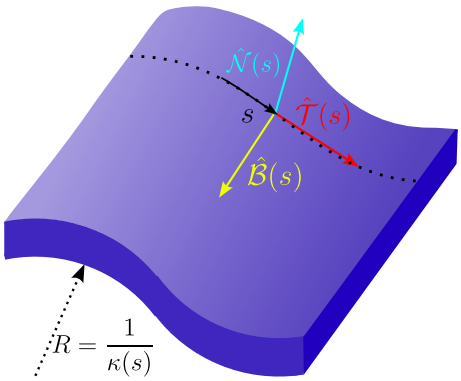

Figure 1: Figure showing the curvilinear coordinate system. It is described by an arclength s measured from some reference point and a set of orthogonal unit vectors $\hat{\boldsymbol{\mathcal{N}}}(s)$, $\hat{\boldsymbol{\mathcal{T}}}(s)$ and $\hat{\boldsymbol{\mathcal{B}}}(s)$ normal, tangential and binormal to the curved nanostructure, respectively. The radius at the arclength point s is given by $R = \frac{1}{\kappa(s)}$, where $\kappa(s)$ is the curvature.

When deriving the different relations for the system, we will start by assuming that the binormal unit vector is independent on the arclength s, i.e. no torsion. Later we will look at the case with torsion included. We will also assume that the structure in the plane follows a differentiable curve, so we can parameterize the surface in terms of the arclength coordinate s and the binormal coordinate b as $\mathbf{r}(s,b) = \boldsymbol{\xi}(s) + b\hat{\boldsymbol{\mathcal{B}}}(s)$. Here $\boldsymbol{\xi}(s)$ is the parametrization of the differentiable curve in the plane of curvature, along the arclength s. Similarly, the three-dimensional space around the surface $\mathbf{R}$ can be parametrized using the normal unit vector, normal coordinate n and the parametrization of the surface:

$$\mathbf{R}(s,n,b) = \mathbf{r}(s,b) + n\hat{\boldsymbol{\mathcal{N}}}(s). \tag{2.26}$$

The unit vectors $\hat{\boldsymbol{\mathcal{N}}}$, $\hat{\boldsymbol{\mathcal{T}}}$ and $\hat{\boldsymbol{\mathcal{B}}}$ are connected through the Frenet-Serret formulas [17, 30]. In the case of no torsion, these relations are

$$\begin{pmatrix} \partial_s \hat{\boldsymbol{\mathcal{T}}}(s) \\ \partial_s \hat{\boldsymbol{\mathcal{N}}}(s) \\ \partial_s \hat{\boldsymbol{\mathcal{B}}}(s) \end{pmatrix} = \begin{pmatrix} 0 & \kappa(s) & 0 \\ -\kappa(s) & 0 & 0 \\ 0 & 0 & 0 \end{pmatrix} \begin{pmatrix} \hat{\boldsymbol{\mathcal{T}}}(s) \\ \hat{\boldsymbol{\mathcal{N}}}(s) \\ \hat{\boldsymbol{\mathcal{B}}}(s) \end{pmatrix}, \tag{2.27}$$

where $\kappa(s) = \frac{1}{R}$ is the curvature at at the arclength point s with radius R. We can now write the total differential displacement of the space $\mathbf{R}$ as:

$$\begin{aligned} \mathrm{d}\mathbf{R}(s,n,b) &= \partial_s \mathbf{R}(s,n,b) + \partial_n \mathbf{R}(s,n,b) + \partial_b \mathbf{R}(s,n,b) \\ &= (1-\kappa(s)n)\mathrm{d}s\hat{\boldsymbol{\mathcal{T}}}(s) + \mathrm{d}n\hat{\boldsymbol{\mathcal{N}}}(s) + \mathrm{d}b\hat{\boldsymbol{\mathcal{B}}}(s) = \sum_i h_i \mathrm{d}q^i \hat{\mathbf{e}}_{(i)}(s), \end{aligned} \tag{2.28}$$

where we have used the fact that $\partial_s \boldsymbol{\xi}(s) = \hat{\boldsymbol{\mathcal{T}}}$ from the definition of the derivative. In the last line of the equation, we have written the total differential displacement like we did in equation (2.15), where q^i are the curvilinear coordinates, $\hat{\mathbf{e}}_{(i)}(s)$ are the curvilinear unit vectors, and the scale factors are given as

$$h_T = 1 - \kappa(s)n, \qquad h_N = 1, \qquad h_B = 1. \tag{2.29}$$

We can now find the metric tensor for the system by taking the square of the total differential difference in equation (2.28)

$$(\mathrm{d}R(s,n,b))^2 = \sum_{i,j} h_i h_j \hat{\mathbf{e}}_{(i)} \cdot \hat{\mathbf{e}}_{(j)} \mathrm{d}q^i \mathrm{d}q^j = \eta_{ij} \mathrm{d}q^i \mathrm{d}q^j, \tag{2.30}$$

where we use the Einstein summation convention in the last equality, and the fact that the basis vectors of the curved system are orthogonal to write the metric tensor as $\eta_{ij} = h_i h_j \delta_{ij}$. Using the expressions for the scale factors h_i we found above, we can write the metric tensor for our curvilinear coordinate system as a diagonal matrix:

$$\eta_{ij} = \begin{pmatrix} H(s,n)^2 & 0 & 0 \\ 0 & 1 & 0 \\ 0 & 0 & 1 \end{pmatrix}, \tag{2.31}$$

where we defined the scale factor

$$H(s,n) = 1 - \kappa(s) n. \tag{2.32}$$

Later, we will see how this scale factor appear in equations like the Usadel equation.

In the following sections we would like to take the covariant derivative of the Usadel equation. To be able to do this, we need to find the expressions for the Christoffel symbols used in the covariant derivative. The Christoffel symbols are related to the metric tensor through equation (2.24)

$$\Gamma^k_{ij} = \frac{1}{2} \eta^{kk} (\partial_j \eta_{ki} + \partial_i \eta_{kj} - \partial_k \eta_{ij}), \tag{2.33}$$

where we have set $l = k$ since the curvilinear metric is diagonal. Most of the components are zero, but the four non-zero components are given as:

$$\Gamma^s_{ss} = \frac{1}{H(s,n)} \partial_s H(s,n), \tag{2.34a}$$

$$\Gamma^n_{ss} = -H(s,n) \partial_n H(s,n), \tag{2.34b}$$

$$\Gamma^s_{ns} = \Gamma^s_{sn} = \frac{1}{H(s,n)} \partial_n H(s,n). \tag{2.34c}$$

Note that the elements in the matrix (2.31) are labeled such that element η_{ss} is the upper left element, η_{nn} the center element, and η_{bb} the lower right element.

2.4.1 Torsion

In the case where we include torsion, the Frenet-Serret-type equations are given as

$$\begin{pmatrix} \partial_s \hat{\boldsymbol{\mathcal{T}}}(s) \\ \partial_s \hat{\boldsymbol{\mathcal{N}}}(s) \\ \partial_s \hat{\boldsymbol{\mathcal{B}}}(s) \end{pmatrix} = \begin{pmatrix} 0 & \kappa(s) & 0 \\ -\kappa(s) & 0 & \tau(s) \\ 0 & -\tau(s) & 0 \end{pmatrix} \begin{pmatrix} \hat{\boldsymbol{\mathcal{T}}}(s) \\ \hat{\boldsymbol{\mathcal{N}}}(s) \\ \hat{\boldsymbol{\mathcal{B}}}(s) \end{pmatrix}, \tag{2.35}$$

where $\kappa(s)$ and $\tau(s)$ denotes the curvature and torsion of the space curve, respectively [33]. For a 1D-line, the inclusion of both torsion and curvature would turn it

into a helix. In the case where $\tau \to 0$, we get the system described above. Here the torsion is given by τ and the curvature κ.

The metric tensor for the curvilinear coordinate system with torsion is given as [33]

$$\eta_{ij} = \begin{pmatrix} H(s,n)^2 + \tau(s)^2(n^2+b^2) & -\tau(s)b & \tau(s)n \\ -\tau(s)b & 1 & 0 \\ \tau(s)n & 0 & 1 \end{pmatrix}. \tag{2.36}$$

2.5 Antiferromagnetism

Antiferromagnets are a type of magnetic material where the magnetic moments of the individual particles are aligned in opposite directions, which creates a pattern of alternating up and down spins as is seen in figure 2. The total magnetization of the antiferromagnet can either be zero when the total net spin is zero, or it can have a small net magnetization in one direction. This can happen if the magnetic moment is stronger in one direction, or if there are more particles with one type of spin direction. Usually, one can construct the lattice of an antiferromagnet with a unit cell consisting of two points, one for each spin direction. The lattice therefore consists of two sublattices, where each sublattice contains only points with the same spin direction.

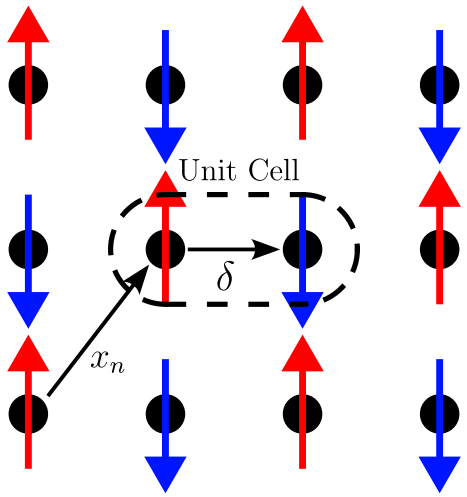

Figure 2: Figure showing a typical unit cell for an antiferromagnetic lattice with up and down spins. x_n is the distance between the unit cells, and δ is the distance between the nearest neighbor lattice cites.

There are different combination of alternating spins that will give us an antiferromagnet. In 3D-space, there are three different ways to structure the spins to achieve this, if we consider the spins on a square lattice, as is seen in figure 3. These are the A-, C-, and G type antiferromagnets. If we want to end up with a spin chain in 1D-space, we need to cleave these 3D-structures into 2D, and then finally into 1D. Cleaving the antiferromagnetic structures in figure 3, we end up with the 2D planes in figure 4, which we can then cleave into the 1D chains in figure 5.

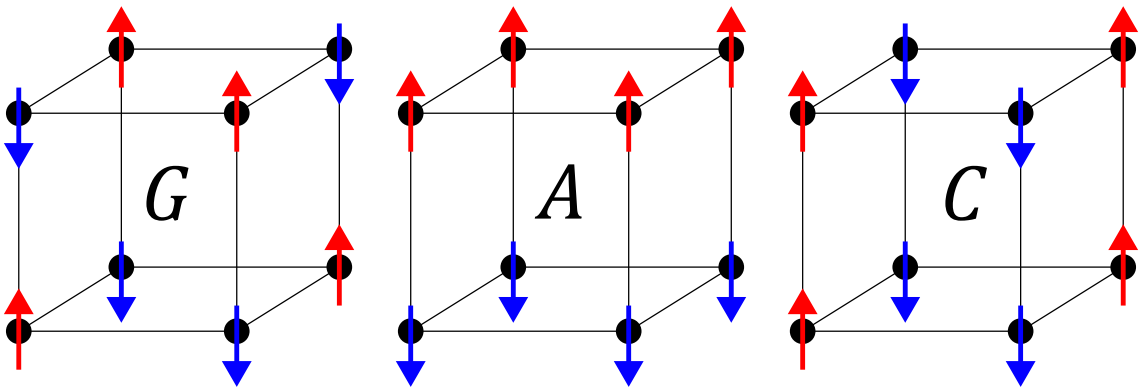

Figure 3: Different spin structures for a 3D square lattice.

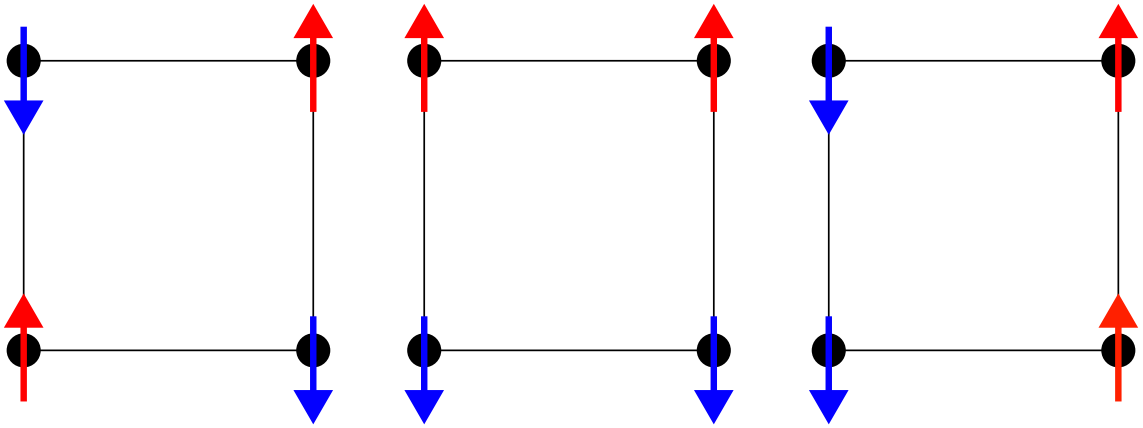

Figure 4: Different spin structures for a 2D square lattice.

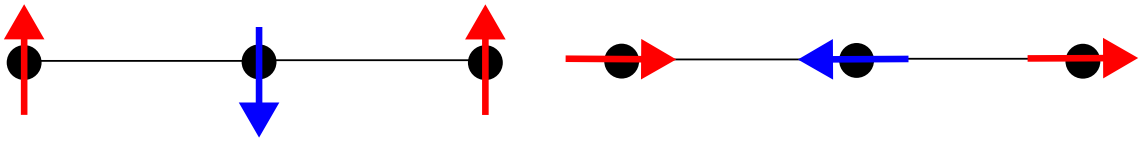

Figure 5: Different spin structures for a 1 lattice chain.

The spin direction is also determined by what direction is most energy efficient to point in. An example which will be relevant for later is the ground state in an antiferromagnetic helix with magnetic dipolar interaction. Here, we get two cases depending on the strength of the curvature and torsion of the helix [34]. The Néel vector is a vector pointing in the direction of the magnetic moment of the antiferromagnet. For this system it is determined by the geometrical parameters curvature and torsion. The first case is the homogeneous state, which is the case when the Néel vector stays at a fixed angle. Here, he Néel vector tilts at an angle ψ away from the binormal unit vector $\hat{\mathbf{e}}_B$ of the helix. The second case is the periodic state, which is the case when the Néel vector rotates. Here, the Néel vector oscillates almost uniformly in the plane perpendicular to the helix axis, with a small oscillation in the binormal direction. These two cases are illustrated in figure 6. It is worth noting that ref. [34] models the Curvilinear antiferromagnet as a classical spin chain with nearest-neighbor exchange and dipolar interaction, which is different form the

model we will use in section 6 when deriving the antiferromagnetic Usadel equation.

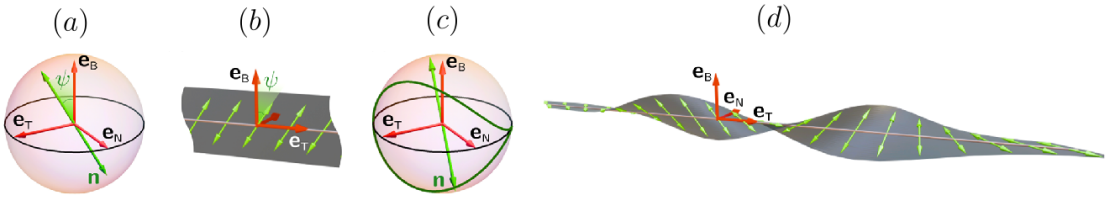

Figure 6: Figure taken from [34]. Schematics of the (a, b) homogeneous and (b, c) periodic states for an antiferromagnetic helix with magnetic dipolar interaction in the TNB reference frame. (a, c) Bloch spheres illustrate the trajectories of the Néel vector $\mathbf{n}$.

2.6 Mixed Representation

In future calculations, it will be useful to use a center off mass and relative representation for the position and time coordinates. To achieve this we do a transformation to the mixed or Wigner representation, given by the following relations:

$$\boldsymbol{r} = \boldsymbol{r}_1 - \boldsymbol{r}_2, \qquad \boldsymbol{R} = \frac{1}{2}(\boldsymbol{r}_1 + \boldsymbol{r}_2), \tag{2.37}$$

$$t = t_1 - t_2, \qquad T = \frac{1}{2}(t_1 + t_2). \tag{2.38}$$

The time and spatial derivatives in the mixed representation are then given by [35]:

$$\frac{\partial}{\partial t_1} = \frac{1}{2}\frac{\partial}{\partial T} + \frac{\partial}{\partial t}, \qquad \frac{\partial}{\partial t_2} = \frac{1}{2}\frac{\partial}{\partial T} - \frac{\partial}{\partial t}, \tag{2.39}$$

$$\nabla_1 = \frac{1}{2}\nabla_{\boldsymbol{R}} + \nabla_{\boldsymbol{r}}, \qquad \nabla_2 = \frac{1}{2}\nabla_{\boldsymbol{R}} - \nabla_{\boldsymbol{r}}, \tag{2.40}$$

$$\nabla_1^2 = \frac{1}{4}\nabla_{\boldsymbol{R}}^2 + \nabla_{\boldsymbol{r}} \cdot \nabla_{\boldsymbol{R}} + \nabla_{\boldsymbol{r}}^2, \qquad \nabla_2^2 = \frac{1}{4}\nabla_{\boldsymbol{R}}^2 - \nabla_{\boldsymbol{r}} \cdot \nabla_{\boldsymbol{R}} + \nabla_{\boldsymbol{r}}^2, \tag{2.41}$$

where ∇_i operates on particle i.

2.7 Notation for Integrals Using Products

We will now define a useful product known as the *bullet product* that will simplify further calculations. This product is defined by

$$A(x_1, x_2) \bullet B(x_2, x_3) = \int \mathrm{d}^4 x_2 \, A(x_1, x_2) B(x_2, x_3), \tag{2.42}$$

where A and B are functions that depend on at least one common spacetime coordinate. If A or B is a function of only one or zero spacetime coordinates, $A \bullet B$ is interpreted as an ordinary matrix product AB with no integral present.

We can also express the bullet product using mixed coordinates, in addition to Fourier transforming the center of mass time T and position $\boldsymbol{R}$ into energy ε and momentum $\boldsymbol{p}$, respectively. The bullet product then becomes [36]

$$A \bullet B = \exp\left\{\frac{i}{2}(\partial_\varepsilon^A \partial_T^B - \partial_T^A \partial_\varepsilon^B)\right\} \exp\left\{\frac{i}{2}(\nabla_{\boldsymbol{R}}^A \nabla_{\boldsymbol{p}}^B - \nabla_{\boldsymbol{p}}^A \nabla_{\boldsymbol{R}}^B)\right\} \cdot A(\boldsymbol{R}, \boldsymbol{p}, \varepsilon, T) B(\boldsymbol{R}, \boldsymbol{p}, \varepsilon, T), \tag{2.43}$$

where the notation $\nabla_{\boldsymbol{R}}^A$, ∂_t^A means we differentiate with respect to $\boldsymbol{R}$ and t, only affecting the function A.

Next we introduce another convenient product known as a *ring product*. This product only consist of the energy/time differentials from the bullet product. We define it as:

$$A \circ B = \exp\left\{\frac{i}{2}(\partial_\varepsilon^A \partial_T^B - \partial_T^A \partial_\varepsilon^B)\right\} A(\boldsymbol{R}, \boldsymbol{p}, \varepsilon, T) B(\boldsymbol{R}, \boldsymbol{p}, \varepsilon, T). \tag{2.44}$$

We can then write the bullet product as:

$$A \bullet B = \exp\left\{\frac{i}{2}(\nabla_{\boldsymbol{R}}^A \nabla_{\boldsymbol{p}}^B - \nabla_{\boldsymbol{p}}^A \nabla_{\boldsymbol{R}}^B)\right\} A(\boldsymbol{R}, \boldsymbol{p}, \varepsilon, T) \circ B(\boldsymbol{R}, \boldsymbol{p}, \varepsilon, T). \tag{2.45}$$

In the stationary limit where $\partial_T = 0$, the ring product reduces to ordinary matrix multiplication. We have the following commutation relations for the bullet- and ring product:

$$[A, B]_\bullet \equiv A \bullet B - B \bullet A, \qquad [A, B]_\circ \equiv A \circ B - B \circ A, \tag{2.46}$$

$$\{A, B\}_\bullet \equiv A \bullet B + B \bullet A, \qquad \{A, B\}_\circ \equiv A \circ B + B \circ A \tag{2.47}$$

If the spatial variation of A and B is small, then the gradient expressions in equation (2.45) are also small. We can then linearize the exponential function in the expression:

$$A \bullet B \approx A \circ B + \frac{i}{2}\Big((\nabla_{\boldsymbol{R}} A) \circ (\nabla_{\boldsymbol{p}} B) - (\nabla_{\boldsymbol{p}} A) \circ (\nabla_{\boldsymbol{R}} B)\Big). \tag{2.48}$$

This is known as the gradient approximation. Using this, we can write the commutator for the bullet product as:

$$[A, B]_\bullet = [A, B]_\circ + \frac{i}{2}\Big(\big\{(\nabla_{\boldsymbol{R}} A) \circ (\nabla_{\boldsymbol{p}} B)\big\} - \big\{(\nabla_{\boldsymbol{p}} A) \circ (\nabla_{\boldsymbol{R}} B)\big\}\Big). \tag{2.49}$$

These approximations will be useful when we later look at the Quasiclassical approximation in section 4.

2.8 Structure

The goal of this thesis is to derive the Usadel equation for an antiferromagnet-superconductor system in curvilinear coordinates. We then want to look at the case of a 1D nanowire and helix, and solve them numerically in order to investigate the density of states and magnetization of the electrons in the curved antiferromagnet.

The beginning of the thesis will be used for studying the equation of motion for the Green's function of the system for both an SF system and an AF-S system. Section 3 gives an overview of the Green's function, and how we can write it in the mixed representation, while section 4 introduces the quasiclassical approximation which will be used to simplify the Green's functions of the system. Section 5 summarizes the derivation of the Usadel equation for a SF system, following the derivation of J.A. Ouassou [37]. The aim of this section is to make the following derivation of the Usadel equation for antiferromagnets easier, as the steps taken in the two derivations are similar but a bit easier to follow in the SF case. Section 6 gives a summary of the derivation of the Usadel equation for an AF-S system, following the work done by Fyhn et.al. [20].

Sections 7 and 8 will look at how curvature can result in effective SOC, which will be inserted in the Usadel equation to look at how it behaves for a curved system. In section 9 we will apply the Usadel equation for curved systems we found in the previous section to the case of a 1D nanowire arch curved in the form of a portion of a circle, and a 1D helix. Here, we will also derive the Pauli matrices in the curvilinear basis, both with and without torsion.

In section 10 we will use the Riccati parametrization on the curvilinear Usadel equation found in the previous section, which we will use in section 11 to look at the weak proximity equations for both the case with and without torsion. In sections 12 and 13 we will look at the numerical results for the density of states and magnetization of the electrons in the system, using the Riccati parametrized equations found in section 10. All numerical modeling and plots thereof are provided by Tancredi Salamone, who collaborated on this work in conjunction with his PhD degree [38]. Finally, in section 14 we will summarize the main results, as well as look at possible continuations of the work preformed in this thesis.

3 Green's Functions

In this section we will look at Green's functions, and how we can combine them into a 8×8 Green's function matrix in Keldysh space which can be used to describe the motion of electrons in a system.

In many particle physics, a Green's function $G_{\sigma_1\sigma_2}(\mathbf{r_1}, t_1, \mathbf{r_2}, t_2)$ tells us something about the probability amplitude of a particle with spin σ_1 at position $\mathbf{r_1}$ at time t_1 moving to position $\mathbf{r_2}$ at time t_2 with spin σ_2. There are several ways to define these Green's functions. One way to define a non-equilibrium Green's function is to use [39]:

$$G_{\sigma_1\sigma_2}(x_1, x_2) \equiv -i \langle n| T\psi_{\sigma_1}(x_1)\psi^\dagger_{\sigma_2}(x_2) |n\rangle , \tag{3.1}$$

where σ_j is the spin of particle j, x_j the spacetime coordinate, $\hat{\psi}_j$ the fermionic annihilation operator ($\psi^\dagger_j$ is then the creation operator), $|n\rangle$ the quantum state of the system, and T the *time ordering operator* defined as:

$$-iT\psi_\sigma(\mathbf{r}, t)\psi^\dagger_{\sigma'}(\mathbf{r}', t') \equiv \begin{cases} -i\psi_\sigma(\mathbf{r}, t)\psi^\dagger_{\sigma'}(\mathbf{r}', t'), & t' < t \\ i\psi^\dagger_{\sigma'}(\mathbf{r}', t')\psi_\sigma(\mathbf{r}, t), & t' > t \end{cases} . \tag{3.2}$$

The time ordering operator has the effect of ordering the product in chronological order, such that the operator with the largest time dependence is on the left. Here we will use the three Green's functions from the Keldysh definitions:

$$G^R_{\sigma_1\sigma_2}(x_1, x_2) \equiv -i\langle\{\psi_{\sigma_1}(x_1), \psi^\dagger_{\sigma_2}(x_2)\}\rangle\Theta(t_1 - t_2), \tag{3.3}$$

$$G^A_{\sigma_1\sigma_2}(x_1, x_2) \equiv +i\langle\{\psi_{\sigma_1}(x_1), \psi^\dagger_{\sigma_2}(x_2)\}\rangle\Theta(t_2 - t_1), \tag{3.4}$$

$$G^K_{\sigma_1\sigma_2}(x_1, x_2) \equiv -i\langle[\psi_{\sigma_1}(x_1), \psi^\dagger_{\sigma_2}(x_2)]\rangle. \tag{3.5}$$

By looking at the definitions, we see that the *retarded Green's function* G^R only exists for $t_1 > t_2$, which means that the creation $\psi^\dagger_{\sigma_2}(x_2)$ of the electron at x_2 happens *before* the annihilation $\psi_{\sigma_1}(x_1)$ of the electron at x_1. For the *advanced Green's function* G^A it is the opposite, so we have annihilation before creation. We can therefore interpret these Green's functions as G^R describing the flow of *electrons*, while G^A describes the flow of *holes*. The *Keldysh Green's function* G^K is special in that it is the only one of the Green's functions that contains information about the system in non-equilibrium [40]. Note that the retarded and advanced Green's function uses anticommutators, while the the Keldysh Green's function uses a commutator.

We will also use the *anomalous Green's function*, which describes correlations between particles at different points in spacetime:

$$F^R_{\sigma_1\sigma_2}(x_1, x_2) \equiv -i\langle\{\psi_{\sigma_1}(x_1), \psi_{\sigma_2}(x_2)\}\rangle\Theta(t_1 - t_2), \tag{3.6}$$

$$F^A_{\sigma_1\sigma_2}(x_1, x_2) \equiv +i\langle\{\psi_{\sigma_1}(x_1), \psi_{\sigma_2}(x_2)\}\rangle\Theta(t_2 - t_1), \tag{3.7}$$

$$F^K_{\sigma_1\sigma_2}(x_1, x_2) \equiv -i\langle[\psi_{\sigma_1}(x_1), \psi_{\sigma_2}(x_2)]\rangle. \tag{3.8}$$

In order to more easily keep track of the different spin-dependent Green's functions defined above, we combine them to form 2×2 matrices in spin space:

$$G^R \equiv \begin{pmatrix} G^R_{\uparrow\uparrow} & G^R_{\uparrow\downarrow} \\ G^R_{\downarrow\uparrow} & G^R_{\downarrow\downarrow} \end{pmatrix} . \tag{3.9}$$

The rest of the Green's functions and anomalous Green's functions are collected the same way. We can further combine the Green's function into 4×4 matrices in particle-hole *Nambu space*:

$$\hat{G}^R \equiv \begin{bmatrix} G^R & F^R \\ F^{R^*} & G^{R^*} \end{bmatrix}, \qquad \hat{G}^A \equiv \begin{bmatrix} G^A & F^A \\ F^{A^*} & G^{A^*} \end{bmatrix}, \qquad \hat{G}^K \equiv \begin{bmatrix} G^K & F^K \\ -F^{K^*} & -G^{K^*} \end{bmatrix}. \tag{3.10}$$

Note the minus signs in the last row of $\hat{G}^K$, which comes from the fact that the Keldysh Green's functions are defined in terms of commutators instead of anticommutators, as is the case for the rest of the Green's functions. Finally, we can combine all of the Green's functions into a 8×8 matrix in *Keldysh space*:

$$\check{G} \equiv \begin{bmatrix} \hat{G}^R & \hat{G}^K \\ 0 & \hat{G}^A \end{bmatrix}. \tag{3.11}$$

Most physical observables of interest in superconductor-ferromagnetic (SF) systems or superconductor-antiferromagnetic (S-AF) systems, such as the density of states and magnetization, can be described by this Green's function matrix.

In equilibrium, the three non-zero components of the Green's function matrix in Keldysh space are related to each other [41]

$$\hat{G}^A = -\tau_z(\hat{G}^R)\tau_z, \tag{3.12a}$$

$$\hat{G}^K = (\hat{G}^R - \hat{G}^A)\tanh(\frac{\beta\varepsilon}{2}), \tag{3.12b}$$

where $\beta = 1/T$ is the inverse temperature. We can therefore determine the complete 8×8 matrix by only considering only the retarded component.

3.1 Green's Function in the Mixed Representation

It will be convenient for us to represent the Greens functions in the mixed representation discussed in section 2.6. We will use this representation when we look at the equations of motion for the Green's function. By using the relations defined in equation (2.37) and (2.38), we can write the Green's function in the mixed representation as:

$$\check{G}(\mathbf{r}_1, t_1, \mathbf{r}_2, t_2) = \check{G}(\mathbf{R} - \mathbf{r}/2, T - t/2, \mathbf{R} + \mathbf{r}/2, T + t/2). \tag{3.13}$$

We will now simplify this notation by writing:

$$\check{G}(\mathbf{R} - \mathbf{r}/2, T - t/2, \mathbf{R} + \mathbf{r}/2, T + t/2) \equiv \check{G}'(\mathbf{R}, T, \mathbf{r}, t) \equiv \check{G}(\mathbf{R}, T, \mathbf{r}, t). \tag{3.14}$$

We will use the same notation $\check{G}$ for the Green's function in both the normal and mixed representation. These are not necessarily the same function, but we will write them the same to simplify the notation.

Next we will use a Fourier-transformation to transform from the relative coordinates $\mathbf{r}, t$ to $\mathbf{p}, \epsilon$, where $\mathbf{p}$ is the momentum of the particle, and ϵ is the energy of the particle. We then get:

$$\check{G}(\mathbf{R}, T, \mathbf{p}, \epsilon) = \int \mathrm{d}t\, e^{i\epsilon t} \int \mathrm{d}^3\mathbf{r}\, e^{-i\mathbf{p}\cdot\mathbf{r}} \check{G}(\mathbf{R}, T, \mathbf{r}, t). \tag{3.15}$$

The mixed representation will allow us to integrate out the rapidly oscillating part of the Green's functions, as we will see later in section 4.

4 Quasiclassical Approximation

In this section we will look at the quasiclassical approximation, which we will use to transform the full Green's functions of the system into functions that describe only the most relevant parts of the system.

The Green function behaves like a wavepacket with a part that varies rapidly in terms of the relative coordinate $\mathbf{r}$ on a length scale of the Fermi-wavelength λ_F, and an envelope part which varies in terms of the center of mass coordinate $\mathbf{R}$ on other characteristic length scales of the system. The envelope part contains useful information about how different parts of the system influence physical observables, and it is therefore desirable to only deal with this part. The superconducting coherence length of the Cooper pairs is much larger than the Fermi-wavelength, $\lambda_F \ll \xi_s$, so one can average over the quickly oscillating part, which averages out the relative coordinate [42]. This is known as the *gradient expansion*, and is equivalent to assuming that all length scales of the system must be much larger than λ_F. This is the starting point of the *quasiclassical approximation*. The key aspect of the quasiclassical approximation is that we only consider momenta of the order of the Fermi-momentum, and therefore confine all physical quantities to the Fermi-surface [42]. We may therefore think of constraining the quasiparticle momentum to the Fermi-surface by considering the Green function

$$\check{G}(\mathbf{R}, \mathbf{p}, \varepsilon, T) \to \delta(\epsilon_p)\check{g}(\mathbf{R}, \hat{\mathbf{p}}_F, \varepsilon, T), \tag{4.1}$$

where the delta-function is the part that constrains the momentum onto the Fermi-surface, $\hat{\mathbf{p}}_F$ is the direction of the momentum vector at the Fermi-surface and $\epsilon_p = \frac{\boldsymbol{p}^2}{2m} - \mu$ is the kinetic energy relative to the Fermi-level μ. Based on this, we define the quasiclassical Green function as [35]:

$$\check{g}(\mathbf{R}, \hat{\mathbf{p}}_F, \varepsilon, T) = \frac{i}{\pi} \int \mathrm{d}\epsilon_p \, \check{G}(\mathbf{R}, \mathbf{p}, \varepsilon, T). \tag{4.2}$$

Equation (4.2) does not determine $\check{g}$ uniquely. We also need the normalization condition [43]

$$\check{g} \circ \check{g} = 1. \tag{4.3}$$

In this thesis, we will work with systems in equilibrium. In that case, we see from equation (2.44) that the ring product reduces to an ordinary matrix multiplication

$$\check{g}^2 = 1. \tag{4.4}$$

This normalization condition will be sufficient for the systems in this thesis.

Similar to equation (3.11), the quasiclassical Green's function can be expressed in matrix form as

$$\check{g} = \begin{pmatrix} \hat{g}^A & \hat{g}^K \\ 0 & \hat{g}^R \end{pmatrix}, \tag{4.5}$$

where $\hat{g}^R$, $\hat{g}^A$, and $\hat{g}^K$ are the retarded, advanced and Keldysh quasiclassical Green's functions respectively in 4×4 Nambu space:

$$\hat{g}^R \equiv \begin{bmatrix} g^R & f^R \\ -f^{R^*} & -g^{R^*} \end{bmatrix}, \qquad \hat{G}^A \equiv \begin{bmatrix} g^A & f^A \\ -f^{A^*} & -g^{A^*} \end{bmatrix}, \qquad \hat{G}^K \equiv \begin{bmatrix} g^K & f^K \\ f^{K^*} & g^{K^*} \end{bmatrix}. \tag{4.6}$$

Looking more closely at e.g. the retarded component, we see that the elements are not entirely independent, but can be expressed as

$$\hat{g}^R = \begin{bmatrix} g^R(\mathbf{R}, +\varepsilon) & f^R(\mathbf{R}, +\varepsilon) \\ -f^{R^*}(\mathbf{R}, -\varepsilon) & -g^{R^*}(\mathbf{R}, -\varepsilon). \end{bmatrix} \tag{4.7}$$

The reason for the different sign of the energy in the last row can be seen when we Fourier-transform from regular to mixed coordinates. Taking the Fourier transformation of $G(\mathbf{R}, T, \mathbf{r}, t)$, from equation (3.15) gives

$$\int \mathrm{d}t\, \mathrm{d}^3\mathbf{r}\, e^{i(\epsilon t - \mathbf{p}\cdot\mathbf{r})} G(\mathbf{R}, T, \mathbf{r}, t) = G(\mathbf{R}, T, \mathbf{p}, \epsilon). \tag{4.8}$$

Meanwhile, taking the Fourier transformation of $G^*(\mathbf{R}, T, \mathbf{r}, t)$ gives

$$\begin{aligned} \int \mathrm{d}t\, \mathrm{d}^3\mathbf{r}\, e^{i(\epsilon t - \mathbf{p}\cdot\mathbf{r})} G(\mathbf{R}, T, \mathbf{r}, t)^* &= \left(\int \mathrm{d}t\, \mathrm{d}^3\mathbf{r}\, e^{-i(\epsilon t - \mathbf{p}\cdot\mathbf{r})} G(\mathbf{R}, T, \mathbf{r}, t) \right)^* \\ &= G^*(\mathbf{R}, T, -\mathbf{p}, -\epsilon). \end{aligned} \tag{4.9}$$

Applying equation (4.2) on the two Green's functions, and noting the extra factor i, we end up with the energy dependence given in equation (4.7). A similar derivation can be done for the anomalous part f. The matrix in equation (4.7) can be rewritten by introducing the *tilde conjugation*

$$g^{R*}(\mathbf{R}, -\varepsilon) \equiv \tilde{g}^R(\mathbf{R}, +\varepsilon). \tag{4.10}$$

The quasiclassical Green's function matrix can then be written as

$$\hat{g}^R = \begin{bmatrix} g^R(\mathbf{R}, +\varepsilon) & f^R(\mathbf{R}, +\varepsilon) \\ -\tilde{f}^R(\mathbf{R}, +\varepsilon) & -\tilde{g}^R(\mathbf{R}, +\varepsilon) \end{bmatrix}. \tag{4.11}$$

Furthermore, the normalization condition $\check{g}^2 = 1$ relates the g components to the f components,

$$gg - f\tilde{f} = 1, \qquad gf - f\tilde{g} = 0. \tag{4.12}$$

5 Usadel Equation

In this section we want to summarize the derivation of the Usadel equation for diffusive transport in a straight SF heterostructure. The Usadel equation is the equation of motion for the Green's functions of the system, and it describes how the charge carriers propagate through the materials. The reason for deriving the Usadel equation for a straight SF system is that it will hopefully make the derivation for antiferromagnetic materials easier to follow, as the steps taken in the two derivations are similar, but differs in complexity.

This section is a summary of the derivation in [44]. We want to find an equation of motion for the electron field described by the Green's function $G_{\sigma\sigma'}(x, x')$. To find this, we first need an expression for the Hamiltonian of the system, which we will use to find the time evolution of the electron field operator $\psi_\sigma(x)$ using the Heisenberg equation (2.4)

$$i\partial_t\psi_\sigma(x) = [\psi_\sigma(x), \mathcal{H}], \qquad i\partial_t\psi^\dagger_\sigma(x) = [\psi^\dagger_\sigma(x), \mathcal{H}]. \tag{5.1}$$

We want the Hamiltonian $\mathcal{H}$ describing our system to have properties describing impurities, superconductivity and ferromagnetism. We will therefore end up with a Hamiltonian of the form

$$\mathcal{H} = \mathcal{H}_0 + \mathcal{H}_\Delta + \mathcal{H}_\mathbf{h} + \mathcal{H}_{sf} + \mathcal{H}_{imp}, \tag{5.2}$$

where:

- $\mathcal{H}_0$ describes the non-interacting part of the system.
- $\mathcal{H}_\Delta$ describes superconductivity, which is zero inside the ferromagnet and non-zero in the superconductor.
- $\mathcal{H}_\mathbf{h}$ describes ferromagnetism, which is zero inside the superconductor, and non-zero inside the ferromagnet.
- $\mathcal{H}_{sf}$ describes spin-flip scattering on magnetic impurities.
- $\mathcal{H}_{imp}$ describes scattering on non-magnetic impurities.

For a derivation of each term, see [44]. This Hamiltonian is more general than the one we will need for our systems. We will not include magnetic impurities in the systems we will look at later for the antiferromagnet, but we include the spin-flip term in this derivation because, as we will see in section 6, this term will be similar to the term we get from the antiferromagnet. The time evolution of $\psi_\sigma(x)$ can now be found by inserting this Hamiltonian $\mathcal{H}$ into equation (5.1), and is given as

$$i\partial_t\psi_\sigma(x) = P(x)\psi_\sigma(x) + \sum_{\sigma'} Q_{\sigma\sigma'}(x)\psi_{\sigma'}(x) + \sum_{\sigma'} R_{\sigma\sigma'}(x)\psi^\dagger_{\sigma'}(x), \tag{5.3a}$$

$$-i\partial_t\psi^\dagger_\sigma(x) = \psi^\dagger_\sigma(x)P(x) + \sum_{\sigma'} \psi^\dagger_{\sigma'}(x)Q^\dagger_{\sigma'\sigma}(x) - \sum_{\sigma'} \psi_{\sigma'}(x)R_{\sigma'\sigma}(x), \tag{5.3b}$$

where we have defined the following operators:

$$P(x) \equiv e\varphi(x) - \mu + V_{imp}(x), \tag{5.4}$$

$$\mathbf{Q}(x) \equiv -\frac{1}{2m}\tilde{\nabla}^2 - \mathbf{h}(x)\cdot\boldsymbol{\sigma} + V_{sf}(\mathbf{r})\mathbf{s}(x)\cdot\boldsymbol{\sigma}, \tag{5.5}$$

$$\mathbf{R}(x) \equiv \Delta(x) i\sigma^2. \tag{5.6}$$

Here, $e < 0$ is the electron charge, $\varphi(x)$ is the scalar field, $\tilde{\nabla} = \nabla - ie\mathbf{A}(x)$ is the gauge covariant derivative with vector field $\mathbf{A}(x)$, μ the chemical potential, $V_{imp}(x)$ the background field representing the non-magnetic impurities, $\mathbf{h}(x)$ the magnetization, $\mathbf{s}(x)$ the impurity spin field, $V_{sf}(\mathbf{r})$ the scattering potential between magnetic impurities, and $\Delta(x)$ the superconducting band gap. Note that $\mathbf{Q}$ and $\mathbf{Q}^\dagger$ differs in that the former contains $\tilde{\nabla}^2 = (\nabla - i\mathcal{A})^2$, while the latter $\tilde{\nabla}^{2\dagger} = (\nabla + i\mathcal{A})^2$ since $\mathcal{A}$ is Hermitian. One should also interpret $\mathbf{Q}^\dagger$ as operating on $\psi^\dagger_{\sigma'}(x)$ from the right. Finally, note that $\mathbf{R}^\dagger = \mathbf{R}^{\mathrm{T}} = -\mathbf{R}$.

5.1 Time evolution of the Green's function

The time evolution of the Green's function is found by differentiating the definition of the Retarded Green's function in equation (3.3) with respect to t and t'

$$i\partial_t G^R_{\sigma\sigma'}(x,x') = -i\Big\langle\Big\{i\partial_t\psi_\sigma(x), \psi^\dagger_{\sigma'}(x')\Big\}\Big\rangle\Theta(t-t') + \delta_{\sigma\sigma'}\delta(x-x'), \tag{5.7}$$

$$i\partial'_t G^R_{\sigma\sigma'}(x,x') = -i\Big\langle\Big\{\psi_\sigma(x), i\partial_{t'}\psi^\dagger_{\sigma'}(x')\Big\}\Big\rangle\Theta(t-t') - \delta_{\sigma\sigma'}\delta(x-x'), \tag{5.8}$$

where $\Theta(t-t')$ is the unit step function. Inserting the equations in (5.3) into the above equation, we get:

$$i\partial_t G^R_{\sigma\sigma'} = PG^R_{\sigma\sigma'} + \sum_{\sigma''} Q_{\sigma\sigma''}G^R_{\sigma''\sigma'} - \sum_{\sigma''} R_{\sigma\sigma''}F^{R^*}_{\sigma''\sigma'} + \delta_{\sigma\sigma'}\delta(x-x'), \tag{5.9}$$

$$-i\partial_{t'} G^R_{\sigma\sigma'} = G^R_{\sigma\sigma'}P' + \sum_{\sigma''} G^R_{\sigma\sigma''}Q'^\dagger_{\sigma''\sigma'} - \sum_{\sigma''} F^R_{\sigma\sigma''}R'_{\sigma''\sigma'} + \delta_{\sigma\sigma'}\delta(x-x'), \tag{5.10}$$

where we used that $F_{\sigma\sigma'} = F_{\sigma'\sigma}$. We also suppressed the spacetime coordinates of the functions. All the Green's functions should be interpreted as depending on both primed and unprimed coordinates, while P, $\mathbf{Q}$, and $\mathbf{R}$ depend on unprimed coordinates, and P', $\mathbf{Q}'$, and $\mathbf{R}'$ depend on primed coordinates. We can now express equations (5.9) and (5.10) in matrix form in 4×4 Nambu space, by also deriving equations of motions for the retarded anomalous Green's function F^R and F^{R*} like we did for equations (5.9) and (5.10). We then end up with two equations in Nambu space

$$i\partial_t \begin{bmatrix} G^R & F^R \\ -F^{R^*} & -G^{R^*} \end{bmatrix} = \begin{bmatrix} P+\mathbf{Q} & -\mathbf{R} \\ -\mathbf{R} & P+\mathbf{Q}^* \end{bmatrix}\begin{bmatrix} G^R & F^R \\ F^{R^*} & G^{R^*} \end{bmatrix} + \delta(x-x'), \tag{5.11}$$

$$-i\partial_{t'} \begin{bmatrix} G^R & -F^R \\ F^{R^*} & -G^{R^*} \end{bmatrix} = \begin{bmatrix} G^R & F^R \\ F^{R^*} & G^{R^*} \end{bmatrix}\begin{bmatrix} P'+\mathbf{Q}'^\dagger & -\mathbf{R}' \\ -\mathbf{R}' & P'+\mathbf{Q}'^{\mathrm{T}} \end{bmatrix} + \delta(x-x'). \tag{5.12}$$

Comparing these to the definition of $\hat{G}^R$ in (3.10), we see that we can write these equations in terms of $\hat{G}^R$

$$i(\boldsymbol{\tau}^3 \otimes \sigma^0)(\partial_t \hat{G}^R) = \mathbf{H}\hat{G}^R + \delta(x - x'), \tag{5.13}$$

$$-i(\partial_{t'} \hat{G}^R)(\boldsymbol{\tau}^3 \otimes \sigma^0) = \hat{G}^R \overline{\mathbf{H}}' + \delta(x - x'), \tag{5.14}$$

where we define

$$\mathbf{H} \equiv \begin{bmatrix} P + \mathbf{Q} & -\mathbf{R} \\ -\mathbf{R} & P + \mathbf{Q}^* \end{bmatrix}, \qquad \overline{\mathbf{H}} \equiv \begin{bmatrix} P' + \mathbf{Q}'^\dagger & -\mathbf{R}' \\ -\mathbf{R}' & P' + \mathbf{Q}'^{\mathrm{T}} \end{bmatrix}. \tag{5.15}$$

The equations of motion for $\hat{G}^A$ and $\hat{G}^K$ are derived in a similar way, and are respectively given as

$$i(\boldsymbol{\tau}^3 \otimes \sigma^0)(\partial_t \hat{G}^A) = \mathbf{H}\hat{G}^A + \delta(x - x'), \tag{5.16}$$

$$-i(\partial_{t'} \hat{G}^A)(\boldsymbol{\tau}^3 \otimes \sigma^0) = \hat{G}^A \overline{\mathbf{H}}' + \delta(x - x'), \tag{5.17}$$

$$i(\boldsymbol{\tau}^3 \otimes \sigma^0)(\partial_t \hat{G}^K) = \mathbf{H}\hat{G}^K, \tag{5.18}$$

$$-i(\partial_{t'} \hat{G}^K)(\boldsymbol{\tau}^3 \otimes \sigma^0) = \hat{G}^K \overline{\mathbf{H}}'. \tag{5.19}$$

Note how we do not get a Dirac delta in the equation for G^K, as it has no step function in its definition (3.5). Finally, we use definition (3.11) to combine the equations for $\hat{G}^R$, $\hat{G}^A$ and $\hat{G}^K$ into two matrix equations in 8×8 Keldysh space that cover all of the Green's functions

$$i(\boldsymbol{\tau}^3 \otimes \sigma^0)(\partial_t \check{G}) = \mathbf{H}\check{G} + \delta(x - x'), \tag{5.20}$$

$$-i(\partial_{t'} \check{G})(\boldsymbol{\tau}^3 \otimes \sigma^0) = \check{G}\overline{\mathbf{H}}' + \delta(x - x'). \tag{5.21}$$

5.2 Quantum Transport equation

The next step in the derivation of the Usadel equation is to attempt to combine equations (5.20) and (5.21) into a single transport equation, described by the Hamiltonian in equation (5.2). Note that we now switch from using primed coordinates $(\mathbf{r}, t)$, $(\mathbf{r}', t')$ to numbered coordinates $(\mathbf{r}_1, t_1)$, $(\mathbf{r}_2, t_2)$ to avoid confusion when we introduce the mixed variables $(\mathbf{R}, T)$, $(\mathbf{r}, t)$. We start by subtracting equation (5.21) from (5.20):

$$i(\tau^3 \otimes \sigma^0)(\partial_{t_1} \check{G}) + i(\partial_{t_2} \check{G})(\tau^3 \otimes \sigma^0) = \mathbf{H}_1 \check{G}(x_1, x_2) - \check{G}(x_1, x_2)\bar{\mathbf{H}}_2. \tag{5.22}$$

If we now transform into relative coordinates (as discussed in section 2.6), consider the contribution from each term in (5.22) separately and introduce bullet-commutators and -anticommutators, we end up with the exact transport equation for the system [44]

$$\begin{aligned} &\frac{\mathbf{p}}{m}\Big(\nabla_{\mathbf{r}} \check{G} - i\Big[\hat{\mathcal{A}}, \check{G}\Big]_\bullet\Big) = \\ &i\big[\epsilon(\tau^3 \otimes \sigma^0) + \Delta(\tau^1 \otimes i\sigma^2) + \mathbf{h} \cdot \hat{\boldsymbol{\sigma}} - e\varphi - V_{imp} - V_{sf}\mathbf{s} \cdot \hat{\boldsymbol{\sigma}}, \check{G}\big]_\bullet \\ &+ \frac{1}{4m}\Big(\big\{\nabla_{\mathbf{r}} \cdot \hat{\mathcal{A}}, \check{G}\big\}_\bullet + \big\{\hat{\mathcal{A}}, \check{G}\big\}_\bullet\Big) - \frac{i}{2m}\big[\hat{\mathcal{A}}^2, \check{G}\big]_\bullet. \end{aligned} \tag{5.23}$$

Here we defined the matrices

$$\hat{\mathcal{A}} = \begin{pmatrix} \mathcal{A} & 0 \\ 0 & -\mathcal{A}^* \end{pmatrix}, \qquad \hat{\boldsymbol{\sigma}} = \begin{pmatrix} \boldsymbol{\sigma} & 0 \\ 0 & -\boldsymbol{\sigma}^* \end{pmatrix}, \tag{5.24}$$

related by the equation

$$\hat{\mathcal{A}} = (e\mathbf{A} + \mathbf{w}\hat{\boldsymbol{\sigma}})(\tau^3 \otimes \sigma^0), \tag{5.25}$$

where $\mathbf{w}(\mathbf{r}, t)$ is a matrix that describes the linearized interaction between the spin and momentum, and we inserted the expressions for P, $\mathbf{Q}$ and $\mathbf{R}$ in equations (5.4) - (5.6). One should note that no approximations were used in the calculation of this transport equation, which means that inaccuracies are due to assumptions and approximations related to the Hamiltonian itself.

5.3 Quasiclassical transport equation

Even though the transport equation (5.23) is exact, it can be difficult to work with in practical situations. This is in part due to the infinite series of differentiations with respect to position, time, energy and momentum found in the bullet products. Therefore, we now want to apply different approximations to find transport equations which are easier to work with. To start off, we want to apply the quasiclassical approximation, discussed in section 4, where we replace the Green's function $\check{G}(\mathbf{R}, T, \mathbf{p}, \varepsilon) \to \check{g}(\mathbf{R}, T, \hat{\mathbf{p}}_F, \varepsilon)$, where $\check{g}$ is the quasiclassical Green's function. This works because in most systems of interest, the characteristic length L of the system is much bigger than the Fermi-wavelength λ_F. We can therefore expand the transport equation in terms of the parameter $\eta \equiv \lambda_F/L$, and only keep leading orders of η. It then turns out that we can discard the second line of the exact transport equation (5.23), as it is of order η^2 while the rest is of order η.

Next, we would like to reduce the bullet products to simpler ring products. Since $\nabla_{\mathbf{R}} \sim 1/L$ and $\nabla_{\mathbf{p}} \sim \lambda_F$ we see that the gradient expansion (2.49) of the bullet product is equivalent to an expansion in η. This means that to leading order in η, we can discard everything except the zeroth order term of the expansion. This allows us to replace the bullet products with ring products.

We will also assume that the background field $\mathcal{A}$ is independent of center-off-mass time T. This implies that the left-hand side of equation (5.23) further reduces to a normal commutator, and can then be written as a covariant derivative of the Green's function, where the covariant derivative in this context is defined as

$$\tilde{\nabla}\check{G} \equiv \nabla_{\mathbf{R}}\check{G} - i\Big[\hat{\mathcal{A}}, \check{G}\Big]. \tag{5.26}$$

Performing the approximations discussed above, along with replacing $\mathbf{p}/m$ with the Fermi velocity $\mathbf{v}_F$ and replacing $\check{G}(\mathbf{R}, T, \mathbf{p}, \varepsilon)$ with the quasiclassical Green's function $\check{g}(\mathbf{R}, \hat{\mathbf{p}}, \varepsilon, T)$, we obtain the quasiclassical transport equation for the system

$$\mathbf{v}_F \cdot \tilde{\nabla}\check{g} = i\big[\epsilon(\tau^3 \otimes \sigma^0) + \Delta(\tau^1 \otimes i\sigma^2) + \mathbf{h} \cdot \hat{\boldsymbol{\sigma}} - e\varphi - V_{imp} - V_{sf}\mathbf{s} \cdot \hat{\boldsymbol{\sigma}}, \check{g}\big]_\circ. \tag{5.27}$$

This is also known as the *Eilenberger equation*. This result is a lot simpler to work with than the transport equation (5.23) as we have discarded multiple terms, in addition to not having an infinite series of differentiations in the bullet commutator. Moreover, since the quasiclassical Green's function is dependent on the direction of $\mathbf{p}$, and not it's magnitude, there is one less degree of freedom to worry about.

5.4 Diffusive Limit

The final step in the derivation of the Usadel equation is to consider *dirty materials*, i.e. materials with a high concentration of non-magnetic impurities and thus a short mean free path. This means that V_{imp} will be the dominant term in the Eilenberger equation. Our goal in this section will be to first expand the Green's function in terms of its isotropic and anisotropic part. We will then find that we can write the anisotropic part in terms of the isotropic part, and we can thus focus on the equation that gives us a solution for only the isotropic part. This equation will be the Usadel equation.

As mentioned, V_{imp} will be the dominant term in the Eilenberger equation. In such systems, there will be a high frequency of random scattering events due to the increased concentration of impurities. This will make it equally probable for electrons to be scattered in any direction, and since the Green's function tells us something about the probability amplitude of a particle moving from one place to another, we can expect that the Green's function should be nearly isotropic. This suggests that we can approximate the Green's function by a first-order expansion in terms of its isotropic and anisotropic part:

$$\check{g}(\mathbf{R}, T, \hat{\mathbf{p}}_F, \epsilon) \approx \check{g}_s(\mathbf{R}, T, \epsilon) + \hat{\mathbf{p}}_F \cdot \check{g}_p(\mathbf{R}, T, \epsilon). \tag{5.28}$$

The s-wave component $\check{g}_s$ is the isotropic part of the Green's function, while $\check{g}_p$ is the p-wave component that describes the linearized anisotropy with respect to the transport direction given by $\hat{\mathbf{p}}_F$. We may also rewrite the impurity and spin-flip potentials for dirty materials as

$$V_{imp} \approx -\frac{i}{2\tau_0}\langle\check{g}\rangle, \qquad V_{sf}\mathbf{s}\cdot\boldsymbol{\sigma} \approx -\frac{i}{2\tau_s}(\tau^3\otimes\sigma^0)\langle\check{g}\rangle(\tau^3\otimes\sigma^0). \tag{5.29}$$

Here, τ_0 is the momentum relaxation time, τ_s is the spin relaxation time, and the angle brackets $\langle\check{g}\rangle$ denotes an average of angles over the Fermi surface, which we can write as $\langle\check{g}\rangle \equiv \int \mathrm{d}\Omega_{\hat{\mathbf{p}}}\,\check{g}/4\pi$ where $\mathrm{d}\Omega \equiv \sin\theta\,\mathrm{d}\theta\,\mathrm{d}\phi$. Expanding $\langle\check{g}\rangle$ in terms of the expansion given in equation (5.28) gives

$$\langle\check{g}\rangle \approx \langle\check{g}_s\rangle + \langle\hat{\mathbf{p}}_F\cdot\check{g}_p\rangle = \langle\check{g}_s\rangle \tag{5.30}$$

since $\hat{\mathbf{p}}_F$ has unit length for all angles. If we insert equation (5.30) into equation (5.29), we get that the impurity potentials can be written as:

$$V_{imp} \approx -\frac{i}{2\tau_0}\check{g}_s, \qquad V_{sf}\mathbf{s}\cdot\boldsymbol{\sigma} \approx -\frac{i}{2\tau_s}(\tau^3\otimes\sigma^0)\check{g}_s(\tau^3\otimes\sigma^0). \tag{5.31}$$

Inserting equations (5.28) and (5.31) into the Eilenberger equation (5.27), rewriting the Fermi velocity as $v_F\hat{\mathbf{p}}_F$ and averaging it over the Fermi surface, we get

$$\frac{1}{3}v_F\tilde{\nabla}\cdot\check{g}_p = i\big[\epsilon(\tau^3\otimes\sigma^0)+\Delta(\tau^1\otimes i\sigma^2)+\mathbf{h}\cdot\hat{\boldsymbol{\sigma}}-e\varphi+\frac{i}{2\tau_s}(\tau^3\otimes\sigma^0)\check{g}_s(\tau^3\otimes\sigma^0),\check{g}_s\big]_\circ. \quad (5.32)$$

Next we want to find a relation between the anisotropic part $\check{g}_p$ and the isotropic part $\check{g}_s$. This is done by looking at the equation we get when we multiply the Eilenberger equation (5.27) with $\hat{\mathbf{p}}_F$ before averaging over the Fermi surface, but after inserting equations (5.28) and (5.31). This equation, along with the normalization condition $\check{g}\circ\check{g}=1$ of the quasiclassical function, gives the relation

$$\check{g}_p = -\tau_0 v_F\check{g}_s\circ\tilde{\nabla}\check{g}_s. \quad (5.33)$$

From this equation we see that we can find a solution for the anisotropic $\check{g}_p$ if we manage to solve the transport equation for the isotropic component $\check{g}_s$. We can therefore insert the above relation into equation (5.32) to get a diffusion equation for the isotropic Green's function $\check{g}_s$:

$$\begin{aligned} iD\tilde{\nabla}\cdot(\check{g}_s\circ\tilde{\nabla}\check{g}_s) = \\ \big[\epsilon(\tau^3\otimes\sigma^0)+\Delta(\tau^1\otimes i\sigma^2)+\mathbf{h}\cdot\hat{\boldsymbol{\sigma}}-e\varphi+\frac{i}{2\tau_s}(\tau^3\otimes\sigma^0)\check{g}_s(\tau^3\otimes\sigma^0),\check{g}_s\big]_\circ, \end{aligned} \quad (5.34)$$

where $D\equiv\frac{1}{3}\tau_0 v_F^2$. This equation is known as the *Usadel equation*, and is the transport equation of the quasiclassical Green's functions of the system. Note how we have reduced an equation for $\check{g}(\mathbf{R},T,\hat{\mathbf{p}}_F,\epsilon)$ into an equation for only the isotropic part $\check{g}_s(\mathbf{R},T,\epsilon)$.

5.5 Equilibrium

The final limit we will look at is when the system is in equilibrium. In this limit, the Green's functions becomes a time independent quantity $\check{g}_s(\mathbf{R},\varepsilon)$, and the ring commutator in the Usadel equation (5.34) reduce to a ordinary commutator. Also, $e\varphi$ is just a scalar in this limit, so it drops out of the equation. Finally one can also show, by considering their definitions, that the retarded, advanced and Keldysh component are, in equilibrium, related by

$$\check{g}^A = -(\tau^3\otimes\sigma^0)\check{g}^{R\dagger}(\tau^3\otimes\sigma^0), \qquad \check{g}^K = (\check{g}^R-\check{g}^A)\tanh(\varepsilon/2T), \quad (5.35)$$

where T is the temperature of the system. This means that it is sufficient to only solve e.g. the 4×4 retarded component in equilibrium. The Usadel equation is now

$$\begin{aligned} iD\tilde{\nabla}\cdot(\hat{g}_s^R\circ\tilde{\nabla}\hat{g}_s^R) = \\ \big[\epsilon(\tau^3\otimes\sigma^0)+\Delta(\tau^1\otimes i\sigma^2)+\mathbf{h}\cdot\hat{\boldsymbol{\sigma}}+\frac{i}{2\tau_s}(\tau^3\otimes\sigma^0)\hat{g}_s^R(\tau^3\otimes\sigma^0),\hat{g}_s^R\big]. \end{aligned} \quad (5.36)$$

If we want to compare this Usadel equation with the one we get when we solve for antiferromagnetic materials, we should restrict our attention to a 1D SF bilayer.

In this case, we assume that the dynamics are effectively one-dimensional and ignore spin-flip scattering processes. In this case, the Usadel equation is given as

$$iD\tilde{\nabla}\cdot(\hat{g}_s^R\circ\tilde{\nabla}\hat{g}_s^R)=\left[\epsilon(\tau^3\otimes\sigma^0)+\Delta(\tau^1\otimes i\sigma^2)+\mathbf{h}\cdot\hat{\boldsymbol{\sigma}},\hat{g}_s^R\right]. \tag{5.37}$$

These are the same conditions we use for the antiferromagnet, except we have an antiferromagnet instead of a ferromagnet. However, we will see that the term we get from the antiferromagnetic part of the Usadel equation looks similar to the term we got from the spin-flip magnetic impurities.

In order to get a unique solution for the Usadel equation, we need to include a set of boundary conditions that describe the interactions between the interfaces of the materials. One set of boundary conditions we can use are the Kuprianov-Lukichev boundary conditions, valid in the dirty limit and for weak transmission regime [45]

$$\hat{g}_{s,j}^R\tilde{\nabla}\hat{g}_{s,j}^R=\frac{1}{2L_j\zeta_j}\left[\hat{g}_{s,1}^R,\hat{g}_{s,2}^R\right] \tag{5.38}$$

where the label j denotes the material j, L_j is the length of material j, and $\zeta_j=\frac{R_B}{R_j}$ is the ratio between the barrier resistance R_B and the bulk resistance in material j, R_j

6 Usadel Equation for Antiferromagnetic metals

Antiferromagnets are materials where the magnetic moment of the atoms align in a regular pattern, pointing in opposite directions. This creates a pattern of alternating up and down spins, in contrast to the ferromagnet discussed in section 5, where the spins point in the same direction. In this section, we will summarize the main steps of the derivation of the Usadel equation for an antiferromagnetic metal, following Fyhn et.al [20]. In later sections, we will also transform the Usadel equation for antiferromagnets into a curved system, and look at the weak proximity effect for such a system.

Consider a bilayer consisting of two materials labeled L (left) and R (right), connected through a tunneling contact. The Hamiltonian is given by

$$\mathcal{H}(t) = \mathcal{H}_L(t) + \mathcal{H}_R(t) + \mathcal{H}_T. \tag{6.1}$$

We also have

$$\mathcal{H}_\alpha = \sum_{n,m\in A_\alpha} c_n^{\alpha\dagger}[H_0^\alpha(t) + V^\alpha(t)]_{nm} c_m^\alpha, \tag{6.2}$$

where $\alpha \in \{L, R\}$ denotes the material and A_α is the set of unit cells in material α. The hopping parameter, t^α, chemical potential, μ^α, and the exchange energy J^α between localized spins and conducting electrons are all collected in H_0^α. V^α contains all additional effects that may be present in the model, such as superconductivity, external spin-splitting fields, spacial geometry, etc.

Since V^α determines and confines the spatial geometry, we can simplify the sum in equation (6.2) by letting the lattice A_α run to infinity in all directions, such that $A_\alpha = \mathbb{Z}^3$, where $\mathbb{Z}$ is the set of integers. We can do this since the potential V^α makes the extra points outside of A_α included in $\mathbb{Z}^3$ zero. This makes the sum in equation (6.2) easier to work with.

In this derivation, we will use a square lattice, where each unit cell is labeled by the 3-tuple n, and contains one orbital associated with the A-sublattice at position $\mathbf{x}_n^\alpha$ and one orbital associated with the B-sublattice at position $\mathbf{x}_n^\alpha + \boldsymbol{\delta}^\alpha$, as is seen in figure 2. $\boldsymbol{\delta}^\alpha$ is therefore the nearest neighbor displacement vector in material α. For example, the unit cell $(1, 1, 1)$ means we are looking at the unit cell where the A-sublattice is located at $\mathbf{x}_{(1,1,1)}^\alpha$ and the B-sublattice at $\mathbf{x}_{(1,1,1)}^\alpha + \boldsymbol{\delta}^\alpha$. The antiferromagnet will have alternating spins on the different sublattices, e.g. spin up on A and spin down on B.

The annihilation operators at the A- and B-sublattice are denoted as $c_{nA\sigma}^\alpha$ and $c_{nB\sigma}^\alpha$, respectively, where σ denotes the spin at unit cell n in material α. We then define

$$c_n^{\alpha\dagger} = (c_{nA\uparrow}^{\alpha\dagger} \quad c_{nA\downarrow}^{\alpha\dagger} \quad c_{nB\uparrow}^{\alpha\dagger} \quad c_{nB\downarrow}^{\alpha\dagger} \quad c_{nA\downarrow}^{\alpha} \quad -c_{nA\uparrow}^{\alpha} \quad c_{nB\downarrow}^{\alpha} \quad -c_{nB\uparrow}^{\alpha}) \tag{6.3}$$

as a 1×8 matrix vector. Furthermore, we only include nearest neighbor hopping, and assume this hopping is only between two different sublattices. Finally, the spin space is rotated such that the Néel vector is always parallel to the z-axis.

Because the lattice used in this section contains two sublattices, and each sublattice can have either spin up or down, the dimension of the Green's functions will be different than the ones discussed in section 3. The retarded, advanced and Keldysh Green's functions are defined as

$$\hat{G}^{R,\alpha\beta}_{nm}(t_1,t_2) = -i\tau_z\langle\{c^{\alpha}_n(t_1), c^{\beta\dagger}_m(t_2)\}\rangle\Theta(t_1-t_2), \tag{6.4a}$$
$$\hat{G}^{A,\alpha\beta}_{nm}(t_1,t_2) = +i\tau_z\langle\{c^{\alpha}_n(t_1), c^{\beta\dagger}_m(t_2)\}\rangle\Theta(t_2-t_1), \tag{6.4b}$$
$$\hat{G}^{K,\alpha\beta}_{nm}(t_1,t_2) = -i\tau_z\langle[c^{\alpha}_n(t_1), c^{\beta\dagger}_m(t_2)]\rangle. \tag{6.4c}$$

Since these definitions contain the different spin values possible for the lattice point, they are similar to the 4×4 Green's function in Nambu space for SF systems discussed in section 3. They have different dimensions however, since the dimension of the operator (6.3) makes them 8×8. The 8×8 matrices can be collected in larger 16×16 matrices,

$$\check{G}^{\alpha\beta}_{nm} = \begin{pmatrix} \hat{G}^{R,\alpha\beta}_{nm} & \hat{G}^{K,\alpha\beta}_{nm} \\ 0 & \hat{G}^{A,\alpha\beta}_{nm} \end{pmatrix}, \tag{6.5}$$

and even larger 32×32 matrices,

$$\breve{G}_{nm} = \begin{pmatrix} \check{G}^{LL}_{nm} & \check{G}^{LR}_{nm} \\ \check{G}^{RL}_{nm} & \check{G}^{RR}_{nm} \end{pmatrix}. \tag{6.6}$$

In this section we use the notation that $\hat{\cdot}$ indicates a 8×8 matrix in Nambu space, $\check{\cdot}$ indicates a 16×16 matrix in Keldysh space and $\breve{\cdot}$ indicates a 32×32 matrix in material space.

Using that any operator P evolves in time according to equation (2.4)

$$i\frac{\mathrm{d}}{\mathrm{d}t}P(t) = [P(t), H], \tag{6.7}$$

and using this equation on the creation $c^{\alpha\dagger}_n$ and annihilation operator c^{α}_n, we get the Gor'kov equations [20, 46]

$$i\tau_z\frac{\partial\breve{G}}{\partial t} - \breve{\Sigma}\bullet\breve{G} = \delta(t_1-t_2)\delta_{nm}, \tag{6.8a}$$
$$\frac{\partial\breve{G}}{\partial t'}i\tau_z + \breve{G}\bullet\breve{\Sigma} = -\delta(t_1-t_2)\delta_{nm}, \tag{6.8b}$$

where

$$\breve{\Sigma} = \begin{pmatrix} \hat{H}^L_0 + \check{V}^L & \hat{T}^{LR} \\ \hat{T}^{RL} & \hat{H}^R_0 + \check{V}^R \end{pmatrix} = \begin{pmatrix} \Sigma^{LL} & \Sigma^{LR} \\ \Sigma^{RL} & \Sigma^{RR} \end{pmatrix} \tag{6.9}$$

is the self energy. The Gor'kov equations are then used to derive the Dyson equations for the system, given as [20, 47]

$$\breve{G} = \breve{G}_0 + \breve{G}_0\bullet\delta\Sigma\bullet\breve{G}, \tag{6.10a}$$
$$\breve{G} = \breve{G}_0 + \breve{G}\bullet\delta\Sigma\bullet\breve{G}_0, \tag{6.10b}$$

where $\breve{\Sigma}_0 = \breve{\Sigma} - \delta\breve{\Sigma}$ and $\breve{G}_0$ inserted into (6.8) solves the the Gor'kov equations with $\breve{\Sigma}\to\breve{\Sigma}_0$. $\breve{G}_0$ is then the Green's function in the absence of impurities. The Gor'kov equations are the equations of motion for the system, and gives the starting point for further derivations.

6.1 Imputity Averaging

The next step in deriving the Usadel equation for antiferromagnetic metals is to average over impurities, and identify the self-energy which relates the impurity-averaged Green's function to the Green's function with no impurities. The impurity averaged Green's function can be found by replacing the impurity potential in the Gor'kov equations with this self energy. We assume that there are $m^{\alpha X}$ number of impurities in material α on sublattice $X \in \{A, B\}$. We also assume that the impurity potentials are local to the position of the impurities, and that the potential strength and position of the i'th impurity in material α on sublattice X are $U_i^{\alpha X}$ and $r_i^{\alpha X}$, respectively. The impurity average is then defined as the sum over all possible impurity locations and impurity potential strengths, weighted by some normalized distribution function $p_{imp}(\{U_i\}, \{r_i\})$ that makes the impurities independent and uniformly distributed:

$$\langle A \rangle_{imp} = \prod_{\alpha \in \{L,R\}} \prod_{X \in \{A,B\}} \prod_{i=1}^{m^{\alpha X}} \int_{-\infty}^{\infty} \mathrm{d}U_i^{\alpha X} \sum_{r_i^{\alpha X} \in \mathbb{Z}^3} p_{imp}(\{U_i\}, \{r_i\}) A(\{U_i\}, \{r_i\}). \quad (6.11)$$

Finally, the strength and locations of impurities are assumed to be uncorrelated. The impurity averaged Green's function, $\breve{G}_{imp} \equiv \langle \breve{G} \rangle_{imp}$ can then be written as

$$\breve{G}_{imp} = \breve{G}_0 + \breve{G}_0 \bullet \breve{\Sigma}_{imp} \bullet \breve{G}_{imp}. \quad (6.12)$$

To find the expression for the impurity self energy $\breve{\Sigma}_{imp}$ the impurity average of the Dyson equations in (6.10) is taken, yielding an expression for the impurity self energy $\breve{\Sigma}_{imp}$ as a function of $\breve{G}_{imp}$, which to second order is given as

$$\begin{aligned} &\big[\breve{\Sigma}_{imp}(t_1, t_2)\big]_{nm}^{\alpha\beta} = \\ &\delta_{\alpha\beta}\delta_{nm} \sum_{X \in \{A,B\}} n_{imp}^{\alpha X} \big(\rho_X \langle U^{X\alpha} \rangle_{imp} + \langle U^{X\alpha} U^{X\alpha} \rangle_{imp} \rho_X (\check{G}_{imp}^{\alpha\alpha})_{nn}(t_1, t_2) \rho_X \big), \end{aligned} \quad (6.13)$$

where $n_{imp}^{\alpha X} \equiv m^{\alpha X}/N^{\alpha}$ is the impurity density on sublattice X in material α, and

$$\rho_A = \frac{1 + \rho_z}{2} \qquad \text{and} \qquad \rho_B = \frac{1 - \rho_z}{2} \quad (6.14)$$

are the projection operators in sublattice space A and B respectively. From now on we drop the subscript on the impurity averaged Green's function, $\breve{G}_{imp} \to \breve{G}$.

Next want to express the self energy $\breve{\Sigma}$ in a block diagonal form. To achieve this, closed equations for $\check{G}^{LL}$ and $\check{G}^{RR}$ are needed by first removing $\check{G}^{LR}$ and $\check{G}^{RL}$ from $\breve{\Sigma}$. This is done by treating the tunneling self-energy as a perturbation in the Dyson equation (6.10). Let

$$\breve{T} = \begin{pmatrix} 0 & \hat{T}^{LR} \\ \hat{T}^{RL} & 0 \end{pmatrix}, \quad (6.15)$$

and let $\breve{G}_0$ be the Green's function with $\hat{T}^{LR} = \hat{T}^{RL} = 0$, i.e. it solves the Gor'kov equations

$$i\tau_z \frac{\partial \breve{G}_0}{\partial t} - \breve{\Sigma}_0 \bullet \breve{G}_0 = \delta(t_1 - t_2)\delta_{nm}, \tag{6.16a}$$

$$\frac{\partial \breve{G}_0}{\partial t'} i\tau_z + \breve{G}_0 \bullet \breve{\Sigma}_0 = -\delta(t_1 - t_2)\delta_{nm}, \tag{6.16b}$$

with $\breve{\Sigma}_0 = \breve{\Sigma} - \breve{T} = \mathrm{diag}(\check{\Sigma}^{LL}, \check{\Sigma}^{RR})$ as we can see from definition (6.9), where now $\delta\breve{\Sigma} = \breve{T}$. Note that $\delta\breve{\Sigma}$ includes the impurity self energy term obtained when we took the impurity average above. The Dyson equations (6.10) are now given as

$$\breve{G} = \breve{G}_0 + \breve{G}_0 \bullet \breve{T} \bullet \breve{G}, \tag{6.17a}$$

$$\breve{G} = \breve{G}_0 + \breve{G} \bullet \breve{T} \bullet \breve{G}_0. \tag{6.17b}$$

Studying the different blocks of the two equations above, and inserting the results for the $\check{G}^{LR}$ and $\check{G}^{RL}$ blocks into the Gor'kov equations (6.8), the blocks $\check{G}^{LR}$ and $\check{G}^{RL}$ can be removed from the Gor'kov equations, which gives a block-diagonal self energy,

$$\breve{\Sigma} = \breve{H}_0 + \breve{V} + \breve{\Sigma}_{imp} + \breve{\Sigma}_T, \tag{6.18}$$

where

$$\breve{H}_0 = \begin{pmatrix} \hat{H}_0^L & \\ & \hat{H}_0^R \end{pmatrix}, \tag{6.19a}$$

$$\breve{V} = \begin{pmatrix} \check{V}^L & \\ & \check{V}^R \end{pmatrix}, \tag{6.19b}$$

$$\breve{\Sigma}_T = \begin{pmatrix} \hat{T}^{LR} \bullet \check{G}_0^{RR} \bullet \hat{T}^{RL} & \\ & \hat{T}^{RL} \bullet \check{G}_0^{LL} \bullet \hat{T}^{LR} \end{pmatrix}. \tag{6.19c}$$

Functions in the quasiclassical framework vary slowly with the center-of-mass (COM) coordinates, and quickly with the relative coordinate. As discussed in section 4, the COM part contains useful information about how different parts of the system influence physical observables. It would therefore be useful to Fourier transform in the relative coordinates, in order to obtain functions in terms of momentum $\mathbf{k}$, energy ε, COM time T and COM position $\mathbf{x}$, also known as Wigner coordinates. The Fourier transform of function A in relative time t is

$$\mathcal{F}_t(A)(T, \varepsilon) = \int_{-\infty}^{\infty} \mathrm{d}t\, A(T + t/2, T - t/2) e^{i\varepsilon t}, \tag{6.20}$$

and the Fourier transform in relative position r is given as

$$\mathcal{F}_r(A)(\mathbf{k}, \mathbf{x}_n \alpha) = \sum_{m \in \mathbb{Z}^3} e^{-i\rho_B \mathbf{k}\cdot\delta^\alpha} A_{(n+m)n} e^{i\rho_B \mathbf{k}\cdot\delta^\alpha} e^{-i\mathbf{k}\cdot\mathbf{x}_m^\alpha}. \tag{6.21}$$

The Gor'kov equations in the Wigner coordinates are given as

$$\tau_z \varepsilon \circ \breve{G} - \breve{\Sigma} \bullet \breve{G} = 1, \tag{6.22a}$$

$$\breve{G} \circ \tau_z \varepsilon - \breve{G} \bullet \breve{\Sigma} = 1. \tag{6.22b}$$

Note that the circle product using Wigner coordinates is the same as in the continuous models for normal metals discussed in section 2.6. Meanwhile, the spatial part of the bullet product is different. The bullet product can however still be expanded as a series of differentiable operators, and the zeroth order term is the same in both cases. We will end up only keeping the zeroth order terms, except for when calculating the kinetic energy term, the tunneling term, and the potential which is large outside the material. These terms must be evaluated explicitly.

6.2 Extracting the Conduction Band

As discussed in section 4, one of the main ideas behind the quasiclassical theory is that the majority of the interesting physics happens close to the Fermi surface. It would therefore be beneficial to isolate the contribution from states close to the Fermi surface. In this case, there will be two energy bands per material α which are not overlapping, so only one of these can pass through the Fermi surface. To separate the two bands, $\hat{H}_0$ must first be diagonalize by writing it in the band-basis:

$$\hat{H}_0^\alpha = S^\alpha D^\alpha (S^\alpha)^T, \tag{6.23}$$

where

$$D^\alpha = \mathrm{diag}(\xi_-^\alpha, \xi_-^\alpha, \xi_-^\alpha, \xi_-^\alpha, \xi_+^\alpha, \xi_+^\alpha, \xi_+^\alpha, \xi_+^\alpha) \tag{6.24}$$

contains the different energies, and S^T denotes the transpose of

$$S^\alpha = \frac{1}{\sqrt{2\eta^\alpha}} \left[\begin{pmatrix} -\sigma_0 & 0 & \sigma_0 & 0 \\ \sigma_0 & 0 & \sigma_0 & 0 \\ 0 & -\sigma_0 & 0 & \sigma_0 \\ 0 & \sigma_0 & 0 & \sigma_0 \end{pmatrix} \bar{s}^\alpha - \begin{pmatrix} \sigma_z & 0 & \sigma_z & 0 \\ \sigma_z & 0 & -\sigma_z & 0 \\ 0 & -\sigma_z & 0 & -\sigma_z \\ 0 & -\sigma_z & 0 & \sigma_z \end{pmatrix} \Delta s^\alpha \right], \tag{6.25}$$

where σ_0 is the 2×2 identity matrix, $\eta^\alpha = \sqrt{(J^\alpha)^2 + (K^\alpha)^2}$, K^α is the kinetic term, $\xi_\pm^\alpha = -\mu^\alpha \pm \eta^\alpha$, $\bar{s}^\alpha = (s_+^\alpha + s_-^\alpha)/2$ and $\Delta s^\alpha = (s_+^\alpha - s_-^\alpha)/2$, with $s_\pm^\alpha = \sqrt{\eta^\alpha \pm J^\alpha}$. Next define

$$(S^\alpha)^T \check{G}^{\alpha\alpha} S^\alpha = \begin{pmatrix} \check{G}_{--}^{\alpha\alpha} & \check{G}_{-+}^{\alpha\alpha} \\ \check{G}_{+-}^{\alpha\alpha} & \check{G}_{++}^{\alpha\alpha} \end{pmatrix}. \tag{6.26}$$

We now want an equation for the Green's function associated with the energy band which crosses the Fermi surface. This can be either $\check{G}_{--}^{\alpha\alpha}$ or $\check{G}_{++}^{\alpha\alpha}$. Here $\check{G}_{--}^{\alpha\alpha}$ is chosen. By extracting only one of the bands, we have reduced the dimensional of the problem by half. This means that when we write $\hat{}$ from now on, we mean the regular 4×4 dimensions used for e.g. the SF case and so on. The Gor'kov equations can then be written as

$$\tau_z \varepsilon \circ \check{G}_{--}^{\alpha\alpha} - \xi_-^\alpha \check{G}_{--}^{\alpha\alpha} - \left[(\check{\Sigma}^\alpha - \hat{H}_0^\alpha) \bullet \check{G}^{\alpha\alpha} \right]_{--} = 1, \tag{6.27a}$$

$$\check{G}_{--}^{\alpha\alpha} \circ \tau_z \varepsilon - \xi_-^\alpha \check{G}_{--}^{\alpha\alpha} - i \nabla_k \xi_-^\alpha \cdot \Delta_R \check{G}_{--}^{\alpha\alpha} - \frac{i J^\alpha \nabla_k \eta^\alpha}{K^\alpha} \cdot \Delta_R \check{G}_{-+}^{\alpha\alpha} \tau_z \sigma_z \tag{6.27b}$$

$$-iK^\alpha \delta^\alpha \cdot \Delta_R \check{G}_{-+}^{\alpha\alpha} - \left[\check{G}^{\alpha\alpha} \bullet (\check{\Sigma}^\alpha - \hat{H}_0^\alpha) \right]_{--} = 1,$$

where $\check{\Sigma}^\alpha$ is the block of $\check{\Sigma}$ in (6.18) corresponding to material α. We also use the notation that we can write a general matrix A in the sublattice basis as

$$(S^\alpha)^T A S^\alpha = \begin{pmatrix} A_{--} & A_{-+} \\ A_{+-} & A_{++} \end{pmatrix}, \tag{6.28}$$

so the $--$ index, for instance, indicate that one should take the upper left block in the conduction basis. Also, the discrete finite difference operator is defined as

$$x_m^\alpha \cdot \Delta_R \check{G}^{\alpha\alpha}(k, n_n) = \check{G}^{\alpha\alpha}(k, x_n^\alpha + x_m^\alpha) - \check{G}^{\alpha\alpha}(k, x_n^\alpha). \tag{6.29}$$

Looking at the Gor'kov equations (6.27), we are only considering the Green's functions which stays in either the left or right material, since they are only denoted by a single index α. This means we we can ignore the α index, as the difference between the left and right materials we look at will now manifests itself in the boundary conditions, which are discussed at the end of this section.

6.3 Quasiclassical Green's function

The next step is to transform into using the quasiclassical Green's function. To do this, the Green's function must be integrated over all momenta, as discussed in section 4. As mentioned above, we only want contributions from the states close to the Fermi surface. This means that we cannot simply integrate over all momenta, as the contributions far from the Fermi surface are small but not negligible. Instead, we must integrate over a contour close to the Fermi surface. The integral is therefore decomposed into one part which includes contributions close to the Fermi surface, and one part which includes the rest, by using the Eilenberger decomposition [48]. To get the quasiclassical equations of motion, we must integrate the Gor'kov equations (6.27) over this contour $\oint \mathrm{d}\xi_-$. The quasiclassical Green's function is now defined as

$$\check{g} = \frac{i}{\pi} \oint \mathrm{d}\xi_- \, \check{G}_{--}. \tag{6.30}$$

Here, only positions inside the materials will be looked at, which means the tunneling self energy term and any potential outside the material can be ignored. Integrating the Gor'kov equations (6.27) over the contours in the complex ξ_- space, subtracting the second equation from the first, and using the assumption that $\check{V} + \check{\Sigma}_{\mathrm{imp}}$ varies slowly with COM position, the equation of motion for the quasiclassical Green's function can be derived as [20],

$$i\mathbf{v}_F \cdot \Delta_R \check{g} + \left[\tau_z \varepsilon - (\check{\Sigma} - \hat{H}_0)_{--} \circ \check{g}\right] = 0. \tag{6.31}$$

This is the Eilenberger equation for antiferromagnetic materials, where $\mathbf{v}_F = \nabla_k \xi_-(\mathbf{k}_F)$ is the Fermi velocity. The Eilenberger equation does not have a unique steady-state solution, so to compensate for this one typically assumes the normalization condition that $\check{g} \circ \check{g} = 1$.

6.4 Diffusive Limit

In order to arrive at the Usadel equation for antiferromagnetic materials, the diffusive limit of the Eilenberger equation (6.31) must be taken. Before we can do this, the impurity self energy (6.13) must be expressed in terms of the quasiclassical Green's function (6.30). We assume that there are, on average, an equal amount of impurities of equal average strength on both sublattices, and the impurities are not magnetic. Using the Eilenberger contour discussed above, the impurity self energy can be written as [20]

$$(\check{\Sigma}_{imp})_{--} = -\frac{i}{2\tau_{imp}}(\check{g}_s + \frac{J^2}{\eta^2}\sigma_z\tau_z\check{g}_s\sigma_z\tau_z), \tag{6.32}$$

where the angular average quasiclassical Green's function in momentum space is defined as

$$\langle\check{g}\rangle \equiv \check{g}_s = \int \frac{\mathrm{d}\Omega}{4\pi}\check{g}. \tag{6.33}$$

We see that the equation for the impurity self energy reduces to the normal state impurity self energy in the absence of antiferromagnetism when $J^\alpha = 0$. However, when $J^\alpha \neq 0$ we get an additional term which is equal to the term one gets when adding magnetic impurities in the quasiclassical theory for normal metals. This means that the impurities in the antiferromagnet behave as if they where magnetic [20]. This antiferromagnetic term proportional to J is similar to the spin-flip scattering term one gets for the ferromagnetic Usadel equation in section 5

We are now ready to derive the equation of motion for the diffusive limit, starting from the Eilenberger equation (6.31). This equation of motion is valid for diffusive systems, where the impurity scattering time is assumed to be small. To start off, the gradient term needs to be replaced with the covariant derivative, in order to be able to include spin-orbit coupling and the vector gauge potential from the electromagnetic field. This is done by extracting the p-wave part of $\check{V}_{--}$, writing it as

$$\check{V}_{--} = \mathbf{v}_F \cdot \hat{\mathbf{A}} + \check{V}_s + \Delta\check{V}, \tag{6.34}$$

where $\check{V}_s = \langle\check{V}_{--}\rangle$ is the s-wave part, and $\mathbf{v}_F \cdot \hat{\mathbf{A}}$ is the p-wave part of $\check{V}_{--}$. The p-wave contribution includes the vector gauge potential from the electromagnetic field, as well as spin-orbit coupling and the spatial variation in the Néel vector. The covariant derivative is then defined as

$$\tilde{\nabla} \circ \check{g} = \Delta_R\check{g} - i\left[\hat{\mathbf{A}}, \check{g}\right]_\circ. \tag{6.35}$$

The Eilenberger equation (6.31) is now

$$i\mathbf{v}_F \cdot \tilde{\nabla} \circ \check{g} + \left[\tau_z\varepsilon - \check{V}_s - \Delta\check{V} - (\check{\Sigma}_{imp})_{--}, \check{g}\right]_\circ = 0. \tag{6.36}$$

where $\check{\Sigma} - \hat{H}_0 = \check{V} + \check{\Sigma}_{imp}$ inside the material, since here the tunneling term is zero. Also, the matrix current is defined as

$$\check{\mathbf{j}} \equiv \langle\mathbf{v}_F\check{g}\rangle. \tag{6.37}$$

We can get an expression for the matrix current by assuming that $\frac{1}{\tau_{imp}}$ is much larger than ε, $\check{V}_s$ and $\Delta\check{V}$, and writing $\check{g} = \check{g}_s + \Delta\check{g}$ where $\check{g}_s = \langle\check{g}\rangle$ is the isotropic part of the quasiclassical Green's function. Next, we assume that $\Delta\check{g}^\alpha$ does not include higher order spherical harmonics with large amplitudes, which is valid under the assumption that $\Delta\check{V}^\alpha$ is small. We can then show that the isotropic Green's function also satisfies the normalization condition $\check{g}_s^\alpha \circ \check{g}_s^\alpha$. This is consistent as long as the change in $\check{g}_s$ over the length of the mean free path $l_{imp} = v_F\tau_{imp}$ is small compared to 1. With these assumptions, the matrix current can be written as

$$\check{\mathbf{j}} = -\check{g}_s \circ \tilde{\nabla} \circ (D\check{g}_s) - \check{g}_s \circ \left[\frac{J^2}{2\eta^2}\sigma_z\tau_z\check{g}_s\sigma_z\tau_z, \check{\mathbf{j}}\right]_\circ, \tag{6.38}$$

where

$$D \equiv \tau_{imp}\langle \mathbf{v}_F \otimes \mathbf{v}_F\rangle \tag{6.39}$$

is the diffusion tensor. The next step is to take the angular average of equation (6.36). We then end up with

$$i\tilde{\nabla} \circ \check{\mathbf{j}} + \left[\tau_z\varepsilon - \check{V}_s + \frac{iJ^2}{2\tau_{imp}\eta^2}\sigma_z\tau_z\check{g}_s\sigma_z\tau_z, \check{g}_s\right]_\circ = 0. \tag{6.40}$$

This the Usadel equation for systems with antiferromagnets, which gives us the equation of motion for the system. As we can see, if we set $J \to 0$, we end up with the usual Usadel equation for normal metals discussed in section 5. This equation can be used to find useful information about the system, such as magnetization and density of states.

6.5 Equilibrium

As Fyhn et.al. points out, a simpler equation for the matrix current $\check{\mathbf{j}}$ can be found in equilibrium by assuming that $(J/\eta)^2[\sigma_z\tau_z, \check{g}_s] \ll 1$. This is valid for time independent situations, and equation (6.38) can then be written as

$$\check{\mathbf{j}} \approx -[1 + (J/\eta)^2]^{-1} D\check{g}_s\tilde{\nabla}\check{g}_s, \tag{6.41}$$

where D is now constant. Since we are in equilibrium, the ring commutator reduces to an ordinary commutator. The final version of the Usadel equation is now

$$[1 + (J/\eta)^2]^{-1} iD\tilde{\nabla}(\check{g}_s\tilde{\nabla} \circ \check{g}_s) = \left[\tau_z\varepsilon - \check{V}_s + \frac{iJ^2}{2\tau_{imp}\eta^2}\sigma_z\tau_z\check{g}_s\sigma_z\tau_z, \check{g}_s\right]. \tag{6.42}$$

6.6 Boundary Conditions

The two materials must have some condition which describes how the electrons will behave when they travel from one material to the other. Let the superconductor be denoted by S, and the antiferromagnet by A. The general boundary condition for the matrix current going out of material $\alpha \in \{S, A\}$ into material $\beta \in \{A, S\}$ is given by [20, 49]

$$\mathbf{e} \cdot \check{\mathbf{j}}_\alpha = \left[\hat{T}_{\alpha\beta}\check{g}_\beta\hat{T}_{\beta\alpha} + i\hat{R}_\alpha, \check{g}_\alpha\right], \tag{6.43}$$

where $\mathbf{e}_n$ is the outwards pointing normal vector, $\hat{T}_{\alpha\beta}$ it the tunneling matrix and $\hat{R}_\alpha$ is the reflection matrix. The tunneling matrix tells us something about the probability for an electron to tunnel through the boundary, while the reflection matrix about the probability for it to be reflected at the boundary. For the boundary conditions, we have either compensated or uncompensated interfaces. In the compensated boundary we assume that the tunneling and reflection are scalars independent of spin and sublattice, given as $\hat{T}_{\alpha\beta} = \hat{T}^*_{\alpha\beta} = t$, $\hat{R}_\alpha = r$. These conditions gives us the same result as the one discussed in the SF case in section 5. The uncompensated boundary conditions are the same as the spin active boundary conditions. In this case it is assume that tunneling can only occur between the superconductor and the A-sublattice in the antiferromagnet, where the boundary contains spins pointing in the direction $\hat{\mathbf{m}}$. In this case the tunneling matrix becomes [49]

$$\begin{aligned}&\hat{T}_{SA} = \hat{T}^\dagger_{AS} = \\ &\frac{t}{2}\left[\sqrt{1+J/\mu} + \sqrt{1-J/\mu} + (\sqrt{1+J/\mu} - \sqrt{1-J/\mu})\tau_z \hat{\mathbf{m}}\cdot\boldsymbol{\sigma}\right].\end{aligned} \tag{6.44}$$

In general, we should also have spin-dependent reflection. The reflection matrix is for simplicity set equal for both sides

$$\hat{R}_A = \hat{R}_S = r\tau_z \hat{\mathbf{m}}\cdot\boldsymbol{\sigma}. \tag{6.45}$$

7 Spin-orbit coupling as a result of curvature

We would like to take the Usadel equation for antiferromangets we found in section 6 and use it to describe curved systems. To achieve this, we first need to look at how curvature can induce a spin-orbit coupling which we will include as a background field in the derivative operator. This section is based on Ref. [30].

When a material with an initially regular atomic lattice with some constant distance between the lattice points becomes bent, the interatomic distances becomes nonuniform, as we can see in figure 7. The deformation due to the curvature is tensile for $n > 0$ and compressive for $n < 0$, where n is the normal coordinate. Suppose we look at a section of the bent material. The strain along the bent direction is defined as

$$\epsilon_{ss} = \frac{L(n) - L_0}{L_0}, \tag{7.1}$$

where $L(n)$ is the length of the bent material at a distance n from the center of the material, and $L(0) \equiv L_0$ is the length of the material before being bent. The length can be expressed in terms of the curvature radius R and curvature angle θ along the material, $L(n) = (R + n)\theta$. We can then write

$$\epsilon_{ss} = \frac{(R+n)\theta - R\theta}{R\theta} = \kappa(s)n, \tag{7.2}$$

where $\kappa(s) = \frac{1}{R}$ is the curvature of the material and s is the arch length parameter.

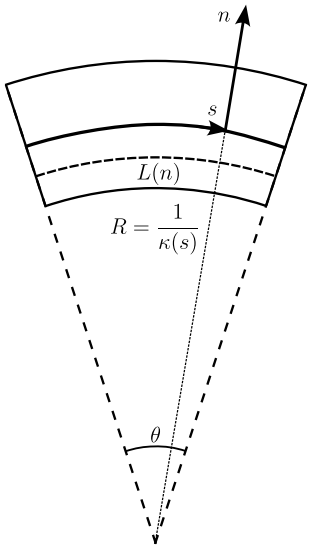

Figure 7: A part of the cross section of a curved nanostructure. n is the normal coordinate, s is the arclength parameter and θ is the curvature angle. $R = \frac{1}{\kappa(s)}$ is the radius of curvature, where $\kappa(s)$ is the curvature. $L(n)$ is the length of the section at a distance n from the center line, indicated by the dotted line.

Since the strain in the material gives rise to different distances between the lattice points along the normal direction, we get a shift in the energy band [18, 50]. This shift in the band energies may be treated as a varying potential, which for small

values of the strain are linear in the strain [50]:

$$V(s,n) = \lambda\epsilon_{ss}(s,n) = \lambda\kappa(s)n, \tag{7.3}$$

where λ is a characteristic energy scale, which for semiconductors is in the order of 1eV [19]. As we know, a varying potential gives rise to an electric field $\mathbf{E} = -\frac{1}{e}\nabla V$. Using the gradient in curvilinear coordinates given in [30], the electric field induced by the strain and the potential (7.3) is given by

$$\mathbf{E}(s,n) = -\frac{\lambda n}{eH(s,n)}\partial_s(\kappa(s))\hat{\boldsymbol{\mathcal{T}}}(s) - \frac{\lambda\kappa(s)}{e}\hat{\boldsymbol{\mathcal{N}}}(s). \tag{7.4}$$

We now average over the normal coordinate by integrating over n, and use the curvilinear Jacobian given in equation [30]:

$$\langle\mathbf{E}\rangle_N(s) = -\frac{\lambda\kappa(s)}{e}\hat{\boldsymbol{\mathcal{N}}}(s). \tag{7.5}$$

This is the average of the electric field over the normal coordinate n at the archlength point s, and is denoted by $\langle ...\rangle_N$. This shows that the curvature $\kappa(s)$ of the material induces an electric field in the normal direction, proportional to the curvature.

We will now find how this electric field is coupled to the spin of the electrons. An electron traveling with a velocity $\mathbf{v}$ in an electric field $\mathbf{E}$ experiences a magnetic field $\mathbf{B} = -\mathbf{v}\times\mathbf{E}$. This magnetic field couples to the magnetic momentum μ_e of the electron through the Zeeman interaction in the Hamiltonian

$$H_{SO} = -\mu_e\cdot\mathbf{B} = \frac{eg}{2m}\mathbf{S}\cdot(\mathbf{v}\times\mathbf{E}), \tag{7.6}$$

where $\mathbf{S}$ is the spin-vector and g is the g-factor, which for an electron is approximately equal to 2. Writing this in terms of the electron momentum $\mathbf{p}$ and the Pauli spin matrix vector $\boldsymbol{\sigma} = 2\mathbf{S}$, we get

$$H_{SO} = \frac{eg}{4m^2}\boldsymbol{\sigma}\cdot(\mathbf{p}\times\mathbf{E}). \tag{7.7}$$

This Hamiltonian shows how the electron momentum is coupled to the spin, which is mediated by the electric field. This type of coupling is known as spin-orbit coupling. We can now insert equation (7.5) for the electric field induced by the curvature into this Hamiltonian and get

$$H_{SO} = -\frac{\alpha_N}{m}\boldsymbol{\sigma}\cdot(\mathbf{p}\times\hat{\boldsymbol{\mathcal{N}}}(s)), \tag{7.8}$$

where $\alpha_N = \frac{g\lambda\kappa(s)}{4m}$ is the Rashba coefficient determining the strength of the curvature-induced spin-orbit coupling. We see that by adjusting the curvature $\kappa(s)$ of the material, we can directly control the spin orbit strength on the electron through the Rashba coefficient.

We will now look at how we can express the spin-orbit coupling in terms of a spin-orbit field $\mathbf{A}$. In addition to the spin-orbit coupling in the normal direction originating from the curved structure, we may also have a second, intrinsic, spin-orbit

term independent of the curvature [51]. This term comes from the fact that we have an asymmetric confinement in the binormal direction. To account for these different types, we may introduce a general spin-orbit vector whose components represents the spin-orbit coupling strength in the different curvilinear directions: $\boldsymbol{\alpha} = \alpha_T \hat{\boldsymbol{\mathcal{T}}}(s) + \alpha_N \hat{\boldsymbol{\mathcal{N}}}(s) + \alpha_B \hat{\boldsymbol{\mathcal{B}}}(s)$ [33]. The magnitude of the spin-orbit interaction, and its axis can now be determined by the magnitude and direction of $\boldsymbol{\alpha}$, respectively. The Hamiltonian of the system, only including the kinetic and spin-orbit part, can now be written as:

$$\hat{H} = \frac{\mathbf{p}^2}{2m} - \frac{\boldsymbol{\alpha}}{2m} \cdot \boldsymbol{\sigma} \times \mathbf{p}. \tag{7.9}$$

Next, we would like to write this as a covariant equation using tensors. To achieve this, we replace $\mathbf{p} = -i\nabla$ with the coordinate covariant derivatives defined in equation (2.23) and rewrite the cross product in covariant form:

$$\hat{H} = -\frac{1}{2m}\eta^{ij}\mathcal{D}_i\mathcal{D}_j + \frac{i}{2m}\alpha_i\mathcal{E}^{ijk}\sigma_j\partial_k. \tag{7.10}$$

Since the ordinary Levi-Cevita symbol ϵ^{ijk} is not a tensor, we introduce the contravariant Levi-Cevita tensor $\mathcal{E}^{ijk} \equiv \frac{1}{\sqrt{\eta}}\epsilon^{ijk}$, where $\sqrt{\eta}$ is defined as the square root of the determinant of the metric tensor η_{ij}. This makes sure that the equations stay in tensorial form. We can now introduce the contravariant spin-orbit field A^k in the last term of the equation

$$A^k = \alpha_i\mathcal{E}^{ijk}\sigma_j. \tag{7.11}$$

The Hamiltonian now takes the form:

$$\hat{H} = -\frac{1}{2m}\eta^{ij}\mathcal{D}_i\mathcal{D}_j + \frac{i}{2m}A^k\partial_k. \tag{7.12}$$

When operating on a scalar function, regular and covariant derivatives are equivalent. This is the case for the Hamiltonian, as it acts on scalar wavefunctions. We can therefore replace $\partial_k \to \mathcal{D}_k$ in the last term of the Hamiltonian. After relabeling the k-index and using the metric tensor to lower the index of the spin-orbit field, we get:

$$\hat{H} = -\frac{1}{2m}\eta^{ij}(\mathcal{D}_i\mathcal{D}_j - iA_i\mathcal{D}_j). \tag{7.13}$$

If we now assume that the spin-orbit coupling is weak, i.e. the physical components $\left|A_{(i)}\right| \ll 1$, we can rewrite this equation in a similar way as for a charged particle moving in a magnetic field

$$\hat{H} = -\frac{1}{2m}\eta^{ij}(\mathcal{D}_i - iA_i)^2, \tag{7.14}$$

where A_i acts as a background SU(2) gauge field [52]. Finally, we need to replace the coordinate covariant derivatives with a coordinate-gauge covariant derivative to ensure that we have the correct transformation properties under local SU(2) rotations. The coordinate-gauge covariant derivative of a covariant vector v_j is defined as:

$$\tilde{\mathcal{D}}_i v_j = \mathcal{D}_i v_j - i[A_i, v_j] = \partial_i v_j - \Gamma^k_{ij} v_k - i[A_i, v_j]. \tag{7.15}$$

The commutator ensures that the transformation is gauge covariant, while the Christoffel symbols ensures that it is coordinate covariant.

8 Usadel Equation for Antiferromagnets in Curvilinear Coordinates

Now we are ready to derive the Usadel equation for curved systems. Here we will insert the different Christoffel symbols in the coordinate-gauge covariant derivative, and consider them in terms of a curvilinear gradient and physical spin-orbit field **A**.

We would like to find an expression for the Usadel equation in curvilinear coordinates. To achieve this, we start off by considering the Usadel equation for antiferromagnets (6.42) we found earlier. We would like to include spin-orbit coupling, and write the equation in covariant form. We therefore replace the derivatives with the coordinate-gauge covariant derivative, and write the scalar product using tensor notation. This gives us the Usadel equation for antiferromagnets in tensorial form, which also includes spin-orbit coupling:

$$iD_F\eta^{ij}[1+(J/\eta)^2]^{-1}\tilde{\mathcal{D}}_i(\check{g}\tilde{\mathcal{D}}_j\check{g}) = \left[\epsilon\tau_z - \check{V}_s + \frac{iJ^2}{2\tau_{imp}\eta^2}\sigma_z\tau_z\check{g}\sigma_z\tau_z, \check{g}\right], \tag{8.1}$$

where $\tilde{\mathcal{D}}_i v_j = \partial_i v_j - \Gamma^k_{ij}v_k - i\left[\hat{A}_i, v_j\right]$ and $\hat{A}_i \equiv (\underline{A}_i, -\underline{A}_i^{\alpha *})$ is the covariant spin-orbit field in 4×4 Nambu space.

We now want to go from the general Usadel equation using tensor notation, to using a curvilinear coordinate system as described in section 2.4. We will start by looking at the case of no torsion. We will see how the equations change when adding torsion when we look at a more specific case for the nanowire arch/helix in the next section. The left hand side of the Usadel equation can be calculated explicitly. Writing it out, we get

$$\begin{aligned} iD_F\eta^{ij}[1+(J/\eta)^2]^{-1}\tilde{\mathcal{D}}_i(\check{g}\tilde{\mathcal{D}}_j\check{g}) = iD_F\eta^{ij}[1+(J/\eta)^2]^{-1}\Big(&\partial_i(\check{g}\partial_j\check{g}) - \Gamma^k_{ij}(\check{g}\partial_k\check{g}) \\ &-i\left[\hat{A}_i, \check{g}\partial_j\check{g}\right] - i\partial_i\big(\check{g}\left[\hat{A}_j, \check{g}\right]\big) + i\Gamma^k_{ij}\check{g}\left[\hat{A}_k, \check{g}\right] - \left[\hat{A}_i, \check{g}\left[\hat{A}_j, \check{g}\right]\right]\Big). \end{aligned} \tag{8.2}$$

In section 2.4 we found the expressions for the Christoffel symbols (2.34) and metric tensor (2.31) for a curvilinear coordinate system with no torsion. In equation (2.28), we multiply the Christoffel symbols with the diagonal metric tensor. As a result, only the terms with equal lower indices ($i=j$) contribute, which are

$$\Gamma^s_{ss} = \frac{1}{H(s,n)}\partial_s H(s,n), \qquad \Gamma^n_{ss} = -H(s,n)\partial_n H(s,n). \tag{8.3}$$

We now insert the metric tensor and Christoffel symbols into equation (8.2). The full Usadel equation (8.1) now takes the form [30]

$$\begin{aligned} iD_F[1+(J/\eta)^2]^{-1}&\left[\tilde{\nabla}_s(\hat{g}\tilde{\nabla}_s\hat{g}) + \frac{1}{H(s,n)}\tilde{\nabla}_n(H(s,n)\hat{g}\tilde{\nabla}_n\hat{g}) + \tilde{\nabla}_b(\hat{g}\tilde{\nabla}_b\hat{g})\right] = \\ &\left[\epsilon\tau_z - \check{V}_s + \frac{iJ^2}{2\tau_{imp}\eta^2}\sigma_z\tau_z\check{g}\sigma_z\tau_z, \check{g}\right], \end{aligned} \tag{8.4}$$

where we have defined the gauge covariant derivative in terms of the physical spin orbit field component $\hat{A}_{(i)}$ defined in the curvilinear basis, such that

$$\tilde{\nabla}_i v_j = \nabla_i v_j - i\Big[\hat{A}_{(i)}, v_j\Big], \tag{8.5}$$

where ∇_i is the component of the curvilinear gradient $\nabla = (\frac{1}{H(s,n)}\partial_s, \partial_n, \partial_b)$ in the i-th direction, and $\hat{A}_{(i)} = (\underline{A}_i, -\underline{A}_i^*)$ where the physical spin-orbit field is given as

$$\mathbf{A} = (\alpha_{(N)}\sigma_{(B)} - \alpha_{(B)}\sigma_{(N)}, \alpha_{(B)}\sigma_{(T)} - \alpha_{(T)}\sigma_{(B)}, \alpha_{(T)}\sigma_{(N)} - \alpha_{(N)}\sigma_{(T)}). \tag{8.6}$$

Equation (8.6) is derived by considering the definition of the contravariant spin-orbit field in equation (7.11), and inserting the determinant of the metric tensor into the equation while performing the summation using curvilinear coordinates [30]. Here we also defined the set of physical curvilinear Pauli matrices $\sigma_{(T),(N),(B)}(s) \equiv \boldsymbol{\sigma} \cdot \{\hat{\boldsymbol{\mathcal{T}}}(s), \hat{\boldsymbol{\mathcal{N}}}(s), \hat{\boldsymbol{\mathcal{B}}}(s)\}$.

We can perform a similar derivation in order to find the curvilinear expressions for the boundary conditions given in (6.43). The covariant form of the boundary conditions can be written as

$$[1 + (J/\eta)^2]^{-1} D\check{g}_\alpha \tilde{\mathcal{D}}_i \check{g}_\alpha = \left[\hat{T}_{\alpha\beta}\check{g}_\beta \hat{T}_{\beta\alpha} + i\hat{R}_\alpha, \check{g}_\alpha\right], \tag{8.7}$$

where $\tilde{\mathcal{D}}_i$ is the coordinate-gauge covariant derivative. Expanding the covariant boundary conditions in curvilinear coordinates like we did above, we achieve

$$[1 + (J/\eta)^2]^{-1} D\check{g}_\alpha \tilde{\nabla}_i \check{g}_\alpha = \left[\hat{T}_{\alpha\beta}\check{g}_\beta \hat{T}_{\beta\alpha} + i\hat{R}_\alpha, \check{g}_\alpha\right], \tag{8.8}$$

where $\tilde{\nabla}_i$ is the gauge covariant derivative in terms of the physical spin-orbit field discussed in equation (8.5).

9 Nanowire Arc

In this section we will apply the Usadel equation for curved systems we found in the previous section to the case of a nanowire arch curved in the form of a portion of a circle, as illustrated in figure 8. In this case, the curvature is constant, $\kappa(s) = \kappa = 1/R$, where R is the radius of the full circle. We will first look at the case with no torsion, and afterwards look at how the equations changes after adding torsion.

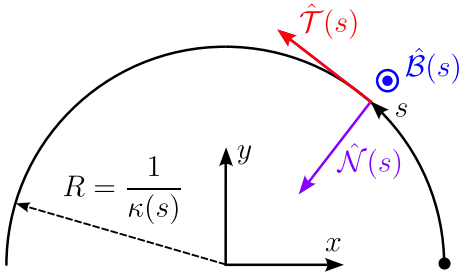

Figure 8: An illustration of a nanowire arch, here chosen to be a semicircle with constant radius of curvature $R = \frac{1}{\kappa(s)}$. The nanowire resides in the xy-plane, where at any arclength point s, measured from the right end of the semicircle, we have a local set of basis vectors $\hat{\boldsymbol{\mathcal{T}}}(s)$, $\hat{\boldsymbol{\mathcal{N}}}(s)$ and $\hat{\boldsymbol{\mathcal{B}}}(s)$, following a right handed curvilinear coordinate system. For the case of no torsion the binormal unit vector is constant.

We assume that the wire is infinitesimally thin and lies in the xy-plane. This means that we may neglect the degrees of freedom in the normal and binormal direction, $n, b \to 0$, and the curvature dependent scale function becomes $H(s,n) = 1 - \kappa(s)n = 1$. The metric tensor in equation (2.31) thus reduces to the same form as the Cartesian metric tensor. For coordinate systems with a Cartesian-like metric, there is no distinction between covariant/contravariant and physical tensor component. We can therefore drop the parenthesis notation for physical components in the following sections.

For a 1D nanowire arc, the curvilinear Usadel equation in (8.4) takes the simple form:

$$iD_F[1 + (J/\eta)^2]^{-1}\tilde{\partial}_s(\check{g}\tilde{\partial}_s\check{g}) = \left[\epsilon\tau_z - \check{V}_s + \frac{iJ^2}{2\tau_{imp}\eta^2}\sigma_z\tau_z\check{g}\sigma_z\tau_z, \check{g}\right], \tag{9.1}$$

where we defined the gauge covariant derivative $\tilde{\partial}_s v_j = \partial_s v_j - i\left[\hat{A}_T, v_j\right]$, corresponding to $H(s,n) = 1$ for the coordinate gauge covariant derivative in curvilinear coordinates used in the curvilinear Usadel equation. Also, $\hat{A}_T = \text{diag}(\underline{A}_T, -\underline{A}_T^*)$, where $\underline{A}_T = \alpha_N\sigma_B - \alpha_B\sigma_N$ is the tangential component of the spin-orbit field (8.6). Only the A_T component of the gauge covariant derivative remains since we can ignore the derivatives in the binormal and normal directions due to taking $n, b \to 0$.

9.0.1 Curvilinear Pauli Matrices

Looking at equation (9.1), the only part of the equation that makes this curved case different from a straight case is that the Pauli matrices changes expressions in the

curvilinear basis. We will therefore need the Pauli Matrices in a curvilinear basis. The curvilinear Pauli matrices are defined as:

$$\sigma_T = \boldsymbol{\sigma} \cdot \hat{\boldsymbol{\mathcal{T}}}(s), \qquad \sigma_N = \boldsymbol{\sigma} \cdot \hat{\boldsymbol{\mathcal{N}}}(s), \qquad \sigma_B = \boldsymbol{\sigma} \cdot \hat{\boldsymbol{\mathcal{B}}}(s), \tag{9.2}$$

where $\boldsymbol{\sigma}$ is the Cartesian Pauli spin vector. As we can see, we need expressions for the three basis vectors. The basis vectors are related through the torsion-free Frenet-Serret formulas given in equation (2.27), and can be expressed in terms of the arc length parametrization $\boldsymbol{\xi}(s)$ as:

$$\hat{\boldsymbol{\mathcal{T}}}(s) = \frac{\mathrm{d}}{\mathrm{d}s}\boldsymbol{\xi}(s), \qquad \hat{\boldsymbol{\mathcal{N}}}(s) = \frac{1}{\kappa(s)}\frac{\mathrm{d}^2}{\mathrm{d}s^2}\boldsymbol{\xi}(s), \qquad \hat{\boldsymbol{\mathcal{B}}}(s) = \hat{\mathbf{e}}_z. \tag{9.3}$$

The arch length parametrization is given by $\boldsymbol{\xi}(s) = \frac{1}{\kappa}\cos(\kappa s)\hat{\mathbf{e}}_x + \frac{1}{\kappa}\sin(\kappa s)\hat{\mathbf{e}}_y$, using a Cartesian coordinate system as shown in figure 8. Using this parametrization, the basis vectors in (9.3) can be written as:

$$\hat{\boldsymbol{\mathcal{T}}}(s) = -\sin(\kappa s)\hat{\mathbf{e}}_x + \cos(\kappa s)\hat{\mathbf{e}}_y, \qquad \hat{\boldsymbol{\mathcal{N}}}(s) = -\cos(\kappa s)\hat{\mathbf{e}}_x - \sin(\kappa s)\hat{\mathbf{e}}_y, \qquad \hat{\boldsymbol{\mathcal{B}}}(s) = \hat{\mathbf{e}}_z. \tag{9.4}$$

Finally, we are able to find expressions for the curvilinear Pauli matrices in equation (9.2):

$$\sigma_T = \begin{pmatrix} 0 & -ie^{-i\kappa s} \\ ie^{i\kappa s} & 0 \end{pmatrix}, \qquad \sigma_N = \begin{pmatrix} 0 & -e^{-i\kappa s} \\ -e^{i\kappa s} & 0 \end{pmatrix}, \qquad \sigma_B = \begin{pmatrix} 1 & 0 \\ 0 & -1 \end{pmatrix}. \tag{9.5}$$

9.1 Nanowire Helix

We would now like to see how the Usadel equation changes when we add torsion to the system, as is seen in figure 9. In this case, we need to use the metric tensor given in equation (2.36)

$$\eta_{ij} = \begin{pmatrix} H(s,n)^2 + \tau(s)^2(n^2+b^2) & -\tau(s)b & \tau(s)n \\ -\tau(s)b & 1 & 0 \\ \tau(s)n & 0 & 1 \end{pmatrix}. \tag{9.6}$$

We can now look at the calculation we did for deriving the Usadel equation in curvilinear coordinates with no torsion in section 8 to see how the equation changes when we add torsion. Looking at the equations, we see that adding torsion to the system changes the number of Christoffel symbols we need to include after inserting the coordinate-gauge covariant derivative, due to the metric tensor having more terms in the case with torsion. In addition, the metric tensor is no longer diagonal so we cannot use the Christoffel symbols for diagonal metric tensors in equation (2.33), but must instead use the full equation (2.24). Fortunately, we would still like to look at a wire which is infinitesimally thin, so we get a nanowire helix. This means that we neglect the degrees of freedom in the normal and binormal direction, $n, b \to 0$. Looking at the metric tensor in equation (9.6), we see that it reduces

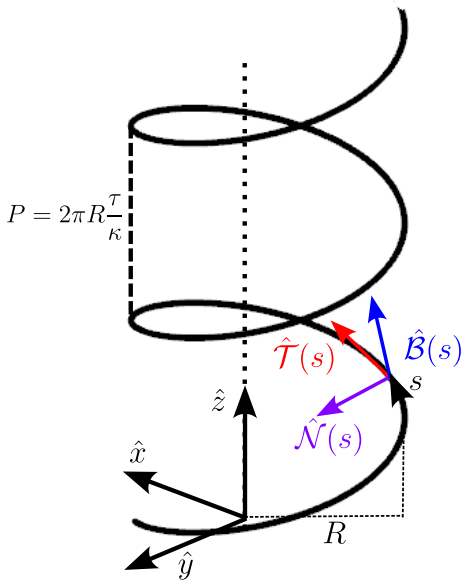

Figure 9: An illustration of a nanowire helix, with a local set of basis vectors $\hat{\boldsymbol{\mathcal{T}}}(s)$, $\hat{\boldsymbol{\mathcal{N}}}(s)$ and $\hat{\boldsymbol{\mathcal{B}}}(s)$, following a right handed curvilinear coordinate system. P is the pitch of the helix, and R is the radius.

to the same metric tensor we got for the case with no torsion, i.e. to a Cartesian metric tensor. We therefore have the same form for the Usadel equation with and without torsion, given in equation (9.1). It is worth repeating that this is only the case for a 1D nanowire where we take the limit $n, b \to 0$. For a 2D or 3D system, the equations with and without torsion would look different due to the different metric tensors and thus different Christoffel symbols.

9.1.1 Curvilinear Pauli Matrices with tortion

The difference between the 1D nanowire arch without torsion and the 1D nanowire helix with torsion lies in the Pauli matrices. For a nanowire helix, the curvilinear basis vectors can be written in a Cartesian coordinate system as [33]

$$\hat{\boldsymbol{\mathcal{T}}}(\varphi) = -\cos(\alpha)\sin(\varphi)\hat{\mathbf{e}}_x + \cos(\alpha)\cos(\varphi)\hat{\mathbf{e}}_y + \sin(\alpha)\hat{\mathbf{e}}_z, \tag{9.7}$$

$$\hat{\boldsymbol{\mathcal{N}}}(\varphi) = -\cos(\varphi)\hat{\mathbf{e}}_x - \sin(\varphi)\hat{\mathbf{e}}_y, \tag{9.8}$$

$$\hat{\boldsymbol{\mathcal{B}}}(\varphi) = \sin(\alpha)\sin(\varphi)\hat{\mathbf{e}}_x - \sin(\alpha)\cos(\varphi)\hat{\mathbf{e}}_y + \cos(\alpha)\hat{\mathbf{e}}_z, \tag{9.9}$$

where φ is the azimuthal angle in the xy-plane, and $\alpha = \arctan(\tau/\kappa)$. Finally, we can use equation (9.2) to get the Pauli matrices for a nanowire helix

$$\begin{aligned}
\sigma_T &= \begin{pmatrix} \sin(\alpha) & -i\cos(\alpha)e^{-i\varphi} \\ i\cos(\alpha)e^{i\varphi} & -\sin(\alpha) \end{pmatrix}, \\
\sigma_N &= \begin{pmatrix} 0 & -e^{-i\varphi} \\ -e^{i\varphi} & 0 \end{pmatrix}, \\
\sigma_B &= \begin{pmatrix} \cos(\alpha) & i\sin(\alpha)e^{-i\varphi} \\ -\sin(\alpha)e^{i\varphi} & -\cos(\alpha) \end{pmatrix}.
\end{aligned} \tag{9.10}$$

10 Parametrization

In this section we will use the Riccati parametrization on the Usadel equation for curved antiferromagnetic materials we found in the previous section. We will end up with an equation of motion for the γ-matrix, which we can use to solve for the Green's function. The equation of motion for the γ-matrix can be solved numerically, and it is a convenient parametrization of the Green's function as the range of 0 to 1 parametrizes an infinite range of variation in $\hat{g}$.

As discussed in section 3, the advanced, Keldysh and retarded Green's function are all related to each other in equilibrium. We can therefore focus on only solving one of them, e.g. the retarded component. Recall that the retarded quasiclassical Green's function was defined as

$$\hat{g}^R(z,\varepsilon) = \begin{pmatrix} g^R(z,+\varepsilon) & f^R(z,+\varepsilon) \\ -f^{R*}(z,-\varepsilon) & -g^{R*}(z,-\varepsilon) \end{pmatrix}. \tag{10.1}$$

As we discussed in section 4, the Green's function has a symmetry between it's components, as we can see by using the tilde conjugation

$$g^*(z,-\varepsilon) \equiv \tilde{g}(z,+\varepsilon). \tag{10.2}$$

We can always get the tilde-version of an equation by taking the tilde-conjugate of the equation, where taking the tilde conjugate simply makes the non-tilde variables into tilde variables, and vice versa. This allows us to parameterize the matrix using the Riccati parametrization [10], defined as

$$\hat{g}^R = \begin{pmatrix} N & 0 \\ 0 & -\tilde{N} \end{pmatrix} \begin{pmatrix} 1+\gamma\tilde{\gamma} & 2\gamma \\ 2\tilde{\gamma} & 1+\tilde{\gamma}\gamma \end{pmatrix}, \tag{10.3}$$

where N is a 2×2 normalization matrix defined as $N = (1-\gamma\tilde{\gamma})^{-1}$. The form of the N-matrix gives some useful identities

$$N\gamma = \gamma\tilde{N}, \qquad \tilde{N}\tilde{\gamma} = \tilde{\gamma}N. \tag{10.4}$$

The Riccati parametrization reduces the problem from solving for the 4×4 Green's functions to solving for the 2×2 γ-matrices.

The left hand side of the Usadel equation for AF-S systems is the same as for the curved SF case with no torsion (except for an extra constant in the antiferromagnet case). We will therefore only solve for the right hand side of the equation. For a derivation of the left hand side, see [30]. We will first consider the case with no torsion, and then look at the system with torsion.

Recall that the Usadel equation for curved antiferromagnets is given as

$$iD_F[1+(J/\eta)^2]^{-1}\tilde{\partial}_s(\check{g}\tilde{\partial}_s\check{g}) = \left[\epsilon\tau_z - \check{V}_s + \zeta\sigma_z\tau_z\check{g}\sigma_z\tau_z, \check{g}\right], \tag{10.5}$$

where we define:

$$\zeta \equiv \frac{iJ^2}{2\tau_{imp}\eta^2}. \tag{10.6}$$

We will now insert the γ-parametrization of $\hat{g}$ on the right hand side, and solve for each term separately.

The first term is given as:

$$\begin{aligned}
[\epsilon\tau_z, \hat{g}] &= \epsilon \begin{pmatrix} 1 & 0 \\ 0 & -1 \end{pmatrix} \begin{pmatrix} N(1+\gamma\tilde{\gamma}) & 2N\gamma \\ -2\tilde{N}\tilde{\gamma} & -\tilde{N}(1+\tilde{\gamma}\gamma) \end{pmatrix} \\
&\quad - \epsilon \begin{pmatrix} N(1+\gamma\tilde{\gamma}) & 2N\gamma \\ -2\tilde{N}\tilde{\gamma} & -\tilde{N}(1+\tilde{\gamma}\gamma) \end{pmatrix} \begin{pmatrix} 1 & 0 \\ 0 & -1 \end{pmatrix} \\
&= \epsilon \begin{pmatrix} N(1+\gamma\tilde{\gamma}) & 2N\gamma \\ 2\tilde{N}\tilde{\gamma} & \tilde{N}(1+\tilde{\gamma}\gamma) \end{pmatrix} - \epsilon \begin{pmatrix} N(1+\gamma\tilde{\gamma}) & -2N\gamma \\ -2\tilde{N}\tilde{\gamma} & \tilde{N}(1+\tilde{\gamma}\gamma) \end{pmatrix} \\
&= \begin{pmatrix} 0 & 4\epsilon N\gamma \\ 4\epsilon\tilde{N}\tilde{\gamma} & 0 \end{pmatrix}.
\end{aligned} \tag{10.7}$$

Next, we solve for the second term for a general potential $\hat{V}_s = \begin{pmatrix} \underline{V}_{11} & \underline{V}_{12} \\ \underline{V}_{21} & \underline{V}_{22} \end{pmatrix}$:

$$\begin{aligned}
\left[-\hat{V}_s, \hat{g}\right] &= - \begin{pmatrix} \underline{V}_{11} & \underline{V}_{12} \\ \underline{V}_{21} & \underline{V}_{22} \end{pmatrix} \begin{pmatrix} N(1+\gamma\tilde{\gamma}) & 2N\gamma \\ -2\tilde{N}\tilde{\gamma} & -\tilde{N}(1+\tilde{\gamma}\gamma) \end{pmatrix} \\
&\quad + \begin{pmatrix} N(1+\gamma\tilde{\gamma}) & 2N\gamma \\ -2\tilde{N}\tilde{\gamma} & -\tilde{N}(1+\tilde{\gamma}\gamma) \end{pmatrix} \begin{pmatrix} \underline{V}_{11} & \underline{V}_{12} \\ \underline{V}_{21} & \underline{V}_{22} \end{pmatrix} \\
&= \begin{pmatrix} -\underline{V}_{11}N(1+\gamma\tilde{\gamma}) + 2\underline{V}_{12}\tilde{N}\tilde{\gamma} & -2\underline{V}_{11}N\gamma + \underline{V}_{12}\tilde{N}(1+\tilde{\gamma}\gamma) \\ -\underline{V}_{21}N(1+\gamma\tilde{\gamma}) + 2\underline{V}_{22}\tilde{N}\tilde{\gamma} & -2\underline{V}_{21}N\gamma + \underline{V}_{22}\tilde{N}(1+\tilde{\gamma}\gamma) \end{pmatrix} \\
&\quad + \begin{pmatrix} N(1+\gamma\tilde{\gamma})\underline{V}_{11} + 2N\gamma\underline{V}_{21} & N(1+\gamma\tilde{\gamma})\underline{V}_{12} + 2N\gamma\underline{V}_{22} \\ -2\tilde{N}\tilde{\gamma}\underline{V}_{11} - \tilde{N}(1+\tilde{\gamma}\gamma)\underline{V}_{21} & -2\tilde{N}\tilde{\gamma}\underline{V}_{12} - \tilde{N}(1+\tilde{\gamma}\gamma)\underline{V}_{22} \end{pmatrix}.
\end{aligned} \tag{10.8}$$

Since we will look at a S-AF system, we will use the potential for a superconductor, $\hat{V}_s = \hat{\Delta} = \begin{pmatrix} 0 & \underline{\Delta} i\sigma_y \\ \underline{\Delta}^* i\sigma_y & 0 \end{pmatrix}$. This term should be zero when we are inside the antiferromagnet. We get:

$$\begin{aligned}
&\left[-\hat{\Delta}, \hat{g}\right] = \\
&\begin{pmatrix} 2\underline{\Delta} i\sigma_y\tilde{N}\tilde{\gamma} & \underline{\Delta} i\sigma_y\tilde{N}(1+\tilde{\gamma}\gamma) \\ -\underline{\Delta}^* i\sigma_y N(1+\gamma\tilde{\gamma}) & -2\underline{\Delta}^* i\sigma_y N\gamma \end{pmatrix} + \begin{pmatrix} 2N\gamma\underline{\Delta}^* i\sigma_y & N(1+\gamma\tilde{\gamma})\underline{\Delta} i\sigma_y \\ -\tilde{N}(1+\tilde{\gamma}\gamma)\underline{\Delta}^* i\sigma_y & -2\tilde{N}\tilde{\gamma}\underline{\Delta} i\sigma_y \end{pmatrix} \\
&= \begin{pmatrix} 2\underline{\Delta} i\sigma_y\tilde{N}\tilde{\gamma} + 2N\gamma\underline{\Delta}^* i\sigma_y & \underline{\Delta} i\sigma_y\tilde{N}(1+\tilde{\gamma}\gamma) + N(1+\gamma\tilde{\gamma})\underline{\Delta} i\sigma_y \\ -\underline{\Delta}^* i\sigma_y N(1+\gamma\tilde{\gamma}) - \tilde{N}(1+\tilde{\gamma}\gamma)\underline{\Delta}^* i\sigma_y & -2\underline{\Delta}^* i\sigma_y N\gamma - 2\tilde{N}\tilde{\gamma}\underline{\Delta} i\sigma_y \end{pmatrix}.
\end{aligned} \tag{10.9}$$

The third and last term is given as:

$$
\begin{aligned}
&[\zeta\sigma_i\tau_z\hat{g}\sigma_i\tau_z,\hat{g}] = \zeta\sigma_i\begin{pmatrix}1 & 0\\ 0 & -1\end{pmatrix}\begin{pmatrix}N(1+\gamma\tilde{\gamma}) & 2N\gamma\\ -2\tilde{N}\tilde{\gamma} & -\tilde{N}(1+\tilde{\gamma}\gamma)\end{pmatrix}\sigma_i\begin{pmatrix}1 & 0\\ 0 & -1\end{pmatrix}\\
&\cdot\begin{pmatrix}N(1+\gamma\tilde{\gamma}) & 2N\gamma\\ -2\tilde{N}\tilde{\gamma} & -\tilde{N}(1+\tilde{\gamma}\gamma)\end{pmatrix} - \zeta\begin{pmatrix}N(1+\gamma\tilde{\gamma}) & 2N\gamma\\ -2\tilde{N}\tilde{\gamma} & -\tilde{N}(1+\tilde{\gamma}\gamma)\end{pmatrix}\sigma_i\begin{pmatrix}1 & 0\\ 0 & -1\end{pmatrix}\\
&\cdot\begin{pmatrix}N(1+\gamma\tilde{\gamma}) & 2N\gamma\\ -2\tilde{N}\tilde{\gamma} & -\tilde{N}(1+\tilde{\gamma}\gamma)\end{pmatrix}\sigma_i\begin{pmatrix}1 & 0\\ 0 & -1\end{pmatrix}\\
&= \zeta\sigma_i\begin{pmatrix}N(1+\gamma\tilde{\gamma}) & 2N\gamma\\ 2\tilde{N}\tilde{\gamma} & \tilde{N}(1+\tilde{\gamma}\gamma)\end{pmatrix}\sigma_i\begin{pmatrix}N(1+\gamma\tilde{\gamma}) & 2N\gamma\\ 2\tilde{N}\tilde{\gamma} & \tilde{N}(1+\tilde{\gamma}\gamma)\end{pmatrix}\\
&- \zeta\begin{pmatrix}N(1+\gamma\tilde{\gamma}) & 2N\gamma\\ -2\tilde{N}\tilde{\gamma} & -\tilde{N}(1+\tilde{\gamma}\gamma)\end{pmatrix}\sigma_i\begin{pmatrix}N(1+\gamma\tilde{\gamma}) & 2N\gamma\\ 2\tilde{N}\tilde{\gamma} & \tilde{N}(1+\tilde{\gamma}\gamma)\end{pmatrix}\sigma_i\begin{pmatrix}1 & 0\\ 0 & -1\end{pmatrix}.
\end{aligned}
\tag{10.10}
$$

We now want to insert a specific direction for the spin basis. Here we will use $\sigma_i = \sigma_B$, where $\sigma_B = \begin{pmatrix}1 & 0\\ 0 & -1\end{pmatrix}$. Since the Pauli matrices are the same with and without torsion, the equation we derive here are valid for both cases. Inserting this into equation (10.10), we get :

$$
\begin{aligned}
&[\zeta\sigma_B\tau_z\hat{g}\sigma_B\tau_z,\hat{g}] = \zeta\sigma_B\begin{pmatrix}N(1+\gamma\tilde{\gamma}) & 2N\gamma\\ 2\tilde{N}\tilde{\gamma} & \tilde{N}(1+\tilde{\gamma}\gamma)\end{pmatrix}\sigma_B\begin{pmatrix}N(1+\gamma\tilde{\gamma}) & 2N\gamma\\ 2\tilde{N}\tilde{\gamma} & \tilde{N}(1+\tilde{\gamma}\gamma)\end{pmatrix}\\
&- \zeta\begin{pmatrix}N(1+\gamma\tilde{\gamma}) & 2N\gamma\\ -2\tilde{N}\tilde{\gamma} & -\tilde{N}(1+\tilde{\gamma}\gamma)\end{pmatrix}\sigma_B\begin{pmatrix}N(1+\gamma\tilde{\gamma}) & 2N\gamma\\ 2\tilde{N}\tilde{\gamma} & \tilde{N}(1+\tilde{\gamma}\gamma)\end{pmatrix}\sigma_B\begin{pmatrix}1 & 0\\ 0 & -1\end{pmatrix}\\
&= \zeta\sigma_B\begin{pmatrix}N(1+\gamma\tilde{\gamma})\sigma_B N(1+\gamma\tilde{\gamma}) + 4N\gamma\sigma_B\tilde{N}\tilde{\gamma} & 2N(1+\gamma\tilde{\gamma})\sigma_B N\gamma + 2N\gamma\sigma_B\tilde{N}(1+\tilde{\gamma}\gamma)\\ 2\tilde{N}\tilde{\gamma}\sigma_B N(1+\gamma\tilde{\gamma}) + 2\tilde{N}(1+\tilde{\gamma}\gamma)\sigma_B\tilde{N}\tilde{\gamma} & 4\tilde{N}\tilde{\gamma}\sigma_B N\gamma + \tilde{N}(1+\tilde{\gamma}\gamma)\sigma_B\tilde{N}(1+\tilde{\gamma}\gamma)\end{pmatrix}\\
&- \zeta\begin{pmatrix}N(1+\gamma\tilde{\gamma})\sigma_B N(1+\gamma\tilde{\gamma}) + 4N\gamma\sigma_B\tilde{N}\tilde{\gamma} & -2N(1+\gamma\tilde{\gamma})\sigma_B N\gamma - 2N\gamma\sigma_B\tilde{N}(1+\tilde{\gamma}\gamma)\\ -2\tilde{N}\tilde{\gamma}\sigma_B N(1+\gamma\tilde{\gamma}) - 2\tilde{N}(1+\tilde{\gamma}\gamma)\sigma_B\tilde{N}\tilde{\gamma} & 4\tilde{N}\tilde{\gamma}\sigma_B N\gamma + \tilde{N}(1+\tilde{\gamma}\gamma)\sigma_B\tilde{N}(1+\tilde{\gamma}\gamma)\end{pmatrix}\\
&\cdot\begin{pmatrix}\sigma_B & 0\\ 0 & \sigma_B\end{pmatrix}.
\end{aligned}
\tag{10.11}
$$

Inserting equations (10.7) - (10.11) into equation (10.5), we get a set of 2×2-matrix equations for γ and $\tilde{\gamma}$. From now on, we only need to consider the $(1,1)$ and $(1,2)$ components of the matrices used to solve for γ, as we can take the tilde conjugate of these equations to get the equations coming from the $(2,1)$ and $(2,2)$ components used to solve for $\tilde{\gamma}$. After simplifying these terms (derived in appendix A), and inserting the parametrization of the left-hand side, we end up with the fully

Riccati parametrized Usadel equation

$$\begin{aligned}
&\tilde{D}_F[(\partial_s^2\gamma) + 2(\partial_s\gamma)\tilde{N}\tilde{\gamma}(\partial_s\gamma)] \\
&= i(\gamma\underline{\Delta}^*\gamma - \underline{\Delta}) - 2i\zeta\Big[\sigma_B N\sigma_B\gamma + \gamma\sigma_B\tilde{N}\sigma_B + \sigma_B N\gamma\sigma_B + \gamma\sigma_B\tilde{N}\tilde{\gamma}\sigma_B\gamma - \gamma\Big] \\
&- 2i\varepsilon\gamma + 2\tilde{D}_F i(\partial_s\gamma)\tilde{N}(A_T^* + \tilde{\gamma}A_T\gamma) + 2\tilde{D}_F i(A_T + \gamma A_T^*\tilde{\gamma})N(\partial_s\gamma) \\
&+ 2\tilde{D}_F(A_T\gamma + \gamma A_T^*)\tilde{N}(A_T^* + \tilde{\gamma}A_T\gamma) + \tilde{D}_F(A_T^2\gamma - \gamma(A_T^*)^2) - \tilde{D}_F i[(\partial_s A_T)\gamma \\
&+ \gamma(\partial_s A_T^*)],
\end{aligned} \tag{10.12}$$

where $\tilde{D}_F \equiv D_F[1 + (J/\eta)^2]^{-1}$. This parametrized equation for for a curved AF-S bilayer is the main result of this thesis. Equation (10.12) is valid for both the case with and without torsion, when we choose the spin direction in the binormal direction and insert this into equation (10.10). If we want the Usadel equation for the spin direction in the normal or tangential direction, the equations for the case with and without torsion would be different, since the Pauli matrices in (9.5) and (9.10) are different. In the next sections we will look at different numerical results using the parametrized equation (10.12).

For a discussion on the parametrized versions of the boundary conditions, see e.g. [53].

11 Weak Proximity Limit

In this section we will look at the weak proximity effect for the Riccati parametrized equation we found in the previous section. We will first look at the case with no torsion, and afterwards look at the case with torsion.

When the superconductor is in contact with the antiferromagnet, some of the Cooper pairs will tunnel from one side to the other. If the transparency of the interface between them is low, only a small number of Cooper pairs are able to tunnel through. This is known as the *weak proximity effect*. In this scenario the components of the γ matrix are expected to be small, i.e. $|\gamma_{ij}| \ll 1$, which means we may neglect terms of the order $\mathcal{O}(\gamma^2)$ [10]. In this limit $N \approx 1$, so the anomalous Green's function given in the upper right block of equation (10.3), $f^R = 2N\gamma$, reduces to $f^R = 2\gamma$. It will also be useful to decompose the anomalous Green's function into singlet/triplet components, where the singlet component is described by a scalar function f_s, and the triplet component are encapsulated in the so-called d-vector [54],

$$f = (f_s + \eta^{ij} d_i \sigma_j) i\sigma_y. \tag{11.1}$$

For a nanowire arch, we can write this equation in curvilinear coordinates as

$$f^R = (f_s + d_T\sigma_T + d_N\sigma_N + d_B\sigma_B) i\sigma_y. \tag{11.2}$$

In matrix form, this equation is given as

$$f^R = 2\gamma = \begin{pmatrix} (id_T + d_N)e^{-i\kappa s} & d_B + f_s \\ d_B - f_s & (id_T - d_N)e^{i\kappa s} \end{pmatrix}, \tag{11.3}$$

where we used the expressions for the Pauli-matrices for a nanowire arch with no torsion given in equation (9.5).

We will consider the weak proximity limit inside the antiferromagnet. This means that $\underline{\Delta} = 0$. In the weak proximity limit, the Riccati parametrized Usadel equation for a nanowire arch in (10.12) reduces to a linear differential equation in γ

$$\begin{aligned} \tilde{D}_F \partial_s^2 \gamma = &-2i\zeta \left[\gamma + \sigma_B \gamma \sigma_B\right] - 2i\varepsilon\gamma + 2i\tilde{D}_F \left[(\partial_s\gamma)A_T^* + A_T(\partial_s\gamma)\right] \\ &+ \tilde{D}_F \left[A_T\gamma A_T^* + \gamma(A_T^*)^2\right] + \tilde{D}_F \left[(A_T)^2\gamma - \gamma(A_T^*)^2\right] \\ &- i\tilde{D}_F \left[(\partial_s A_T)\gamma + \gamma(\partial_s A_T^*)\right]. \end{aligned} \tag{11.4}$$

We now want to express each term of the above equation in matrix form, using the weak proximity representation of the γ-matrix given in equation (11.3). Here, we will only solve for the antiferromagnet ζ-term of the equation. For a derivation of the remaining terms, see [30]. Multiplying the weak proximity γ-matrix with the spin vector in the binormal direction, the antiferromagnet part in equation (11.4) is given as

$$-2i\zeta \left[\gamma + \sigma_B\gamma\sigma_B\right] = -2i\zeta \begin{pmatrix} (id_T + d_N)e^{-\kappa s} & 0 \\ 0 & (id_T - d_N)e^{i\kappa s} \end{pmatrix}. \tag{11.5}$$

Comparing the components of the matrix representation of the weak proximity Riccati parametrized Usadel equation in (11.4), we get four coupled differential equations

$$\begin{aligned}\frac{\tilde{D}_F}{2}(\partial_s - i\kappa)^2(id_T + d_N) = &-2i\zeta(id_T + d_N) - i\varepsilon(id_T + d_N) + \tilde{D}\kappa\alpha_B d_B \\ &+ 2\tilde{D}_F\left[\alpha_N^2(id_T + d_N) + \alpha_N\alpha_B d_B + \alpha_B^2(id_T)\right] \\ &+ 2i\tilde{D_F}\left[\alpha_N(\partial_s - i\kappa)(id_T + d_N) + \alpha_B\partial_s d_B\right],\end{aligned} \tag{11.6}$$

$$\begin{aligned}\frac{\tilde{D}_F}{2}(\partial_s + i\kappa)^2(id_T - d_N) = &-2i\zeta(id_T - d_N) + -i\varepsilon(id_T - d_N) - \tilde{D}\kappa\alpha_B d_B \\ &+ 2\tilde{D}_F\left[\alpha_N^2(id_T - d_N) - \alpha_N\alpha_B d_B + \alpha_B^2(id_T)\right] \\ &+ 2i\tilde{D_F}\left[-\alpha_N(\partial_s + i\kappa)(id_T - d_N) + \alpha_B\partial_s d_B\right],\end{aligned} \tag{11.7}$$

$$\begin{aligned}\frac{\tilde{D}_F}{2}\partial_s^2(d_B + f_s) = &-i\varepsilon(d_B + f_s) - \tilde{D}_F\kappa\alpha_B d_N + 2\tilde{D}_F\left[\alpha_B^2 d_B + \alpha_N\alpha_B d_N\right] \\ &- 2\tilde{D}_F\left[\alpha_B(\partial_s(d_T) - \kappa d_N)\right],\end{aligned} \tag{11.8}$$

$$\begin{aligned}\frac{\tilde{D}_F}{2}\partial_s^2(d_B - f_s) = &-i\varepsilon(d_B - f_s) - \tilde{D}_F\kappa\alpha_B d_N + 2\tilde{D}_F\left[\alpha_B^2 d_B + \alpha_N\alpha_B d_N\right] \\ &- 2\tilde{D}_F\left[\alpha_B(\partial_s(d_T) - \kappa d_N)\right],\end{aligned} \tag{11.9}$$

where α_j is the strength of the spin-orbit field in the direction j. These four equations can be simplified by adding and subtracting equation (11.7) from (11.6), and equation (11.9) from (11.8). We then end up with four coupled differential equations for the curvilinear components of the d-vector and the singlet

$$\begin{aligned}\frac{iD_F}{2}\partial_s^2 d_T = &\,2\zeta i d_T + \epsilon d_T + iD_F[2(\alpha_N^2 + \alpha_B^2) + \kappa(\frac{\kappa}{2} + 2\alpha_N)]d_T \\ &+ iD_F(2\alpha_N + \kappa)\partial_s d_N + 2iD_F\alpha_B\partial_s d_B,\end{aligned} \tag{11.10}$$

$$\begin{aligned}\frac{iD_F}{2}\partial_s^2 d_N = &\,2\zeta i d_N + \epsilon d_N + iD_F[2\alpha_N^2 + \kappa(\frac{\kappa}{2} + 2\alpha_N)]d_N \\ &- iD_F(2\alpha_N + \kappa)\partial_s d_T + iD_F\alpha_B(2\alpha_N + \kappa)d_B,\end{aligned} \tag{11.11}$$

$$\begin{aligned}\frac{iD_F}{2}\partial_s^2 d_B = &\,\epsilon d_B + 2iD_F\alpha_B^2 d_B + iD_F\alpha_B(2\alpha_N + \kappa)d_N \\ &- 2iD_F\alpha_B\partial_s d_T,\end{aligned} \tag{11.12}$$

$$\frac{iD_F}{2}\partial_s^2 f_s = \epsilon f_s. \tag{11.13}$$

From these equations we see how the different components interact with each other. For instance, starting with only singlets will not generate any triplet components, and vice versa. For the triplet components (11.10) - (11.12) we see that we only get mixing between the triplet states when either the spin-orbit coupling strength in the normal and binormal direction, α_N, α_B or the curvature κ are non-zero. Comparing these results to the case of a ferromagnet [16], we see that the weak proximity equations for an antiferromagnet does not have the terms proportional to the exchange field components h_i which gives a mixing between the states. Instead, we have the

term proportional to $\xi \equiv \frac{iJ^2}{2\tau_{imp}\eta^2}$ which contributes in an additive way to the tangential and normal component, but does not contribute to the binormal or singlet component. We will need to add torsion in order to get triplet generation from the singlet components.

11.1 Helix

We will now look at the weak proximity effect for a nanowire helix. In this case, the anomalous Green's function in equation (11.2) takes the form

$$f^R = \begin{pmatrix} i\cos(\alpha)e^{-i\varphi}d_T + e^{-i\varphi}d_N - i\sin(\alpha)e^{-i\varphi}d_B & f_s + \sin(\alpha)d_T + \cos(\alpha)d_B \\ -f_s + \sin(\alpha)d_T + \cos(\alpha)d_B & i\cos(\alpha)e^{i\varphi}d_T - e^{i\varphi}d_N - i\sin(\alpha)e^{i\varphi}d_B \end{pmatrix}, \tag{11.14}$$

where we used the Pauli matrices for a nanowire helix in (9.10).

Again, we consider the weak proximity effect inside the antiferromagnet, so $\underline{\Delta} = 0$. We start by looking at the antiferromagnetic ζ-term in equation (11.4), and insert the weak proximity γ matrix:

$$\begin{aligned} &-2i\zeta(\gamma + \sigma_B\gamma\sigma_B) = \\ &-i\zeta\left[\begin{pmatrix} i\cos(\alpha)e^{-i\varphi}d_T + e^{-i\varphi}d_N - i\sin(\alpha)e^{-i\varphi}d_B & f_s + \sin(\alpha)d_T + \cos(\alpha)d_B \\ -f_s + \sin(\alpha)d_T + \cos(\alpha)d_B & i\cos(\alpha)e^{i\varphi}d_T - e^{i\varphi}d_N - i\sin(\alpha)e^{i\varphi}d_B \end{pmatrix}\right] \\ &+ \begin{pmatrix} \cos(\alpha) & i\sin(\alpha)e^{-i\varphi} \\ -\sin(\alpha)e^{i\varphi} & -\cos(\alpha) \end{pmatrix} \\ &\cdot \begin{pmatrix} i\cos(\alpha)e^{-i\varphi}d_T + e^{-i\varphi}d_N - i\sin(\alpha)e^{-i\varphi}d_B & f_s + \sin(\alpha)d_T + \cos(\alpha)d_B \\ -f_s + \sin(\alpha)d_T + \cos(\alpha)d_B & i\cos(\alpha)e^{i\varphi}d_T - e^{i\varphi}d_N - i\sin(\alpha)e^{i\varphi}d_B \end{pmatrix} \\ &\cdot \begin{pmatrix} \cos(\alpha) & i\sin(\alpha)e^{-i\varphi} \\ -\sin(\alpha)e^{i\varphi} & -\cos(\alpha) \end{pmatrix}. \end{aligned} \tag{11.15}$$

Adding and multiplying the matrices, we get

$$\begin{aligned} -2i\zeta[\gamma + \sigma_B\gamma\sigma_B]^{(1,1)} &= i\cos(\alpha)e^{-i\varphi}\{1 + \sin^2(\alpha) + \cos^2(\alpha)\}d_T \\ &+ \{e^{-i\varphi} + \cos^2(\alpha)e^{-i\varphi} - \sin^2(\alpha)e^{i\varphi}\}d_N - i\sin(\alpha)e^{i\varphi}\{e^{-2i\varphi} + \cos^2(\alpha) + \sin^2(\alpha)\}d_B \\ &- i\cos(\alpha)\sin(\alpha)(e^{-i\varphi} + e^{i\varphi}\}f_s, \end{aligned} \tag{11.16}$$

$$\begin{aligned} -2i\zeta[\gamma + \sigma_B\gamma\sigma_B]^{(1,2)} &= -\sin(\alpha)e^{-2i\varphi}\{-e^{2i\varphi} + \cos^2(\alpha) + \sin^2(\alpha)\}d_T \\ &+ i\cos(\alpha)\sin(\alpha)(1 + e^{-2i\varphi})d_N - \cos(\alpha)\{-1 + \cos^2(\alpha) + \sin^2(\alpha)\}d_B \\ &+ \{1 + \sin^2(\alpha)e^{-2i\varphi} - \cos^2(\alpha)\}f_s, \end{aligned} \tag{11.17}$$

$$\begin{aligned} -2i\zeta[\gamma + \sigma_B\gamma\sigma_B]^{(2,1)} &= -\sin(\alpha)e^{2i\varphi}\{-e^{-2i\varphi} + \cos^2(\alpha) + \sin^2(\alpha)\}d_T \\ &- i\cos(\alpha)\sin(\alpha)(1 + e^{2i\varphi})d_N - \cos(\alpha)\{-1 + \cos^2(\alpha) + \sin^2(\alpha)\}d_B \\ &- \{1 + \sin^2(\alpha)e^{2i\varphi} - \cos^2(\alpha)\}f_s, \end{aligned} \tag{11.18}$$

$$-2i\zeta[\gamma+\sigma_B\gamma\sigma_B]^{(2,2)} = i\cos(\alpha)e^{i\varphi}\{1+\sin^2(\alpha)+\cos^2(\alpha)\}d_T \\ -\{e^{-i\varphi}+\cos^2(\alpha)e^{i\varphi}-\sin^2(\alpha)e^{-i\varphi}\}d_N - i\sin(\alpha)e^{-i\varphi}\{e^{2i\varphi}+\cos^2(\alpha)+\sin^2(\alpha)\}d_B \\ +i\cos(\alpha)\sin(\alpha)\{e^{-i\varphi}+e^{i\varphi}\}f_s. \tag{11.19}$$

Simplifying the terms, we end up with

$$-2i\zeta[\gamma+\sigma_B\gamma\sigma_B]^{(1,1)} = -i\zeta\Big[2i\cos(\alpha)e^{-i\varphi}d_T+\big\{[1+\cos^2(\alpha)]e^{-i\varphi}-\sin^2(\alpha)e^{i\varphi}\big\}d_N \\ -2i\sin(\alpha)\cos(\varphi)d_B-2i\cos(\alpha)\sin(\alpha)\cos(\varphi)f_s\Big], \tag{11.20}$$

$$-2i\zeta[\gamma+\sigma_B\gamma\sigma_B]^{(1,2)} = -i\zeta\Big[-\sin(\alpha)[e^{-2i\varphi}-1]d_T+i\cos(\alpha)\sin(\alpha)[1+e^{-2i\varphi}]d_N \\ -\{\cos^2(\alpha)-\sin^2(\alpha)e^{-2i\varphi}-1\}f_s\Big], \tag{11.21}$$

$$-2i\zeta[\gamma+\sigma_B\gamma\sigma_B]^{(2,1)} = -i\zeta\Big[-\sin(\alpha)[e^{2i\varphi}-1]d_T-i\cos(\alpha)\sin(\alpha)[1+e^{2i\varphi}]d_N \\ +\{\cos^2(\alpha)-\sin^2(\alpha)e^{2i\varphi}-1\}f_s\Big], \tag{11.22}$$

$$-2i\zeta[\gamma+\sigma_B\gamma\sigma_B]^{(2,2)} = -i\zeta\Big[2i\cos(\alpha)e^{i\varphi}d_T+\big\{\sin^2(\alpha)e^{-i\varphi}-[1+\cos^2(\alpha)]e^{i\varphi}\big\}d_N \\ -2i\sin(\alpha)\cos(\varphi)d_B+2i\cos(\alpha)\sin(\alpha)\cos(\varphi)f_s\Big]. \tag{11.23}$$

Adding and subtracting equation (11.23) from (11.20), and equation (11.22) from (11.21), we end up with the four equations

$$(1,1)+(2,2) = -i\zeta\Big[2i\cos(\alpha)d_T-i\sin^2(\alpha)\sin(2\varphi)d_N-2i\cos(\alpha)\sin(\alpha)\cos^2(\varphi)d_B \\ +2\cos(\alpha)\sin(\alpha)\cos(\varphi)\sin(\varphi)f_s\Big], \tag{11.24}$$

$$(1,1)-(2,2) = -i\zeta\Big[i(1+\cos^2(\alpha)-\sin^2(\alpha)\cos(2\varphi))d_N+2i\sin(\alpha)\cos(\varphi)\sin(\varphi)d_B \\ +2\cos(\alpha)\sin(\alpha)\cos^2(\varphi)f_s\Big], \tag{11.25}$$

$$(1,2)+(2,1) = -i\zeta\Big[\sin(\alpha)(1-\cos(2\varphi))d_T+\cos(\alpha)\sin(\alpha)\sin(2\varphi)d_N\Big], \tag{11.26}$$

$$(1,2)-(2,1) = -i\zeta\Big[-\sin(\alpha)\sin(2\varphi)d_T - \cos(\alpha)\sin(\alpha)(1+\cos(2\varphi))d_N \\ - i(\cos^2(\alpha)-\sin^2(\alpha)e^{-2i\varphi}-1)f_s\Big]. \tag{11.27}$$

To further simplify the equations, we will multiply and sum the equations (11.24) $\cos(\alpha)$+ (11.25) $\sin(\alpha)$ and (11.24) $\sin(\alpha)$ − (11.25) $\cos(\alpha)$. We will also write these equations in terms of κ and τ by using $\cos(\alpha) = \kappa\tilde{L}$, $\sin(\alpha) = \tau\tilde{L}$, where $1/\tilde{L} = \sqrt{\kappa^2+\tau^2}$ is the length of one turn of the helix. We then get:

$$(11.24)\cos(\alpha) + (11.25)\sin(\alpha) = \\ -i\zeta\Big[2i\kappa^2\tilde{L}^2 d_T + i\tau\tilde{L}(1+\kappa^2\tilde{L}^2 - \tau\tilde{L}^2(\kappa\sin(2\varphi)+\tau\cos(2\varphi)))d_N \\ - 2i\tau\tilde{L}^2\cos(\varphi)(\kappa^2\tilde{L}\cos(\varphi)-\tau\sin(\varphi))d_B \\ + 2\kappa\tau\tilde{L}^3\cos(\varphi)(\kappa\sin(\varphi)+\tau\cos(\varphi))f_s\Big], \tag{11.28}$$

$$(11.24)\sin(\alpha) - (11.25)\cos(\alpha) = \\ -i\zeta\Big[2i\kappa\tau\tilde{L}^2 d_T - i\tilde{L}(\kappa(1+\kappa^2\tilde{L}^2)+\tau^2\tilde{L}(\tau\tilde{L}\sin(2\varphi)-\cos(2\varphi)))d_N \\ - 2i\kappa\tau\tilde{L}^2\cos(\varphi)(\tau\tilde{L}\cos(\varphi)+\sin(\varphi))d_B \\ + 2\kappa\tau\tilde{L}^3\cos(\varphi)(\tau\sin(\varphi)-\kappa\cos(\varphi))f_s\Big]. \tag{11.29}$$

Writing the last to terms (11.26) and (11.27) in terms of κ, τ and $\tilde{L}$, we get

$$(1,2)+(2,1) = -i\zeta\Big[\tau\tilde{L}(1-\cos(2\varphi))d_T + \kappa\tau\tilde{L}^2\sin(2\varphi)d_N\Big], \tag{11.30}$$

$$(1,2)-(2,1) = -i\zeta\Big[-\tau\tilde{L}\sin(2\varphi)d_T - \kappa\tau\tilde{L}^2(1+\cos(2\varphi))d_N - i(\tilde{L}^2(\kappa^2-\tau^2e^{-2i\varphi})-1)f_s\Big]. \tag{11.31}$$

Combining equations (11.28) - (11.31) with the rest of the terms in equation (11.4) derived in [38], we end up with the weak proximity equations for a nanowire helix where $\alpha_N = \alpha_B = 0$:

$$i\frac{\tilde{D}_F}{2}\big(\partial_s^2 d_T - 2\kappa\partial_s d_N - \kappa^2 d_T + \kappa\tau d_B\big) = \epsilon d_T \\ -i\zeta\Big[2i\kappa^2\tilde{L}^2 d_T + i\tau\tilde{L}(1+\kappa^2\tilde{L}^2-\tau\tilde{L}^2(\kappa\sin(2\varphi)+\tau\cos(2\varphi)))d_N \\ - 2i\tau\tilde{L}^2\cos(\varphi)(\kappa^2\tilde{L}\cos(\varphi)-\tau\sin(\varphi))d_B + 2\kappa\tau\tilde{L}^3\cos(\varphi)(\kappa\sin(\varphi)+\tau\cos(\varphi))f_s\Big], \tag{11.32}$$

$$i\frac{\tilde{D}_F}{2}\big(\partial_s^2 d_N + 2\kappa\partial_s d_T - 2\tau\partial_s d_B - (\kappa^2+\tau^2)d_N\big) = \epsilon d_N \\ -i\zeta\Big[2i\kappa\tau\tilde{L}^2 d_T - i\tilde{L}(\kappa(1+\kappa^2\tilde{L}^2)+\tau^2\tilde{L}(\tau\tilde{L}\sin(2\varphi)-\cos(2\varphi)))d_N \\ - 2i\kappa\tau\tilde{L}^2\cos(\varphi)(\tau\tilde{L}\cos(\varphi)+\sin(\varphi))d_B + 2\kappa\tau\tilde{L}^3\cos(\varphi)(\tau\sin(\varphi)-\kappa\cos(\varphi))f_s\Big], \tag{11.33}$$

$$i\frac{\tilde{D}_F}{2}\left(\partial_s^2 d_B+2\tau\partial_s d_N-\tau^2 d_B+\kappa\tau d_T\right)=\varepsilon d_B-i\zeta\left[\tau\tilde{L}(1-\cos(2\varphi))d_T+\kappa\tau\tilde{L}^2\sin(2\varphi)d_N\right], \tag{11.34}$$

$$i\frac{\tilde{D}_F}{2}\partial_s^2 f_s=\epsilon f_s-i\zeta\left[-\tau\tilde{L}\sin(2\varphi)d_T-\kappa\tau\tilde{L}^2(1+\cos(2\varphi))d_N-i(\tilde{L}^2(\kappa^2-\tau^2e^{-2i\varphi})-1)f_s\right]. \tag{11.35}$$

If we want to go to the case of a nanowire arc, we let $\kappa \to 0$. The above equations then reduces to the equations (11.10) - (11.13) when $\alpha_N = \alpha_B = 0$. Looking at equations (11.33) - (11.35), we see that we get mixing between the different singlet and triplet components when the torsion $\kappa \neq 0$. We also note that if we let the curvature $\kappa \to 0$, the triplet states will not be converted to singlet states, but the singlet state will be converted to the normal triplet component. Finally, we see that we do not need any spin-orbit coupling to achieve mixing nor a nanowire helix.

12 Density of States

Here we will look at the density of states for the nanowire helix. The normalized density of states is related to the Green's function through the equation

$$N_F \cdot N(s,\varepsilon) = \frac{1}{2} N_F \,\mathrm{Re}\big\{\mathrm{Tr}\big\{\hat{g}^R(s,\varepsilon)\big\}\big\}, \tag{12.1}$$

where N_F is the density of states at the Fermi-surface [55]. This equation can be expressed in terms of the γ-matrix in the Riccati parametrization as

$$N(s,\varepsilon) = \frac{1}{2}\,\mathrm{Re}\{\mathrm{Tr}\{N(1+\gamma\tilde{\gamma})\}\}. \tag{12.2}$$

The density of states in the center of the helix with one turn for different values of curvature κ, torsion τ and $(J/\mu)^2$ are given in figure 10 for compensated boundary conditions, and in figure 11 for the uncompensated boundary conditions with no spin-orbit coupling, $\alpha_B = \alpha_N = 0$. The density of states for one turn along the entire antiferromagnet is given in figure 12.

The normalized density of states at zero energy, $N(s,0)$, can be used to gain further insight into the underlying physics. $N(s,0)$ can be expressed in terms of the singlet f_s and triplet component $\mathbf{d}$ of the γ-matrix as [56]

$$N(s,0) = 1 - \frac{|f_s(s,0)|}{2} + \frac{|\mathbf{d}(s,0)|}{2}. \tag{12.3}$$

Since the triplet component has a positive contribution to the normalized density of states, and the singlet contributes negatively, we can look at the zero energy density of states to see if the system predominantly contains triplets $\mathbf{d}$ or singlets f_s. When the system contains more triplets $\mathbf{d}$ than singlets, we expect a peak in the zero energy normalized density of states. Conversely, when the singlet state f_s is dominating, we expect a gap in the normalized density of states around zero energy due to the negative contribution to the density of states.

Next we will look at some numerical results for the density of states. All numerical modeling and plots are provided by Tancredi Salamone, who collaborated on this work in conjunction with his PhD degree. Salamone has developed a working code for a curved SF system, which will be made available in conjunction with his PHD-thesis. I have derived the Riccati parametrized Usadel equation for the AF-S system, which Salamone has added to his code. Comparing the two figures 10 and 11 with different boundary conditions, we see that we need spin-active boundary conditions in order to get a significant peak at zero energy. We also see that increasing the torsion τ increases the amount of triplets $\mathbf{d}$ we have in the system. It also appears that we get a dip in the triplet generation for the increased values of τ at zero energy when we increase the fraction J^2/μ^2. This shows that there exist some optimal relationship between the values of κ, τ and J^2/μ^2 which gives the biggest triplet generation.

For the density of states along the entire antiferromagnet in figure 12, we see that we start off with mostly singlets at the boundary with the superconductor, which gets transformed into triplets along the antiferromagnet. Comparing this with the case of two turns of the helix in figure 13, we see that the triplets stays as triplets after the first turn. This is because while the triplets does get converted back to the singlet component, more triplets are generated than are converted.

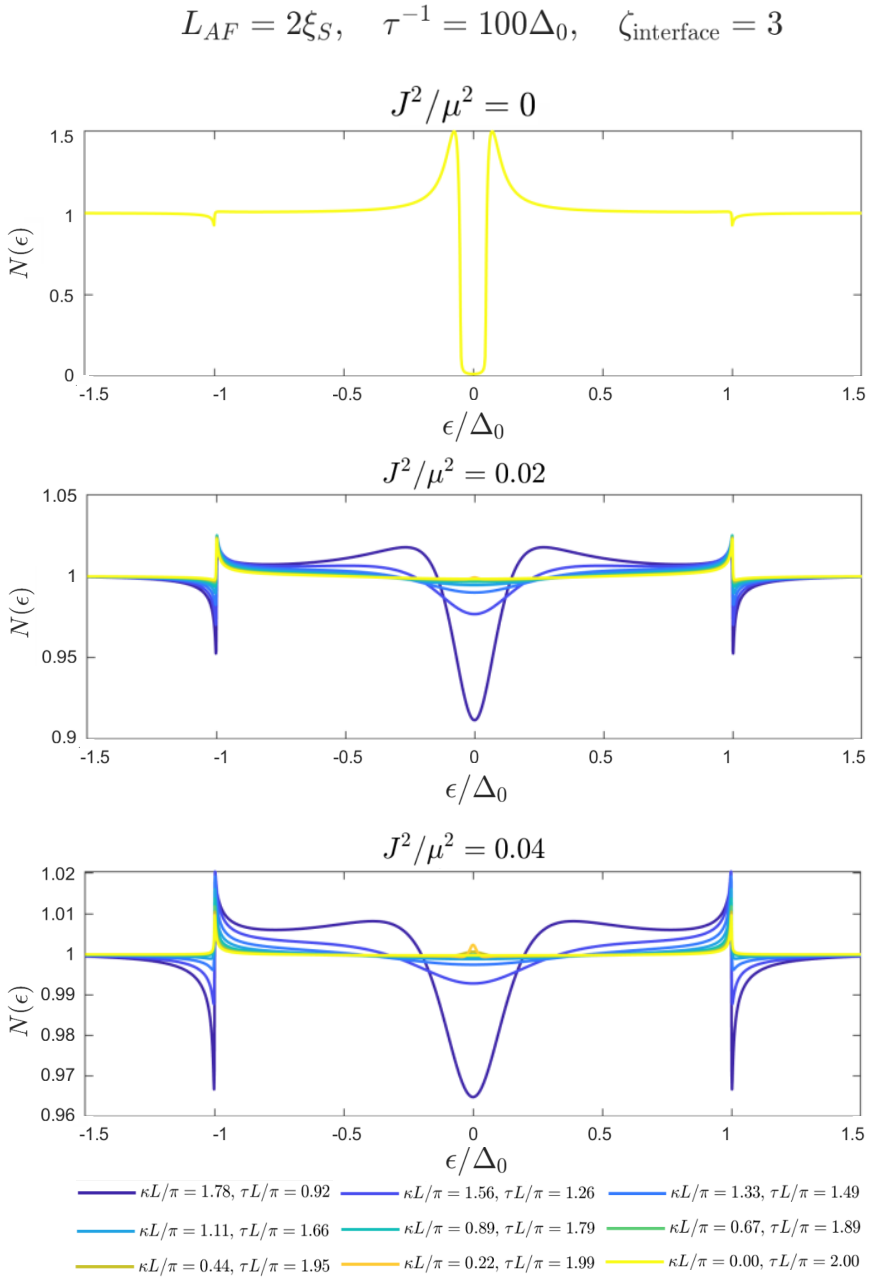

Figure 10: The density of states in the midpoint of the antiferromagnet in a S-AF bilayer with compensated boundary conditions. $L_{AF} = 2\xi_s$, where L_{AF} is the length of the antiferromagnet and ξ_s is the superconducting coherence length. $\zeta_j = 3$ is the ratio between the barrier resistance and the bulk resistance. ε/Δ_0 is given along the x-axis, and the normalized density of states $N(\varepsilon)$ is given along the y-axis. The different plots shows different values of J^2/μ^2. The different colored functions show different ratios of curvature κ and torsion τ. No spin-orbit coupling is included, so $\alpha_B = \alpha_N = 0$.

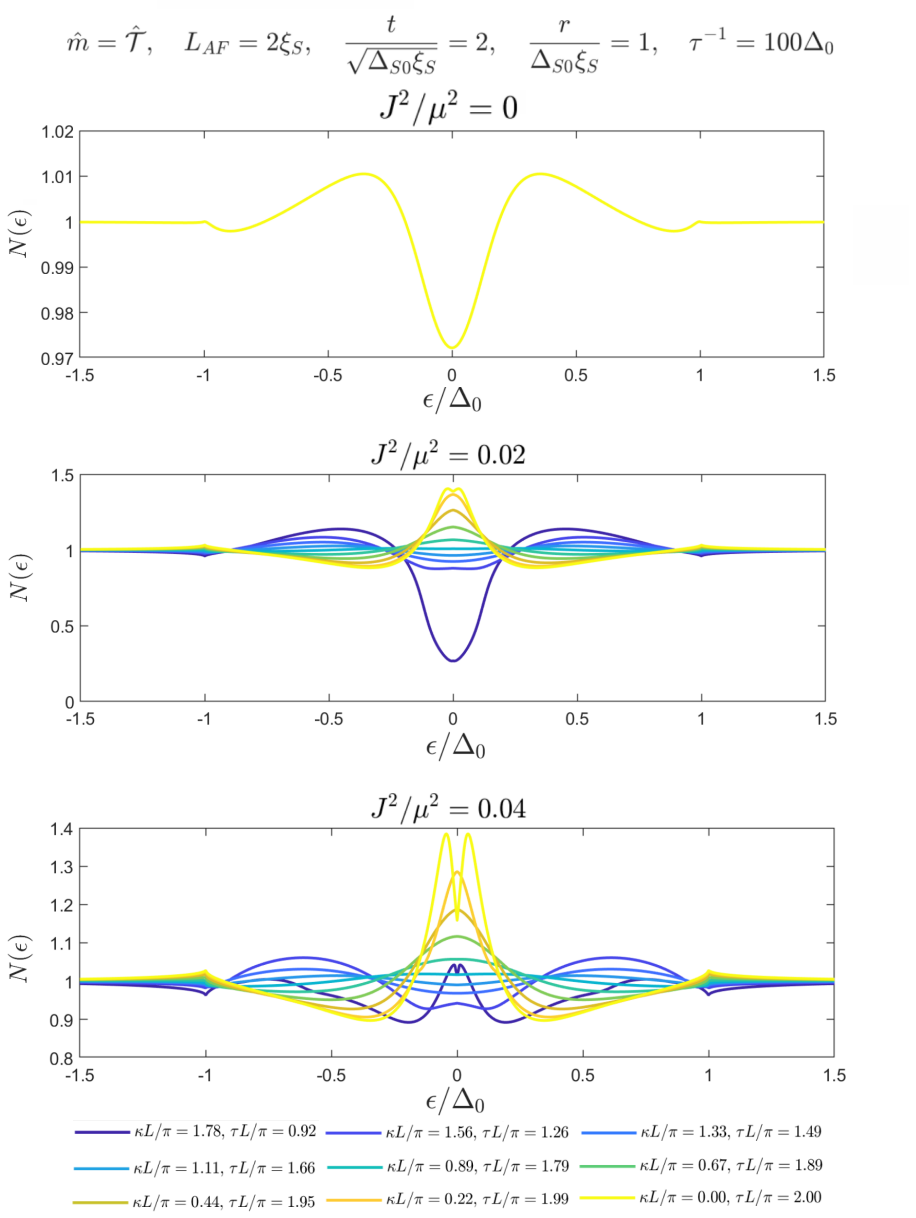

Figure 11: The density of states in the midpoint of the antiferromagnet in a S-AF bilayer with uncompensated boundary conditions. $L_{AF} = 2\xi_s$, where L_{AF} is the length of the antiferromagnet and ξ_s is the superconducting coherence length. t is the tunneling constant, r is the reflection constant and the direction of the magnetization at the boundary is given as $\hat{\mathbf{m}} = \hat{\boldsymbol{\mathcal{T}}}$ as discussed in section 6. $n_{turns} = 1$ is the number of turns for the helix. ε/Δ_0 is given along the x-axis, and the normalized density of states $N(\varepsilon)$ is given along the y-axis, where Δ_0 is the superconducting cap. The different plots shows different values of J^2/μ^2. The different colored functions show different ratios of curvature κ and torsion τ. No spin-orbit coupling is included, so $\alpha_B = \alpha_N = 0$.

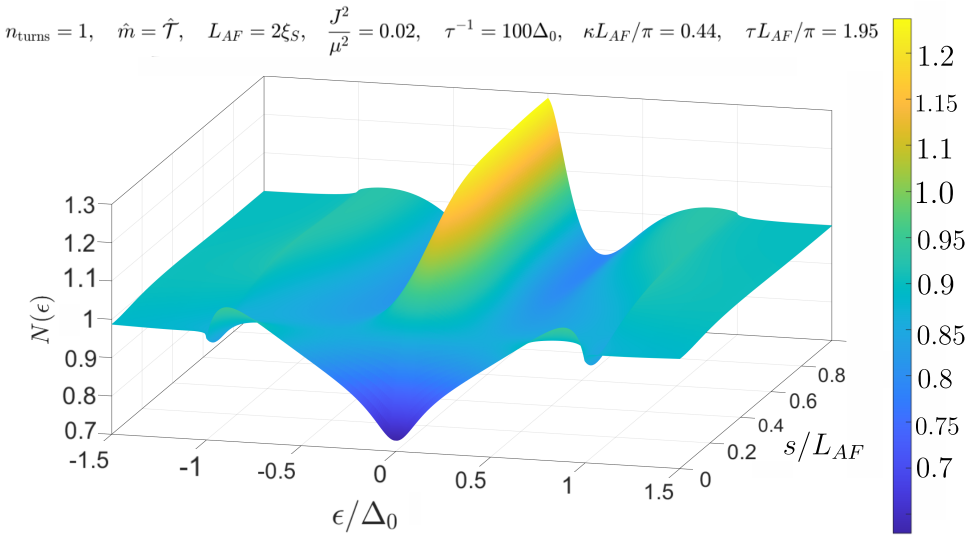

Figure 12: The density of state along the entire antiferromagnet in a S-AF bilayer with uncompensated boundary conditions. $L_{AF} = 2\xi_s$, where L_{AF} is the length of the antiferromagnet and ξ_s is the coherence length. The direction of the magnetization at the boundary is given as $\hat{\mathbf{m}} = \hat{\boldsymbol{\mathcal{T}}}$. $n_{turns} = 1$ is the number of turns for the helix. $J^2/\mu^2 = 0.02$. The curvature $\kappa = 0.44\pi/L_{AF}$ and the torsion $\kappa = 1.95\pi/L_{AF}$. ε/Δ_0 is given along one axis, s/L_{AF} is the length along the antiferromagnet and is given along the other axis, where Δ_0 is the superconducting gap. The normalized density of states $N(\varepsilon)$ is given along the last axis. No spin-orbit coupling is included, so $\alpha_B = \alpha_N = 0$.

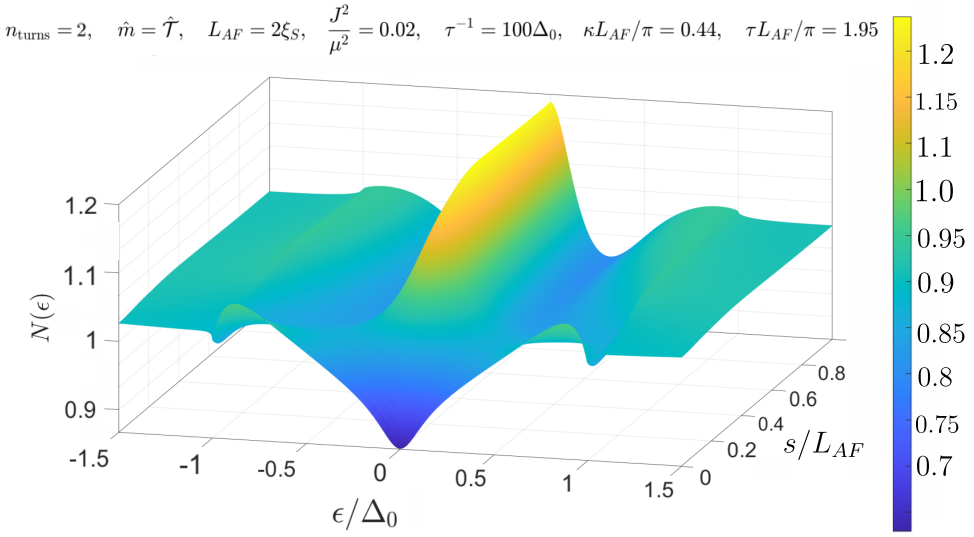

Figure 13: The density of state along the entire antiferromagnet in a S-AF bilayer with the same conditions as in figure 12, but for two turns instead of one

13 Magnetization

In the quasiclassical limit the magnetization is given as [55, 57]

$$\mathbf{M} = M_0 \int \mathrm{d}\varepsilon \, \mathrm{Tr}\{\boldsymbol{\sigma} \hat{g}^K\}, \tag{13.1}$$

where M_0 is the constant reference magnetization given by $M_0 = g\mu_B N_0 \Delta/16$, where μ_B is the Bohr magneton, g is the g-factor, and N_0 is the density of states at the Fermi-level. As mentioned in section 3, in thermal equilibrium the Keldysh component of the quasiclassical Green's function is related to the retarded component

$$\hat{g}^K = (\hat{g} + \tau_z(\hat{g}^R)^\dagger \tau_z) \tanh(\frac{\beta\varepsilon}{2}). \tag{13.2}$$

We can now use the weak proximity limit to get a better understanding of how the singlet and triplet components influence the magnetization. Due to the small value of the induced magnetism, a first order approximation of γ will vanish. We therefore need a second order weak proximity limit, keeping terms of order $\mathcal{O}(\gamma^2)$. The retarded component of the quasiclassical Green's function is then given as

$$\hat{g}^R \approx \begin{pmatrix} 2\gamma\tilde{\gamma} + 1 & 2\gamma \\ -2\tilde{\gamma} & -2\tilde{\gamma}\gamma - 1 \end{pmatrix}, \tag{13.3}$$

while the adjoint is given as

$$(\hat{g}^R)^\dagger \approx \begin{pmatrix} 2\tilde{\gamma}^\dagger\gamma^\dagger + 1 & -2\tilde{\gamma}^\dagger \\ 2\gamma^\dagger & -2\gamma^\dagger\tilde{\gamma}^\dagger - 1 \end{pmatrix}. \tag{13.4}$$

The Keldysh component can now be written in terms of the γ-matrices using equation (13.2)

$$\hat{g}^K = \begin{pmatrix} 2(\gamma\tilde{\gamma} + \tilde{\gamma}^\dagger\gamma^\dagger + 1) & 2(\gamma + \tilde{\gamma}^\dagger) \\ -2(\tilde{\gamma} + \gamma^\dagger) & -2(\tilde{\gamma}\gamma + \gamma^\dagger\tilde{\gamma}^\dagger + 1) \end{pmatrix} \tanh(\frac{\beta\varepsilon}{2}) \tag{13.5}$$

We can now use the Pauli spin vector for a nanowire helix given in equation (9.10). We start by looking at the component of the magnetization in the tangential direction. To second order in the component γ_{ij}, it can be expressed as

$$\begin{aligned} M_T = 2M_0 \int \mathrm{d}\varepsilon \\ \Big\{ & \sin(\alpha)\big[\gamma_{11}\tilde{\gamma}_{11} + \gamma_{12}\tilde{\gamma}_{21} + \text{c.c.} + 1\big] - i\cos(\alpha)e^{-i\varphi}\big[\gamma_{21}\tilde{\gamma}_{11} + \gamma_{22}\tilde{\gamma}_{21} + \text{c.c.}\big] \\ & - \sin(\alpha)\big[\gamma_{21}\tilde{\gamma}_{12} + \gamma_{22}\tilde{\gamma}_{22} + \text{c.c.} + 1\big] + i\cos(\alpha)e^{i\varphi}\big[\gamma_{11}\tilde{\gamma}_{12} + \gamma_{12}\tilde{\gamma}_{22} + \text{c.c.}\big] \\ & - \sin(\alpha)\big[\tilde{\gamma}_{11}\gamma_{11} + \tilde{\gamma}_{12}\gamma_{21} + \text{c.c.} + 1\big] - i\cos(\alpha)e^{i\varphi}\big[\tilde{\gamma}_{21}\gamma_{11} + \tilde{\gamma}_{22}\gamma_{21} + \text{c.c.}\big] \\ & + \sin(\alpha)\big[\tilde{\gamma}_{21}\gamma_{12} + \tilde{\gamma}_{22}\gamma_{22} + \text{c.c.} + 1\big] - i\cos(\alpha)e^{-i\varphi}\big[\tilde{\gamma}_{11}\gamma_{12} + \tilde{\gamma}_{12}\gamma_{22} + \text{c.c.}\big] \Big\} \tanh(\frac{\beta\varepsilon}{2}), \end{aligned} \tag{13.6}$$

where c.c. denotes the complex conjugate, which is not the same as tilde conjugation. Since we integrate over all energies, we can however make the simplification [30]

$$\int \mathrm{d}\varepsilon \, (\gamma_{ij}(\varepsilon)\tilde{\gamma}_{kl}(\varepsilon))^* \tanh\left(\frac{\beta\varepsilon}{2}\right) = -\int \mathrm{d}\varepsilon \, \tilde{\gamma}_{ij}(\varepsilon)\gamma_{kl}(\varepsilon) \tanh\left(\frac{\beta\varepsilon}{2}\right). \tag{13.7}$$

Using this, equation (13.6) can be simplified to

$$\begin{aligned} M_T = 4M_0 \int \mathrm{d}\varepsilon \\ \Big\{ &\sin(\alpha)\big[\gamma_{11}\tilde{\gamma}_{11} + \gamma_{12}\tilde{\gamma}_{21} + 1\big] - i\cos(\alpha)e^{-i\varphi}\big[\gamma_{21}\tilde{\gamma}_{11} + \gamma_{22}\tilde{\gamma}_{21}\big] \\ &- \sin(\alpha)\big[\gamma_{21}\tilde{\gamma}_{12} + \gamma_{22}\tilde{\gamma}_{22} + 1\big] + i\cos(\alpha)e^{i\varphi}\big[\gamma_{11}\tilde{\gamma}_{12} + \gamma_{12}\tilde{\gamma}_{22}\big] \\ &- \sin(\alpha)\big[\tilde{\gamma}_{11}\gamma_{11} + \tilde{\gamma}_{12}\gamma_{21} + 1\big] - i\cos(\alpha)e^{i\varphi}\big[\tilde{\gamma}_{21}\gamma_{11} + \tilde{\gamma}_{22}\gamma_{21}\big] \\ &+ \sin(\alpha)\big[\tilde{\gamma}_{21}\gamma_{12} + \tilde{\gamma}_{22}\gamma_{22} + 1\big] - i\cos(\alpha)e^{-i\varphi}\big[\tilde{\gamma}_{11}\gamma_{12} + \tilde{\gamma}_{12}\gamma_{22}\big] \Big\} \tanh\left(\frac{\beta\varepsilon}{2}\right). \end{aligned} \tag{13.8}$$

We now look at each of the sine and cosine terms separately. The sine term is given as

$$\begin{aligned} M_{Ts} &= 4M_0 \sin(\alpha) \int \mathrm{d}\varepsilon \Big\{ \big[\gamma_{11}\tilde{\gamma}_{11} + \gamma_{12}\tilde{\gamma}_{21}\big] - \big[\gamma_{21}\tilde{\gamma}_{12} + \gamma_{22}\tilde{\gamma}_{22}\big] - \big[\tilde{\gamma}_{11}\gamma_{11} + \tilde{\gamma}_{12}\gamma_{21}\big] \\ &\quad + \big[\tilde{\gamma}_{21}\gamma_{12} + \tilde{\gamma}_{22}\gamma_{22}\big] \Big\} \tanh\left(\frac{\beta\varepsilon}{2}\right) \\ &= 8M_0 \sin(\alpha) \int \mathrm{d}\varepsilon \, \big[\gamma_{12}\tilde{\gamma}_{21} - \gamma_{21}\tilde{\gamma}_{12}\big] \tanh\left(\frac{\beta\varepsilon}{2}\right). \end{aligned} \tag{13.9}$$

Inserting the d-vector formalism of the γ-matrix in curvilinear coordinates for a nanowire helix in equation (9.10) into the above equation, we get the expression

$$M_{Ts} = 4M_0 \sin(\alpha) \int \mathrm{d}\varepsilon \, \big[\sin(\alpha)(\tilde{d_T} f_s - d_T \tilde{f_s}) + \cos(\alpha)(\tilde{d_B} f_s - d_B \tilde{f_s})\big] \tanh\left(\frac{\beta\varepsilon}{2}\right). \tag{13.10}$$

The cosine terms of equation (13.8) are calculated in a similar way, and are given as

$$M_{Tc} = 4M_0 \cos(\alpha) \int \mathrm{d}\varepsilon \, \big[\cos(\alpha)(\tilde{d_T} f_s - d_T \tilde{f_s}) - \sin(\alpha)(\tilde{d_B} f_s - d_B \tilde{f_s})\big] \tanh\left(\frac{\beta\varepsilon}{2}\right). \tag{13.11}$$

Combining the sine term in equation (13.10) with the cosine terms in equation (13.11), we get that the magnetization in the tangential direction is given as

$$M_T = M_{Ts} + M_{Tc} = 4M_0 \int \mathrm{d}\varepsilon \, \big[(\tilde{d_T} f_s - d_T \tilde{f_s})\big] \tanh\left(\frac{\beta\varepsilon}{2}\right). \tag{13.12}$$

The magnetization in the normal and binormal direction are derived in a similar way and are given as

$$M_B = 4M_0 \int \mathrm{d}\varepsilon \, \big[(\tilde{d_B} f_s - d_B \tilde{f_s})\big] \tanh\left(\frac{\beta\varepsilon}{2}\right), \tag{13.13}$$

$$M_N = 4M_0 \int \mathrm{d}\varepsilon \left[\tilde{d}_N f_s - d_N \tilde{f}_s\right] \tanh\left(\frac{\beta\varepsilon}{2}\right). \tag{13.14}$$

The magnetization vector can now be expressed in terms of the d-vector as

$$\mathbf{M} = 4M_0 \int \mathrm{d}\varepsilon \left[\tilde{\mathbf{d}} f_s - \mathbf{d} \tilde{f}_s\right] \tanh\left(\frac{\beta\varepsilon}{2}\right). \tag{13.15}$$

This is the same expression as one gets when looking at a curved ferromagnet with no torsion [30].

The magnetization for different values of torsion κ and curvature τ are given in figure 14 for spin-active boundary conditions with one turn. As we can see, increasing the torsion increases the distance it takes for the magnetization to decay. Also, we need non-zero torsion for the tangential and normal component to be non-zero. We can see why this is the case by looking at the equations for the weak proximity. When $\tau = 0$, we get the weak proximity equations equations with $\alpha_N = \alpha_B = 0$ in equations (11.10) - (11.13). We always have a binormal component since the electrons start with spins in the binormal direction. However, as we can see we from the equations we get no conversion from the triplet component in the binormal direction to the other directions. This makes it so we get no components for the magnetization in the normal or tangential direction. We therefore need torsion in order to get magnetization in the normal and tangential direction. Comparing the case for one turn in figure 14 to two turns in figure 15, we see that we get small oscillations in the second turn. The amplitude increases for increased torsion, until we reach zero curvature where we have a very small oscillation. This shows that there exist an optimal value between κ and τ if we want to have oscillations with large amplitudes in the second turn. For zero torsion we get no oscillations in the second turn for the same reason we get no component in the normal and tangential direction.

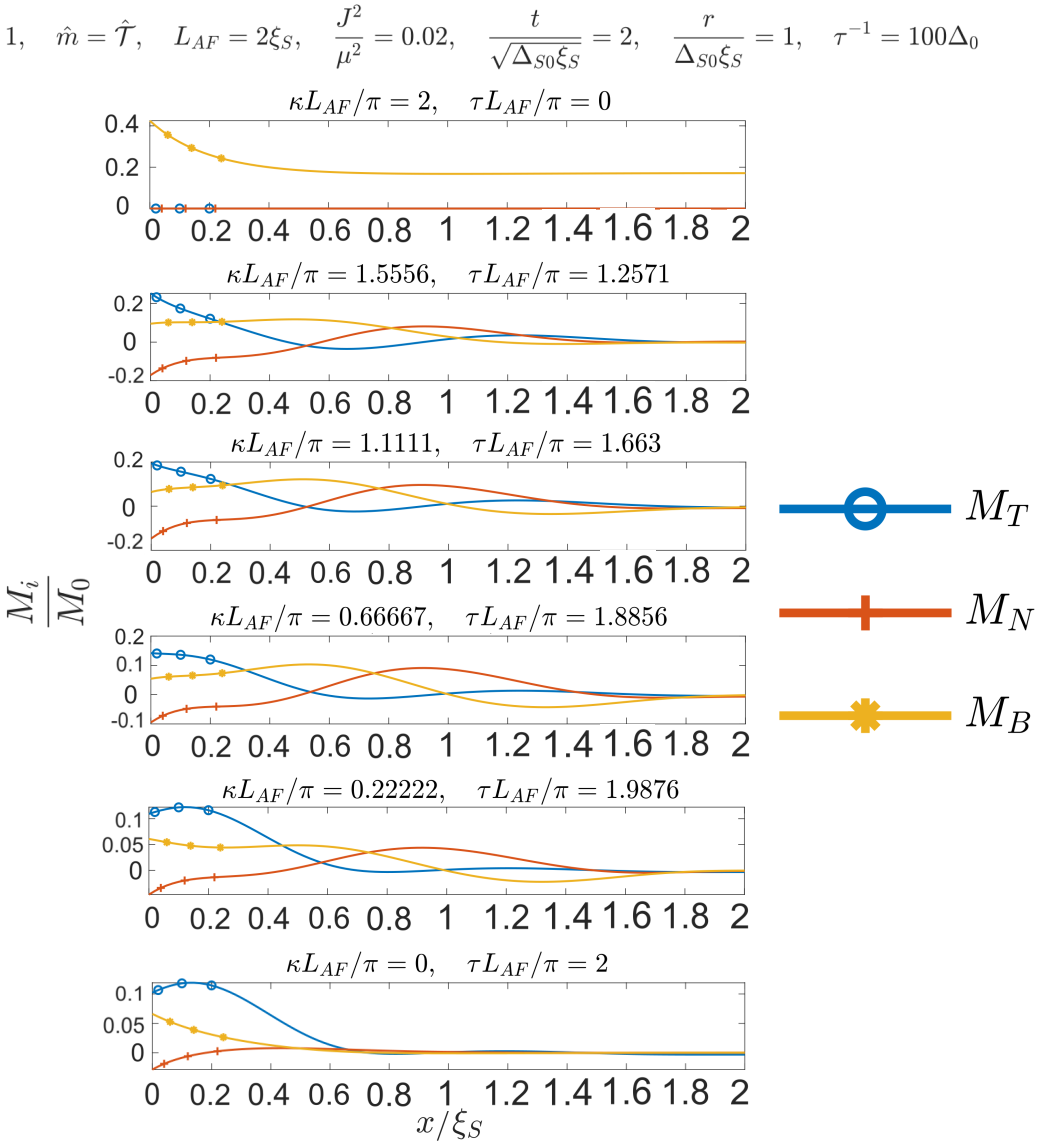

Figure 14: The magnetization inside an antiferromagnet in a S-AF bilayer with uncompensated boundary conditions. $L_{AF} = 2\xi_s$, where L_{AF} is the length of the antiferromagnet and ξ_s is the coherence length. t is the tunneling constant, r is the reflection constant and the direction of the magnetization at the boundary is given as $\hat{\mathbf{m}} = \hat{\boldsymbol{\mathcal{T}}}$ as discussed in section 6. $n_{turns} = 1$ is the number of turns for the helix. $J^2/\mu^2 = 0.02$. The distance along the antiferromagnet is given along the x-axis. The normalized magnetization M_i/M_0 is given along the y-axis. The different plots show different ratios of curvature κ and torsion κ. The blue, red and yellow functions are the magnetization in the in the $\hat{\boldsymbol{\mathcal{T}}}(s)$, $\hat{\boldsymbol{\mathcal{N}}}(s)$ and $\hat{\boldsymbol{\mathcal{B}}}(s)$ directions, respectively. No spin-orbit coupling is included, so $\alpha_B = \alpha_N = 0$.

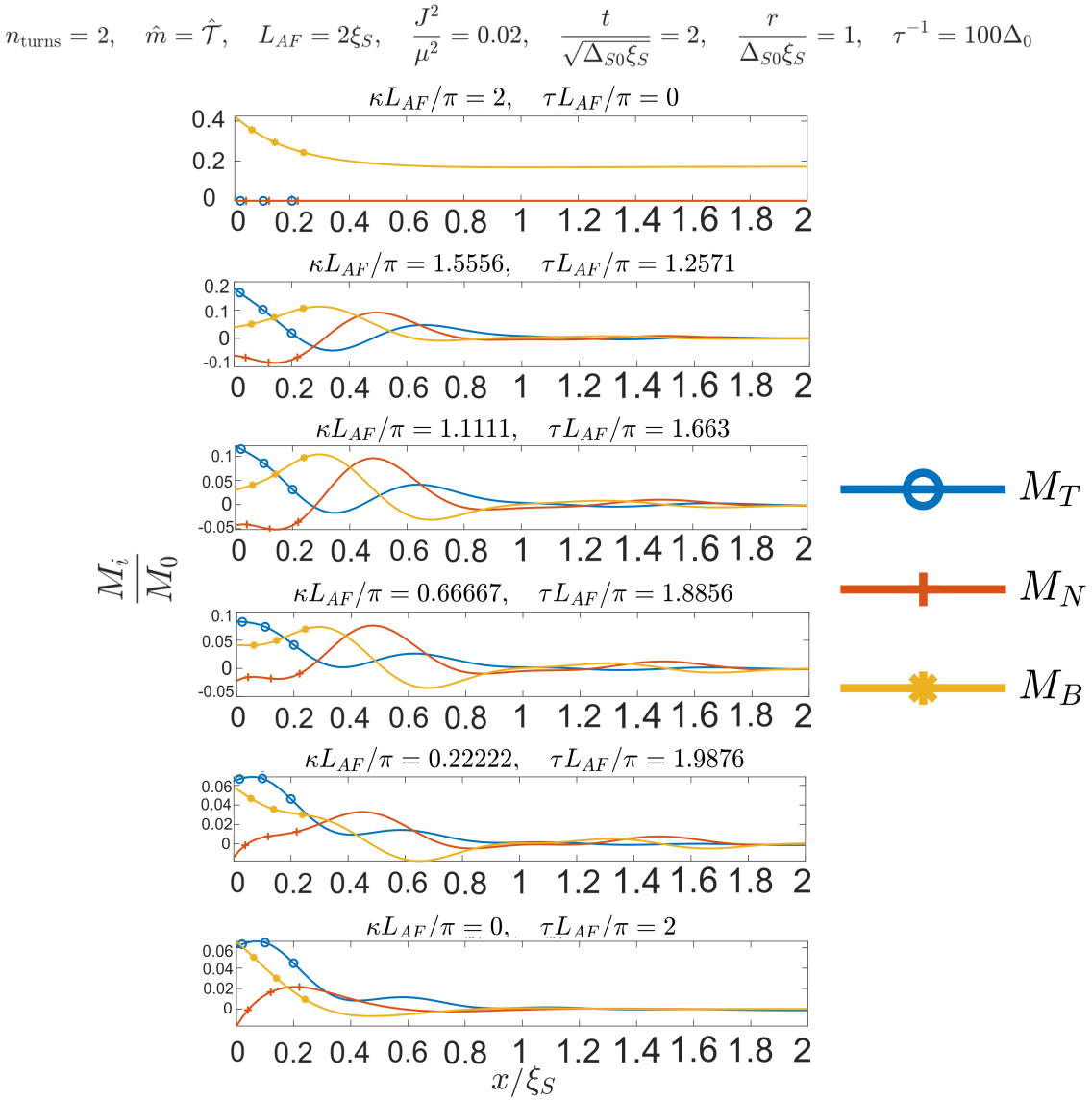

Figure 15: The magnetization inside an antiferromagnet in a S-AF bilayer with the same parameters as in figure 14, but with two turns instead of one

14 Summary and Outlook

In this thesis, we derived the Riccati parametrization for the curved antiferromagnet-superconductor Usadel equation. We started with the AF-S equation of motion derived by Fyhn et.al. [20], and used tensor notation to rewrite it in terms of a curvilinear coordinate system in the 1D case. The density of states and magnetization were then solved numerically using the Riccati parametrized equations.

From looking at the weak proximity equations for the case with and without torsion, we saw that we needed torsion in order to get mixing between the triplet and singlet components. We also saw that we did not need spin-orbit coupling in the case with torsion for mixing to happen. In addition, letting the curvature $\kappa \to 0$ made it so the triplet would not be converted to the singlet, but the singlet would be converted to the normal component. Looking at the density of states at zero energy, we saw that we needed to use uncompensated boundary conditions to get a significant positive contribution for triplet components. There also appeared to be an optimal value for the curvature κ, torsion τ and fraction J^2/μ^2 which gives the biggest peak for triplet generation, where μ is the chemical potential and J is the exchange energy between localized spins and conducting electrons. When looking at the density of states along the curved antiferromagnet, we saw that the singlet components leaking in from the superconductor were quickly converted into triplet components. For the Magnetization, we saw that increasing the torsion increased the distance it took for the magnetization to decay. Furthermore, we saw that adding a second loop for the helix gave small oscillations in the second loop, due to the mixing of the different singlet and triplet components. We saw that we needed torsion to get magnetization in the normal and tangential direction, as there is no mixing between the singlet/binormal component and the normal/tangential component when $\tau = 0$.

An application using what we have discussed could be to use a antiferromagnetic helix as a way to convert and transport triplet components through a system in 1D. A component inside a computer could perhaps use this as a way to transport spin triplets as information carriers.

Possibilities for further work could be to take the Riccati parametrization for different spin directions, not just in the binormal case as is considered in this thesis. This could lead to different results for the density of states and magnetization of the electrons, especially when also looking at the spin direction used for the uncompensated boundary conditions. In this thesis we chose to solve for the binormal direction as the Pauli matrix in this case was the simplest. This choice is also similar to the homogeneous case discussed in [34]. It would also be interesting to see the results for a nanowire with non-constant curvature and torsion. This could allow for a process where one can vary the amount of triplet components generated along the nanowire, by adjusting the curvature and torsion. In the clean limit, elliptical quantum rings have been studied [58], where it was found that the triplet $\mathbf{d}$-vector exhibits winding along the curved profile. Finally, one could also look at a 2D and

3D curved structures. One could then study the effect of vortices in the ferromagnet. It would therefore also be interesting to study the system with a time-dependence.

References

1. Van Remortel, N. The nature of natural units. *Nature Physics* **12,** 1082–1082 (2016).
2. Rauchs, M., Blandin, A., Dek, A. & Wu, Y. *Cambridge Bitcoin Electricity Consumption Index* Available at `https://ccaf.io/cbnsi/cbeci/comparisons`. Accessed 8. May 2023.
3. U.S. Energy Information Administration. Available at `https://tinyurl.com/42ty4nbc`. Accessed 8. May 2023.
4. Cooper, L. N. Bound electron pairs in a degenerate Fermi gas. *Physical Review* **104,** 1189 (1956).
5. De Gennes, P. & Guyon, E. Superconductivity in" normal" metals. *Phys. Letters* **3** (1963).
6. Werthamer, N. Theory of the superconducting transition temperature and energy gap function of superposed metal films. *Physical Review* **132,** 2440 (1963).
7. Hauser, J. HC Theuerer and NR Werthamer. *Phys. Rev* **136,** A637 (1964).
8. De Gennes, P. Boundary effects in superconductors. *Reviews of Modern Physics* **36,** 225 (1964).
9. Bergeret, F. & Tokatly, I. Spin-orbit coupling as a source of long-range triplet proximity effect in superconductor-ferromagnet hybrid structures. *Physical Review B* **89,** 134517 (2014).
10. Jacobsen, S. H., Ouassou, J. A. & Linder, J. Critical temperature and tunneling spectroscopy of superconductor-ferromagnet hybrids with intrinsic Rashba-Dresselhaus spin-orbit coupling. *Physical Review B* **92,** 024510 (2015).
11. Eschrig, M. *et al.* Spin-polarized supercurrents for spintronics. *Phys. Today* **64,** 43 (2011).
12. Fominov, Y. V., Volkov, A. & Efetov, K. Josephson effect due to the long-range odd-frequency triplet superconductivity in S F S junctions with Néel domain walls. *Physical Review B* **75,** 104509 (2007).
13. Volkov, A., Bergeret, F. & Efetov, K. B. Odd triplet superconductivity in superconductor-ferromagnet multilayered structures. *Physical review letters* **90,** 117006 (2003).
14. Eschrig, M. & Löfwander, T. Triplet supercurrents in clean and disordered half-metallic ferromagnets. *Nature Physics* **4,** 138–143 (2008).
15. Annunziata, G., Manske, D. & Linder, J. Proximity effect with noncentrosymmetric superconductors. *Physical Review B* **86,** 174514 (2012).
16. Salamone, T., Hugdal, H. G., Amundsen, M. & Jacobsen, S. H. Curvature control of the superconducting proximity effect in diffusive ferromagnetic nanowires. *Physical Review B* **105,** 134511 (2022).

17. Salamone, T., Svendsen, M. B., Amundsen, M. & Jacobsen, S. Curvature-induced long-range supercurrents in diffusive superconductor-ferromagnet-superconductor Josephson junctions with a dynamic 0- π transition. *Physical Review B* **104,** L060505 (2021).

18. Bardeen, J. & Shockley, W. Deformation potentials and mobilities in non-polar crystals. *Physical review* **80,** 72 (1950).

19. Van de Walle, C. G. Band lineups and deformation potentials in the model-solid theory. *Physical review B* **39,** 1871 (1989).

20. Fyhn, E. H., Brataas, A., Qaiumzadeh, A. & Linder, J. Quasiclassical theory for antiferromagnetic metals. *Physical Review B* **107,** 174503 (2023).

21. Baltz, V. *et al.* Antiferromagnetic spintronics. *Reviews of Modern Physics* **90,** 015005 (2018).

22. Pimenov, A. *et al.* Magnetic and magnetoelectric excitations in TbMnO 3. *Physical Review Letters* **102,** 107203 (2009).

23. Baierl, S. *et al.* Terahertz-driven nonlinear spin response of antiferromagnetic nickel oxide. *Physical review letters* **117,** 197201 (2016).

24. Cansever, H. *et al.* Resonance behavior of embedded and freestanding microscale ferromagnets. *Scientific Reports* **12,** 14809 (2022).

25. Lebrun, R. *et al.* Tunable long-distance spin transport in a crystalline antiferromagnetic iron oxide. *Nature* **561,** 222–225 (2018).

26. Onnes, H. K. Further experiments with liquid helium. C. On the change of electric resistance of pure metals at very low temperatures etc. IV. The resistance of pure mercury at helium temperatures. *Communications from the Physical Laboratory at Leiden* **120** (1911).

27. Bardeen, J., Cooper, L. N. & Schrieffer, J. R. Theory of superconductivity. *Physical review* **108,** 1175 (1957).

28. Mackenzie, A. & Maeno, Y. P-wave superconductivity. *Physica B: Condensed Matter* **280,** 148–153 (2000).

29. Linder, J. & Balatsky, A. V. Odd-frequency superconductivity. *Reviews of Modern Physics* **91,** 045005 (2019).

30. Svendsen, M. B. M. *Curvature in Superconductor-Ferromagnet structures* , M.Sc. thesis, (2021).

31. Neuenschwander, D. *Tensor Calculus for Physics* (Johns Hopkins University Press, Baltimore, 2014).

32. Jones, M. & Love, B. C. Bayesian fundamentalism or enlightenment? On the explanatory status and theoretical contributions of Bayesian models of cognition. *Behavioral and brain sciences* **34,** 169–188 (2011).

33. Ortix, C. Quantum mechanics of a spin-orbit coupled electron constrained to a space curve. *Physical Review B* **91,** 245412 (2015).

34. Pylypovskyi, O. V. *et al.* Curvilinear one-dimensional antiferromagnets. *Nano Letters* **20,** 8157–8162 (2020).

35. Chandrasekhar, V. in *Superconductivity* 279–313 (Springer Berlin Heidelberg, 2008).

36. Svendsen, M. B. M. *Diffusive Spin-Orbit Coupled Superconductor-Ferromagnet Proximity Systems* , Project thesis, (2020).

37. Ouassou, J. A. *Density of States and Critical Temperature in Superconductor/Ferromagnet Structures with Spin-Orbit Coupling* , M.Sc. thesis, (2015).

38. Salamone, T. *In preparation* PhD thesis (2023).

39. Lifshitz, E. & Pitaevskii, L. in *Physical Kinetics* (Pergamon, Oxford, 1981).

40. Belzig, W., Wilhelm, F. K., Bruder, C., Schön, G. & Zaikin, A. D. Quasiclassical Green's function approach to mesoscopic superconductivity. *Superlattices and microstructures* **25,** 1251–1288 (1999).

41. Linder, J., Yokoyama, T. & Sudbø, A. Role of interface transparency and spin-dependent scattering in diffusive ferromagnet/superconductor heterostructures. *Physical Review B* **77,** 174514 (2008).

42. Jacobsen, S. H., Ouassou, J. A. & Linder, J. *Advanced Magnetic and Optical Materials* chap. Superconducting Order in Magnetic Heterostructures (Wiley, 2017).

43. Shelankov, A. On the derivation of quasiclassical equations for superconductors. *Journal of low temperature physics* **60,** 29–44 (1985).

44. Ouassou, J. A. *Full Proximity Effect in Spin-Textured Superconductor—Ferromagnet Bilayers* , Specialization Project, (2014), 13.

45. Kuprianov, M. Y. & Lukichev, V. F. Influence of boundary transparency on the critical current of dirty SS'S structures. *Zh. Eksp. Teor. Fiz* **94,** 149 (1988).

46. Gor'kov, L. P. Microscopic derivation of the Ginzburg-Landau equations in the theory of superconductivity. *Sov. Phys. JETP* **9,** 1364–1367 (1959).

47. Dyson, F. J. The S matrix in quantum electrodynamics. *Physical Review* **75,** 1736 (1949).

48. Eilenberger, G. Transformation of Gorkov's equation for type II superconductors into transport-like equations. *Zeitschrift für Physik A Hadrons and nuclei* **214,** 195–213 (1968).

49. Fyhn, E. H., Brataas, A., Qaiumzadeh, A. & Linder, J. Superconducting proximity effect and long-ranged triplets in dirty metallic antiferromagnets. *arXiv preprint arXiv:2210.09325* (2022).

50. Van de Walle, C. G. & Martin, R. M. Theoretical calculations of heterojunction discontinuities in the Si/Ge system. *Physical Review B* **34,** 5621 (1986).

51. Gentile, P., Cuoco, M. & Ortix, C. *Curvature-induced Rashba spin–orbit interaction in strain-driven nanostructures* in *Spin* **3** (2013), 1340002.

52. Fröhlich, J. & Studer, U. M. Gauge invariance and current algebra in nonrelativistic many-body theory. *Reviews of modern physics* **65,** 733 (1993).

53. Ouassou, J. A. *Manipulating superconductivity in magnetic nanostructures in and out of equilibrium* 2019.

54. Balian, R. & Werthamer, N. Superconductivity with pairs in a relative p wave. *Physical review* **131,** 1553 (1963).

55. Amundsen, M. *Proximity effects in superconducting hybrid structures with spin-dependent interactions* PhD thesis (2020).

56. Vasyukov, D. *et al.* A scanning superconducting quantum interference device with single electron spin sensitivity. *Nature nanotechnology* **8,** 639–644 (2013).

57. Alexander, J., Orlando, T., Rainer, D. & Tedrow, P. Theory of Fermi-liquid effects in high-field tunneling. *Physical Review B* **31,** 5811 (1985).

58. Ying, Z.-J., Cuoco, M., Ortix, C. & Gentile, P. Tuning pairing amplitude and spin-triplet texture by curving superconducting nanostructures. *Physical Review B* **96,** 100506 (2017).

A Riccati Parametrization of Antiferromagnetic Term

We will now simplify the commutators terms in the Usadel equation,

$$iD_F[1+(J/\eta)^2]^{-1}\tilde{\partial}_s(\check{g}\tilde{\partial}_s\check{g}) = \big[\epsilon\tau_z - \check{V}_s + \zeta\sigma_z\tau_z\check{g}\sigma_z\tau_z, \check{g}\big]. \tag{A.1}$$

After inserting the γ-matrix for $\check{g}$, the three terms on the right hand side are given as

$$[\epsilon\tau_z, \hat{g}] = \begin{pmatrix} 0 & 4\epsilon N\gamma \\ 4\epsilon\tilde{N}\tilde{\gamma} & 0 \end{pmatrix}, \tag{A.2}$$

$$\Big[-\hat{\Delta}, \hat{g}\Big] = \begin{pmatrix} 2\underline{\Delta}i\sigma_y\tilde{N}\tilde{\gamma} + 2N\gamma\underline{\Delta}^* i\sigma_y & \underline{\Delta}i\sigma_y\tilde{N}(1+\tilde{\gamma}\gamma) + N(1+\gamma\tilde{\gamma})\underline{\Delta}i\sigma_y \\ -\underline{\Delta}^* i\sigma_y N(1+\gamma\tilde{\gamma}) - \tilde{N}(1+\tilde{\gamma}\gamma)\underline{\Delta}^* i\sigma_y & -2\underline{\Delta}^* i\sigma_y N\gamma - 2\tilde{N}\tilde{\gamma}\underline{\Delta}i\sigma_y \end{pmatrix}, \tag{A.3}$$

$$\begin{aligned}
&[\zeta\sigma_B\tau_z\hat{g}\sigma_B\tau_z, \hat{g}] = \\
&\zeta\sigma_B \begin{pmatrix} N(1+\gamma\tilde{\gamma})\sigma_B N(1+\gamma\tilde{\gamma}) + 4N\gamma\sigma_B\tilde{N}\tilde{\gamma} & 2N(1+\gamma\tilde{\gamma})\sigma_B N\gamma + 2N\gamma\sigma_B\tilde{N}(1+\tilde{\gamma}\gamma) \\ 2\tilde{N}\tilde{\gamma}\sigma_B N(1+\gamma\tilde{\gamma}) + 2\tilde{N}(1+\tilde{\gamma}\gamma)\sigma_B\tilde{N}\tilde{\gamma} & 4\tilde{N}\tilde{\gamma}\sigma_B N\gamma + \tilde{N}(1+\tilde{\gamma}\gamma)\sigma_B\tilde{N}(1+\tilde{\gamma}\gamma) \end{pmatrix} \\
&-\zeta \begin{pmatrix} N(1+\gamma\tilde{\gamma})\sigma_B N(1+\gamma\tilde{\gamma}) + 4N\gamma\sigma_B\tilde{N}\tilde{\gamma} & -2N(1+\gamma\tilde{\gamma})\sigma_B N\gamma - 2N\gamma\sigma_B\tilde{N}(1+\tilde{\gamma}\gamma) \\ -2\tilde{N}\tilde{\gamma}\sigma_B N(1+\gamma\tilde{\gamma}) - 2\tilde{N}(1+\tilde{\gamma}\gamma)\sigma_B\tilde{N}\tilde{\gamma} & 4\tilde{N}\tilde{\gamma}\sigma_B N\gamma + \tilde{N}(1+\tilde{\gamma}\gamma)\sigma_B\tilde{N}(1+\tilde{\gamma}\gamma) \end{pmatrix} \\
&\cdot \begin{pmatrix} \sigma_B & 0 \\ 0 & \sigma_B \end{pmatrix}.
\end{aligned} \tag{A.4}$$

We now want to simplify these terms. First, we will operate the $(1,1)$ components of the matrices above with γ from the right. Then, we subtract this from the $(1,2)$ component, and finally operate with $\frac{1}{2}N^{-1} = \frac{1}{2}(1-\gamma\tilde{\gamma})$ from the left. Let us first consider the $\epsilon\tau_z$-term in equation (A.2). We get:

$$\frac{1}{2}N^{-1}\big([\epsilon\tau_z, \hat{g}]^{(1,2)} - [\epsilon\tau_z, \hat{g}]^{(1,1)}\gamma\big) = \frac{1}{2}N^{-1}\big(4\epsilon N\gamma\big) = 2\epsilon\gamma. \tag{A.5}$$

Next, we consider the $\hat{\Delta}$-term in equation (A.3):

$$\begin{aligned}
&\frac{1}{2}N^{-1}\Big(\Big[-\hat{\Delta}, \hat{g}\Big]^{(1,2)} - \Big[-\hat{\Delta}, \hat{g}\Big]^{(1,1)}\gamma\Big) \\
&= \frac{1}{2}N^{-1}\big(\underline{\Delta}\tilde{N}(1+\tilde{\gamma}\gamma) + N(1+\gamma\tilde{\gamma})\underline{\Delta} - 2\underline{\Delta}\tilde{N}\tilde{\gamma}\gamma - 2N\gamma\underline{\Delta}^*\gamma\big) \\
&= \frac{1}{2}(1-\gamma\tilde{\gamma})\underline{\Delta}\tilde{N}(1+\tilde{\gamma}\gamma) + \frac{1}{2}(1+\gamma\tilde{\gamma})\underline{\Delta} - (1-\gamma\tilde{\gamma})\underline{\Delta}\tilde{N}\tilde{\gamma}\gamma - \gamma\underline{\Delta}^*\gamma \\
&= \frac{1}{2}(1-\gamma\tilde{\gamma})\underline{\Delta}\tilde{N} + \frac{1}{2}(1-\gamma\tilde{\gamma})\underline{\Delta}\tilde{N}\tilde{\gamma}\gamma - (1-\gamma\tilde{\gamma})\underline{\Delta}\tilde{N}\tilde{\gamma}\gamma + \frac{1}{2}(1+\gamma\tilde{\gamma})\underline{\Delta} - \gamma\underline{\Delta}^*\gamma \\
&= \frac{1}{2}(1-\gamma\tilde{\gamma})\underline{\Delta}\tilde{N}(1-\tilde{\gamma}\gamma) + \frac{1}{2}(1+\gamma\tilde{\gamma})\underline{\Delta} - \gamma\underline{\Delta}^*\gamma \\
&= \underline{\Delta} - \gamma\underline{\Delta}^*\gamma.
\end{aligned} \tag{A.6}$$

Finally, we look at the ζ term in equation (A.4):

$$\begin{aligned}
&\frac{1}{2}N^{-1}\big([\zeta\sigma_B\tau_z\hat{g}\sigma_B\tau_z,\hat{g}]^{(1,2)}-[\zeta\sigma_B\tau_z\hat{g}\sigma_B\tau_z,\hat{g}]^{(1,1)}\gamma\big)=\\
&\frac{1}{2}\zeta\Big[2(1-\gamma\tilde{\gamma})\sigma_BN(1+\gamma\tilde{\gamma})\sigma_BN\gamma+2(1-\gamma\tilde{\gamma})\sigma_BN\gamma\sigma_B\tilde{N}(1+\tilde{\gamma}\gamma)+2(1+\gamma\tilde{\gamma})\sigma_BN\gamma\sigma_B\\
&+2\gamma\sigma_B\tilde{N}(1+\tilde{\gamma}\gamma)\sigma_B-(1-\gamma\tilde{\gamma})\sigma_BN(1+\gamma\tilde{\gamma})\sigma_BN(1+\gamma\tilde{\gamma})\gamma-4(1-\gamma\tilde{\gamma})\sigma_BN\gamma\sigma_B\tilde{N}\tilde{\gamma}\gamma\\
&+(1+\gamma\tilde{\gamma})\sigma_BN(1+\gamma\tilde{\gamma})\sigma_B\gamma+4\gamma\sigma_B\tilde{N}\tilde{\gamma}\sigma_B\gamma\Big].
\end{aligned}\tag{A.7}$$

Expanding the terms, we get

$$\begin{aligned}
&\frac{1}{2}N^{-1}\big([\zeta\sigma_B\tau_z\hat{g}\sigma_B\tau_z,\hat{g}]^{(1,2)}-[\zeta\sigma_B\tau_z\hat{g}\sigma_B\tau_z,\hat{g}]^{(1,1)}\gamma\big)=\\
&\frac{\zeta}{2}\Big[2(\sigma_BN-\gamma\tilde{\gamma}\sigma_BN+\sigma_BN\gamma\tilde{\gamma}-\gamma\tilde{\gamma}\sigma_BN\gamma\tilde{\gamma})\sigma_BN\gamma+2(\sigma_BN\gamma\sigma_B\tilde{N}-\gamma\tilde{\gamma}\sigma_BN\gamma\sigma_B\tilde{N}\\
&+\sigma_BN\gamma\sigma_B\tilde{N}\tilde{\gamma}\gamma-\gamma\tilde{\gamma}\sigma_BN\gamma\sigma_B\tilde{N}\tilde{\gamma}\gamma)+2(\sigma_BN\gamma\sigma_B+\gamma\tilde{\gamma}\sigma_BN\gamma\sigma_B)\\
&+2(\gamma\sigma_B\tilde{N}\sigma_B+\gamma\sigma_B\tilde{N}\tilde{\gamma}\gamma\sigma_B)-4(\sigma_BN\gamma\sigma_B\tilde{N}\tilde{\gamma}\gamma-\gamma\tilde{\gamma}\sigma_BN\gamma\sigma_B\tilde{N}\tilde{\gamma}\gamma)+4\gamma\sigma_B\tilde{N}\tilde{\gamma}\sigma_B\gamma\\
&-(\sigma_BN\sigma_BN+\sigma_BN\sigma_BN\gamma\tilde{\gamma}-\gamma\tilde{\gamma}\sigma_BN\sigma_BN-\gamma\tilde{\gamma}\sigma_BN\sigma_BN\gamma\tilde{\gamma}+\sigma_BN\gamma\tilde{\gamma}\sigma_BN\\
&+\sigma_BN\gamma\tilde{\gamma}\sigma_BN\gamma\tilde{\gamma}-\gamma\tilde{\gamma}\sigma_BN\gamma\tilde{\gamma}\sigma_BN-\gamma\tilde{\gamma}\sigma_BN\gamma\tilde{\gamma}\sigma_BN\gamma\tilde{\gamma})\gamma+\\
&(\sigma_BN+\gamma\tilde{\gamma}\sigma_BN+\sigma_BN\gamma\tilde{\gamma}+\gamma\tilde{\gamma}\sigma_BN\gamma\tilde{\gamma})\sigma_B\gamma\Big].
\end{aligned}\tag{A.8}$$

Next we add and subtract similar terms

$$\begin{aligned}
&\frac{1}{2}N^{-1}\big([\zeta\sigma_B\tau_z\hat{g}\sigma_B\tau_z,\hat{g}]^{(1,2)}-[\zeta\sigma_B\tau_z\hat{g}\sigma_B\tau_z,\hat{g}]^{(1,1)}\gamma\big)=\\
&\frac{\zeta}{2}\Big[(\sigma_BN-\gamma\tilde{\gamma}\sigma_BN+\sigma_BN\gamma\tilde{\gamma}-\gamma\tilde{\gamma}\sigma_BN\gamma\tilde{\gamma})\sigma_BN\gamma+2(\sigma_BN\gamma\sigma_B\tilde{N}-\gamma\tilde{\gamma}\sigma_BN\gamma\sigma_B\tilde{N}\\
&-\sigma_BN\gamma\sigma_B\tilde{N}\tilde{\gamma}\gamma-\gamma\tilde{\gamma}\sigma_BN\gamma\sigma_B\tilde{N}\tilde{\gamma}\gamma)+2(\sigma_BN\gamma\sigma_B+\gamma\tilde{\gamma}\sigma_BN\gamma\sigma_B)\\
&+2(\gamma\sigma_B\tilde{N}\sigma_B+\gamma\sigma_B\tilde{N}\tilde{\gamma}\gamma\sigma_B)+4\gamma\tilde{\gamma}\sigma_BN\gamma\sigma_B\tilde{N}\tilde{\gamma}\gamma+4\gamma\sigma_B\tilde{N}\tilde{\gamma}\sigma_B\gamma\\
&-(\sigma_BN\sigma_BN\gamma\tilde{\gamma}-\gamma\tilde{\gamma}\sigma_BN\sigma_BN\gamma\tilde{\gamma}+\sigma_BN\gamma\tilde{\gamma}\sigma_BN\gamma\tilde{\gamma}-\gamma\tilde{\gamma}\sigma_BN\gamma\tilde{\gamma}\sigma_BN\gamma\tilde{\gamma})\gamma\\
&+(\sigma_BN+\gamma\tilde{\gamma}\sigma_BN+\sigma_BN\gamma\tilde{\gamma}+\gamma\tilde{\gamma}\sigma_BN\gamma\tilde{\gamma})\sigma_B\gamma\Big].
\end{aligned}\tag{A.9}$$

Then we collect similar terms

$$\begin{aligned}
&\frac{1}{2}N^{-1}\big([\zeta\sigma_B\tau_z\hat{g}\sigma_B\tau_z,\hat{g}]^{(1,2)}-[\zeta\sigma_B\tau_z\hat{g}\sigma_B\tau_z,\hat{g}]^{(1,1)}\gamma\big)=\\
&\frac{\zeta}{2}\Big[(\sigma_BN-\gamma\tilde{\gamma}\sigma_BN+\sigma_BN\gamma\tilde{\gamma}-\gamma\tilde{\gamma}\sigma_BN\gamma\tilde{\gamma})\sigma_BN\gamma(1-\tilde{\gamma}\gamma)+2(\sigma_BN\gamma\sigma_B(\tilde{N}+1)\\
&-\gamma\tilde{\gamma}\sigma_BN\gamma\sigma_B(\tilde{N}-1)-\sigma_BN\gamma\sigma_B\tilde{N}\tilde{\gamma}\gamma-\gamma\tilde{\gamma}\sigma_BN\gamma\sigma_B\tilde{N}\tilde{\gamma}\gamma)\\
&+2(\gamma\sigma_B\tilde{N}\sigma_B+\gamma\sigma_B\tilde{N}\tilde{\gamma}\gamma\sigma_B)+4\gamma\tilde{\gamma}\sigma_BN\gamma\sigma_B\tilde{N}\tilde{\gamma}\gamma+4\gamma\sigma_B\tilde{N}\tilde{\gamma}\sigma_B\gamma\\
&+(\sigma_BN+\gamma\tilde{\gamma}\sigma_BN+\sigma_BN\gamma\tilde{\gamma}+\gamma\tilde{\gamma}\sigma_BN\gamma\tilde{\gamma})\sigma_B\gamma\Big].
\end{aligned}\tag{A.10}$$

On the first line we use the fact that $N\gamma = \gamma\tilde{N}$ and $\tilde{N}^{-1} = (1-\tilde{\gamma}\gamma)$. On the second line we use that we can write $\tilde{N}\tilde{\gamma}\gamma = \tilde{N}(1-\tilde{N}^{-1}) = \tilde{N}-1$. We then get

$$\begin{aligned}
&\frac{1}{2}N^{-1}\big([\zeta\sigma_B\tau_z\hat{g}\sigma_B\tau_z,\hat{g}]^{(1,2)} - [\zeta\sigma_B\tau_z\hat{g}\sigma_B\tau_z,\hat{g}]^{(1,1)}\gamma\big) = \\
&\frac{\zeta}{2}\Big[(\sigma_B N - \gamma\tilde{\gamma}\sigma_B N + \sigma_B N\gamma\tilde{\gamma} - \gamma\tilde{\gamma}\sigma_B N\gamma\tilde{\gamma})\sigma_B\gamma + 4(\sigma_B N\gamma\sigma_B - \gamma\tilde{\gamma}\sigma_B N\gamma\sigma_B(\tilde{N}-1)) \\
&+ 2(\gamma\sigma_B\tilde{N}\sigma_B + \gamma\sigma_B\tilde{N}\tilde{\gamma}\gamma\sigma_B) + 4\gamma\tilde{\gamma}\sigma_B N\gamma\sigma_B\tilde{N}\tilde{\gamma}\gamma + 4\gamma\sigma_B\tilde{N}\tilde{\gamma}\sigma_B\gamma \\
&+ (\sigma_B N + \gamma\tilde{\gamma}\sigma_B N + \sigma_B N\gamma\tilde{\gamma} + \gamma\tilde{\gamma}\sigma_B N\gamma\tilde{\gamma})\sigma_B\gamma\Big].
\end{aligned} \tag{A.11}$$

Adding and subtracting similar terms gives

$$\begin{aligned}
&\frac{1}{2}N^{-1}\big([\zeta\sigma_B\tau_z\hat{g}\sigma_B\tau_z,\hat{g}]^{(1,2)} - [\zeta\sigma_B\tau_z\hat{g}\sigma_B\tau_z,\hat{g}]^{(1,1)}\gamma\big) = \\
&\frac{\zeta}{2}\Big[2(\sigma_B N + \sigma_B N\gamma\tilde{\gamma})\sigma_B\gamma + 4\sigma_B N\gamma\sigma_B + 2(\gamma\sigma_B\tilde{N}\sigma_B + \gamma\sigma_B\tilde{N}\tilde{\gamma}\gamma\sigma_B) + 4\gamma\sigma_B\tilde{N}\tilde{\gamma}\sigma_B\gamma\Big].
\end{aligned} \tag{A.12}$$

Finally we use that $N\gamma\tilde{\gamma} = N(1-N^{-1}) = N-1$ and $\sigma_B\sigma_B = \begin{pmatrix} 1 & 0 \\ 0 & 1 \end{pmatrix}$ to get

$$\begin{aligned}
&\frac{1}{2}N^{-1}\big([\zeta\sigma_B\tau_z\hat{g}\sigma_B\tau_z,\hat{g}]^{(1,2)} - [\zeta\sigma_B\tau_z\hat{g}\sigma_B\tau_z,\hat{g}]^{(1,1)}\gamma\big) = \\
&2\zeta\Big[\sigma_B N\sigma_B\gamma + \gamma\sigma_B\tilde{N}\sigma_B + \sigma_B N\gamma\sigma_B + \gamma\sigma_B\tilde{N}\tilde{\gamma}\sigma_B\gamma - \gamma\Big].
\end{aligned} \tag{A.13}$$

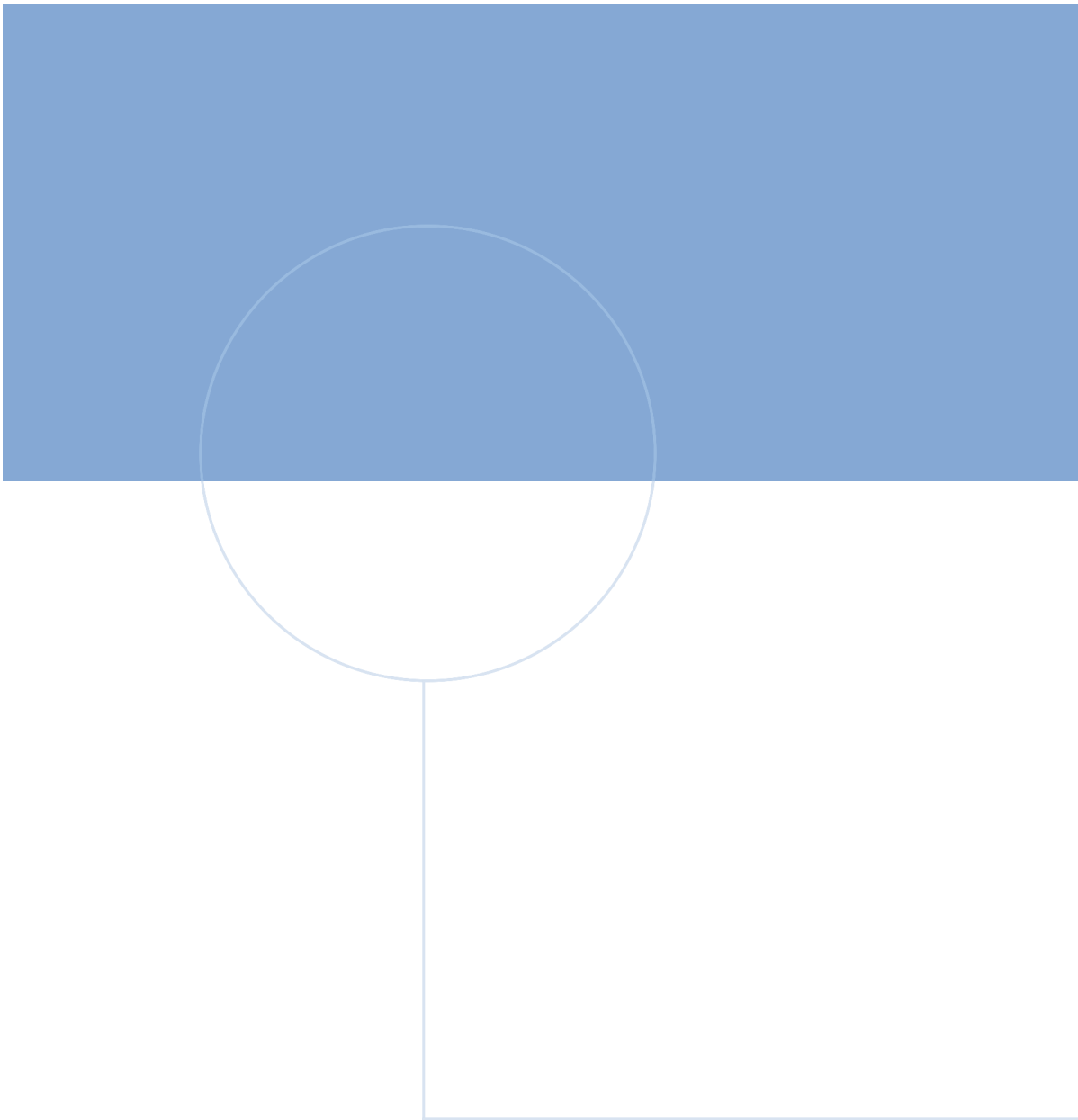

NTNU

Norwegian University of
Science and Technology